



**TOGETHER**  
*for a sustainable future*

## OCCASION

This publication has been made available to the public on the occasion of the 50<sup>th</sup> anniversary of the United Nations Industrial Development Organisation.



**TOGETHER**  
*for a sustainable future*

## DISCLAIMER

This document has been produced without formal United Nations editing. The designations employed and the presentation of the material in this document do not imply the expression of any opinion whatsoever on the part of the Secretariat of the United Nations Industrial Development Organization (UNIDO) concerning the legal status of any country, territory, city or area or of its authorities, or concerning the delimitation of its frontiers or boundaries, or its economic system or degree of development. Designations such as “developed”, “industrialized” and “developing” are intended for statistical convenience and do not necessarily express a judgment about the stage reached by a particular country or area in the development process. Mention of firm names or commercial products does not constitute an endorsement by UNIDO.

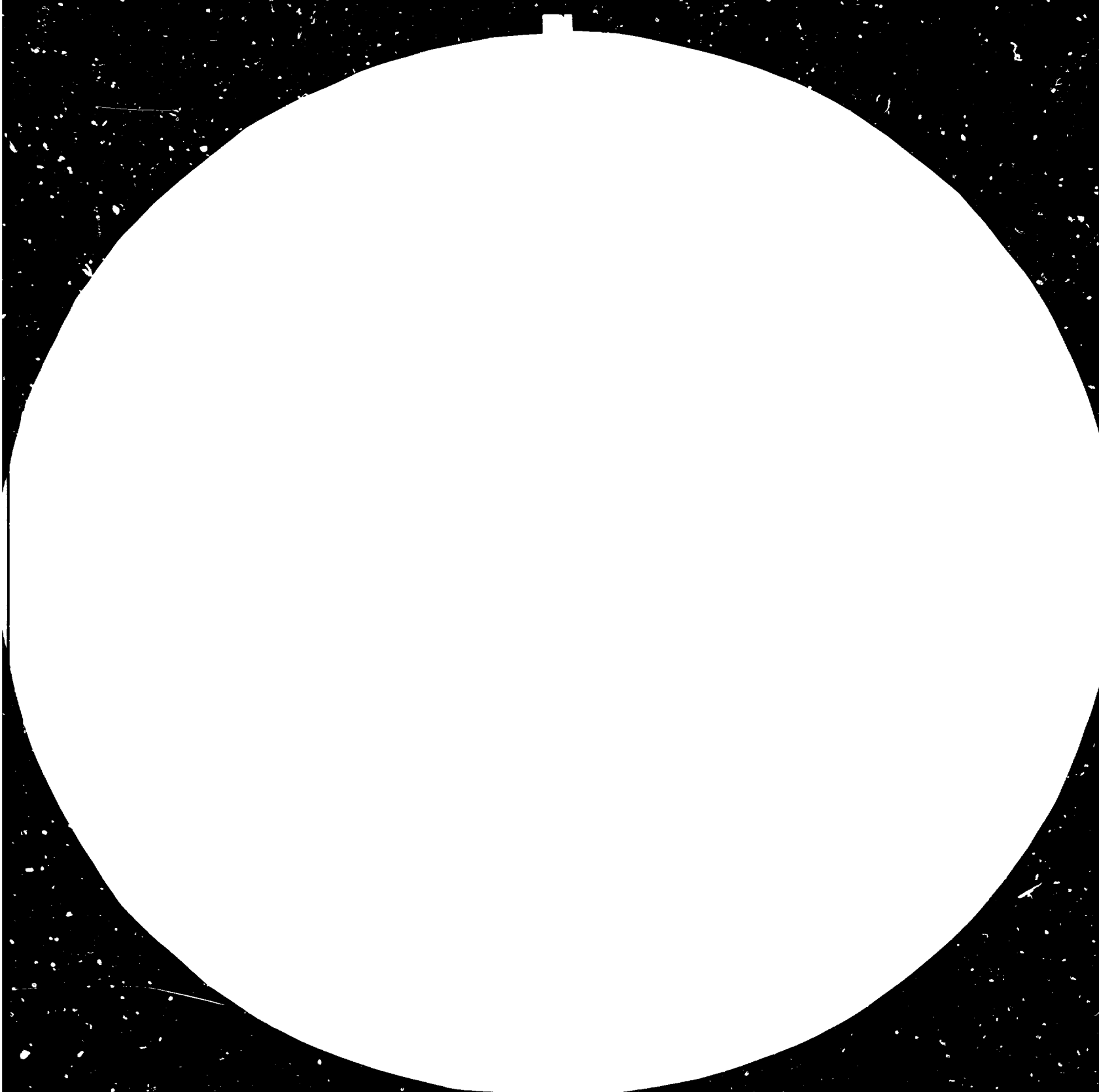
## FAIR USE POLICY

Any part of this publication may be quoted and referenced for educational and research purposes without additional permission from UNIDO. However, those who make use of quoting and referencing this publication are requested to follow the Fair Use Policy of giving due credit to UNIDO.

## CONTACT

Please contact [publications@unido.org](mailto:publications@unido.org) for further information concerning UNIDO publications.

For more information about UNIDO, please visit us at [www.unido.org](http://www.unido.org)





28



3.2



4.0



## MICROSCOPY RESOLUTION TEST CHART

NATIONAL BUREAU OF STANDARDS  
1963-A19  
U.S. GOVERNMENT PRINTING OFFICE: 1963  
O - 348-084

UNITED NATIONS



NATIONS UNIES

UNITED NATIONS INDUSTRIAL DEVELOPMENT ORGANIZATION

13155

World Review on Energy Conservation  
in the  
Bauxite/Alumina Industry

György Leng  
Károly Solymar.

1315

ALUTERV-FKI

Budapest

1983

UNITED NATIONS INDUSTRIAL DEVELOPMENT ORGANIZATION

WORLD REVIEW ON ENERGY CONSERVATION IN THE  
BAUXITE/ALUMINA INDUSTRY

by

György L a n g  
Hungarian Aluminium Corporation

and

dr. Károly S o l y m á r  
ALUTERV-FKI

Edited by: dr. Pál G a d ó  
dr. Zbigniew S a r t o w s k i

The opinions expressed in this volume are those of the contributors and do not necessarily reflect the views of the secretariat of UNIDO.

Printed in  
ALUTERV-FKI  
Budapest, 1983.

## ACKNOWLEDGEMENT

I would like to express my thanks here, to Dr. János Zámbo, director of ALUTERV-FKI for making possible the work on this study.

I am very glad to have co-operated with my coauthor Mr György Lang who elaborated special topics on energy at a high scientific level.

I thank also the precious support in editing to Dr Pál Gadó and Dr Zbigniew Sartowski.

I am thankful for their co-operation to Miss Ildikó Kovács /drawings/, Mrs Mária Birkás and Mrs Éva Fehér /typing/, and Mr Péter Laky /printing/.

Budapest, Nov. 1983.

Dr. Károly Solymár

## I.

## LIST OF ABBREVIATIONS

## Nomenclature and units

A	area of heat transfer surface in $m^2$
a	weight fraction of alumina in ton/ton
$C_A$	concentration of alumina in $kp Al_2O_3/m^3$
$C_N$	caustic concentration in $kp Na_2O/m^3$
G	unit mass rate of steam in ton/ton alumina
H	heat value per unit volume in $MJ/m^3$
$h'$	enthalpy of saturated water in $MJ/ton$
$h''$	enthalpy of saturated vapor in $MJ/ton$
K	heat transfer coefficient in $MJ/h, m^2, ^\circ C$
M	unit mass of process fluid in ton/ton alumina
Q	unit quantity of heat in $MJ/ton$ alumina
q	specific heat capacity in $MJ/ton, ^\circ C$
r	latent heat of vapor in $MJ/ton$
S	entropy of process fluid $MJ/ton, ^\circ K$
T	temperature in $^\circ C$ or $^\circ K$
$T_i'$	feed temperature of stream i in $^\circ C$
$T_i''$	discharge temperature of stream i in $^\circ C$
V	unit volume in $m^3/ton$ alumina
W	unit water equivalent $Mcal/^\circ C, ton$ alumina
w	unit water content in ton water/ton
X	mass or volume fraction in ton/ton or $m^3/m^3$
$\eta$	efficiency in %
$\Phi$	efficiency of heat transfer in %

## Conversion of units

$$BTU = 1,055 \text{ KJ}$$

$$Mcal = 4,1868 \text{ MJ}$$

$$^\circ C = \frac{^\circ F - 32}{9} \cdot 5$$

## II.

### CONTENTS

	page
TABLES	V.
FIGURES	VIII.
EXECUTIVE SUMMARY	XIV.
INTRODUCTION	1
1. Expected development of the world aluminium industry	7
1.1 Expected rate of growth	7
1.2 The energy demand of aluminium production	12
1.3 Potential of the developing countries	14
2. World bauxite resources and energetic aspects of their utilization	18
2.1 World bauxite resources	18
2.2 Energy consumption in bauxite production	21
2.3 Utilization of the bauxite reserves	26
3. Main trends of the technical development of the Bayer process	27
3.1 Characteristics of the process	27
3.2 Determining factors of the technical development	30
3.3 Flowsheet modifications, optimization of the concentration	38
3.4 Tube digestion	41
3.4.1 Development and general characteristics of the tube digestion	41
3.4.2 Development and characteristics of the Hungarian tube digester	42
3.4.3 Experiences from pilot plant tests	44



### III.

	page
3.4.4 Construction of the Hungarian tube digester and outlooks for the future	48
3.5 Bauxite digestion with catalytic additives	49
3.5.1 Catalyzers and their effects	49
3.5.2 Typical results of catalyzed digestion in Hungarian alumina plants	50
3.5.3 Application field of the Hungarian digestion technology with catalytic additives	54
3.6 Two-stage digestion of diasporic bauxites	58
3.6.1 Digestibility of diasporic bauxites	58
3.6.2 Equilibrium solubility of diasporic bauxites and two-stage digestion technology	65
3.7 Recent trends in the precipitation	69
3.8 Reduction of caustic soda losses	71
3.8.1 Distribution of the NaOH losses within the Bayer process	71
3.8.2 Digestion of bauxite using catalysing additives	73
3.8.3 Causticization of soda on the washer line	75
3.8.4 Causticization of red mud	76
3.8.5 Complex causticization	77
3.8.6 Comparison of the methods for regenerating NaOH	81
3.9 Energy consumption of the different stages of the Bayer process	84
4. Overall energy survey of the Bayer process	88
5. Thermal properties of plant fluids	94
5.1 Solubility of alumina in caustic liquors	94
5.2 Effects of bauxite composition	96
5.3 Volume of liquor required for digestion	98
5.4 Density and specific heat of aluminate liquor	101

#### IV.

	page
5.5 Calculations with solids and slurries	102
5.6 Boiling point elevation	103
6. Heat transfer in alumina plants	104
6.1 Surface heat exchangers	104
6.2 Flash-type heat exchangers	107
6.3 Multistep flash heat recovery	109
7. Energy audits of digestion, clarification and precipitation	112
7.1 Digestion	112
7.2 Clarification	118
7.3 Precipitation	123
8. Evaporation	128
8.1 Multieffect evaporators	128
8.2 Co-current evaporator stations	129
8.3 Counter current evaporator stations	131
8.4 Economy of vapour extraction for heating purposes	132
8.5 Flash evaporators	134
8.6 Thermo-compression	135
8.7 Energy audit of the evaporation section	138
9. Calcination	142
9.1 Alumina and water balance	146
9.2 Heat generation by combustion	148
9.3 Practical calculations on combustion	149
9.4 Energy audit of calcination	155
10. Electrical energy	158
11. Cogeneration of electricity and heat	162
REFERENCES	168

## V.

## TABLES

	page
Table 1. Geographic distribution of production, 1980	8
Table 2. Demand forecasts for aluminium inputs	9
Table 3. Capacity and investment predictions for aluminium	10
Table 4. World aluminium production and capacity, 1982	11
Table 5. Energy cost per ton of aluminium	12
Table 6. Classification system for bauxite resources	19
Table 7. World bauxite resources, classified according to their state of development	20
Table 8. Unit energy rates in MJ per ton bauxite for open cut surface mining with different cover layer volumes at an output capacity of 400 000 tpy	24
Table 9. Unit energy rates in MJ per ton bauxite for underground mining in 200 metres depth and an output capacity of 500 000 tpy	25
Table 10. Mineralogical composition of some characteristic bauxites	33
Table 11. Typical composition of the bauxite from Halimba processed by tube digestion	44

## VI.

	page
Table 12. Phase composition of an Australian bauxite and the red muds gained therefrom at 235° C without additives and applying hydrogarnet catalyzer	55
Table 13. Phase composition of a Guinean bauxite and the red muds gained therefrom at 235° C without additives and applying hydrogarnet catalyzer	56
Table 14. Chemical compositions of bauxite samples	59
Table 15. Mineralogical compositions of bauxites and their characteristic red muds	64
Table 16. Phase composition of bauxite and of its characteristic red mud	82
Table 17. Saturation $C_A/C_N$ ratios	95
Table 18. Average bauxite composition	96
Table 19. Average red mud composition	97
Table 20. Unit extraction liquor volumes /m <sup>3</sup> /t/	100
Table 21. Number of flashing steps and heat recovery	112
Table 22. Solids concentrations and liquid volumes in underflow	121
Table 23. Steam consumption rate per unit of evaporated water	129

## VII.

	page
Table 24. Economy of thermocompression	137
Table 25. Energy balances of calciners	146
Table 26. Combustion equations	149
Table 27. Gas volumes and compositions	149
Table 28. Oxygen and air requirements and resulting flue gas volumes and compositions	151
Table 29. Flue gas compositions for different fuels and excess air conditions	152
Table 30. Specific combustion air volumes $/V_{\text{Air}}/$ for different excess air ratios $/n/$ and fuels	153
Table 31. Specific wet flue gas volumes $/V_{\text{FGW}}/$ for different excess air ratios $/n/$ and fuels	153
Table 32. Specific heat content of flue gases $/q_{\text{FG}}/$ and air $/q_{\text{Air}}/$ at different temperatures	154
Table 33. Break up of electrical energy consumption	158
Table 34. Primary heat equivalents	166

## VIII.

### FIGURES

	page
Fig. 1. The expected primary aluminium production of the world in 2000	7
Fig. 2. The world primary aluminium producing capacity by type of power	15
Fig. 3. The total and per capita energy consumption of the industrialized and developing countries between 1981 and 2000	17
Fig. 4. Main phases of the bauxite mining from exploration to refinery's gate	22
Fig. 5. Block-diagram of the Bayer process using low-temperature digestion	28
Fig. 6. Layout of the Gladstone alumina plant	29
Fig. 7. Expected world production of bauxite and alumina	30
Fig. 8. Total capacity in percent and specific investment cost as a function of the plant size	32
Fig. 9. Structure of production costs and energy consumption	34
Fig. 10. Alumina yield after digestion, silica related bound NaOH losses and specific bauxite consumption as function of the $\text{SiO}_2$ content on processing a bauxite with 50 % $\text{Al}_2\text{O}_3$	36

## IX.

	page
Fig. 11. Bayer cycle in the $\text{Na}_2\text{O}-\text{Al}_2\text{O}_3-\text{H}_2\text{O}$ system for the Ajka Alumina Plant, Hungary	38
Fig. 12. I-T Diagram for the Bayer cycle of the Ajka Alumina Plant, Hungary	39
Fig. 13. Hungarian tube digester system	43
Fig. 14. Kinetics of boehmite dissolution in the Hungarian pilot tube digester	45
Fig. 15. Comparison of heat transfer coefficients measured in the Hungarian pilot tube digester and an up-to-date system consisting of preheaters plus autoclave line, respectively	46
Fig. 16. Relation between the heat transfer coefficients measured in the Hungarian pilot tube digester after a cycle of 30 days and the $\text{TiO}_2$ content of the scalings	47
Fig. 17. Variation of the heat transfer coefficient proving the effectiveness of the acid cleaning	47
Fig. 18. Digestion of Hungarian goethitic bauxite without and with additive	50
Fig. 19. Decrease of $\text{Fe}_2\text{O}_3$ content in the aluminate liquor /without control filtration/ after introducing digestion with additives into production of Hungarian alumina plants	51

X.

	page
Fig. 20. Increase of solid concentration in the cone of the last washer in Hungarian alumina plants as a consequence of applying digestion with catalytic additives	52
Fig. 21. Decrease of free Na <sub>2</sub> O content in the last washer in Hungarian alumina plants as a consequence of applying catalytic additives during digestion	53
Fig. 22. Comparison of the phase compositions of the respective red muds obtained from a Guinean bauxite sample without additives and using catalyzed digestion	57
Fig. 23. Digestibility of diasporic bauxites	60
Fig. 24. Digestibility curves of diasporic bauxites	61
Fig. 25. Digestibility curves of the Lang Son bauxite /Vietnam/	63
Fig. 26. Equilibrium solubility of diasporic bauxites compared to that of a boehmitic one	65
Fig. 27. Two-stage digestion for processing diasporic and boehmitic bauxites	67
Fig. 28. Relative magnitude of the contributions to NaOH losses and their diminution	72



XI.

	page
Fig. 29. Alumina yield, bound $\text{Na}_2\text{O}$ in red mud and the efficiency of goethite - hematite transformation in dependence from the $\text{CaO}$ content in the red mud during digestion using additives	74
Fig. 30. Efficiency of causticization at the Dorr line and loss of $\text{Al}_2\text{O}_3$ versus caustic concentration	75
Fig. 31. The efficiency of red mud causticization as a function of the temperature of treatment	76
Fig. 32. Typical phase transformations occurring during complex causticization	78
Fig. 33. Flow sheet of the complex causticization	79
Fig. 34. The change of $\text{Na}_2\text{O}/\text{SiO}_2$ ratio in red mud versus $\text{CaO}$ content during complex causticization	80
Fig. 35. Specific $\text{CaO}$ consumption in various treatments for the regeneration of $\text{NaOH}$	81
Fig. 36. Distribution of energy consumption in a medium level alumina plant among the process stages	84
Fig. 37. Radiation and waste heat losses of the alumina hydrate manufacturing	85
Fig. 38. Energy consumption of the Bayer alumina plant	87

## XII.

	page
Fig. 39. The Bayer cycle	89
Fig. 40. T-Q diagram of the process	90
Fig. 41. Surface heat exchangers	104
Fig. 42. Heat transfer efficiency	106
Fig. 43. Flash-type heat exchange	107
Fig. 44. Q-T diagram of heat transmission	108
Fig. 45. Q/T diagram of flash heat recovery	110
Fig. 46. Flow sheet of digestion	115
Fig. 47. T-Q diagram of digestion	116
Fig. 48. Flow-sheet of settling-washing	120
Fig. 49. Functional flow sheet of precipitation	124
Fig. 50. Cocurrent-flow evaporator	130
Fig. 51. Counter-current evaporator	131
Fig. 52. Case solution No. 1.	132
Fig. 53. Case solution No. 2.	133
Fig. 54. Flash type evaporator	135
Fig. 55. Thermocompression type evaporator	136

XIII.

age		page
89	Fig. 56. Evaporation flow sheet	138
90	Fig. 57. Functional flow sheet of calcination	143
04	Fig. 58. Retrofitting of rotary kiln with GSC/gas suspension calciner/	144
06		
07	Fig. 59. Fluid flash calciner	145
08	Fig. 60. Calcination flow sheet	156
10	Fig. 61. Head and efficiency curves	159
15	Fig. 62. Head-capacity curves	160
16	Fig. 63. Variable speed drive efficiencies	161
20	Fig. 64. Thermal power station	163
24	Fig. 65. Cogeneration plant	164
30		
31		
32		
33		
35		
36		

EXECUTIVE SUMMARY

0.1 EXPECTED DEVELOPMENT OF THE WORLD ALUMINIUM INDUSTRY

The aluminium industry's typical features are high energy consumption and high investment requirement.

The demand for finished aluminium goods will rise by about 4-5 % per annum over the next 20 years - from around 18 million tons in 1980 to 38 million tons in 2000.

The aluminium production is one of the most energy intensive technologies. The total energy requirement of the aluminium production can exceed 200 GJ/ton.

Major trends of the further development are the transfer of alumina production from the developed countries to the bauxite producers and the shift of smelting capacity to low-cost energy sources, particularly to hydropower. Hydropower is widely distributed in developing countries. The aluminium industry is already being shifted to favourable locations in developing countries, a world wide restructuring of this industry has already started. It is reasonable to generate one half /2400 Mtoe/yr/ of the "Lima energy gap" mainly from hydropower and biomass in the developing countries.

0.2 WORLD BAUXITE RESOURCES AND ENERGETIC ASPECTS OF THEIR UTILIZATION

The world's bauxite resources are located mainly in the developing countries while the processing is concentrated in the developed ones. The explored bauxite deposits of the world are increasing faster than the rate of growth of production. The bauxite resources identified world wide

plants will be able to compete with these only by a permanent modernisation of the technology.

A general trend of the technological development is to produce sandy type alumina hydrate at higher caustic soda concentration.

Main roads for saving energy in the bauxite processing are:

- retrofitting existing alumina plants by additional or more efficient heat recovery equipment,
- converting energy supply from expensive oil or natural gas to lower cost coal,
- developing process modifications in order to reduce energy consumption,
- instrumentation and computerized process control.

The following technological possibilities can be preferred to save energy and raw materials:

- flowsheet modifications, optimization of the concentration
- tube digestion
- digestion with catalytic additives
- two-stage digestion of diasporic bauxites
- increasing of the liquor productivity in the precipitation /intensive purification of the circuit/
- reduction of the caustic soda losses by causticization
- application of special chemicals /synthetic flocculants and dewatering aids/

are estimated to be approx. 50 billion metric tons.

The value of bauxite in Bayer recovery is basically determined by the costs of replacing the caustic soda losses and by the amount of dry bauxite to be processed for 1 ton of alumina.

90 per cent of the world's bauxite resources are of lateritic origin, mostly gibbsitic types and can be excavated by high productivity machinery by open pit mining. The average specific energy consumption of the mining operations can vary between 0.2-0.5 GJ/t alumina and this value is relatively very low related to the energy consumption of a typical alumina plant /16-20 GJ/t/. The energy consumption of the transportation, however, is much higher and the bauxite shipment from Australia to an European alumina plant can require as much energy as the total energy consumption of the most up-to-date refinery /approximately 8 GJ/t alumina/. Consequently, the new alumina plants will be located mostly near to the mining areas.

### 0.3 MAIN TRENDS OF THE TECHNICAL DEVELOPMENT OF THE BAYER PROCESS

Bauxite is the main raw material for the alumina production and its ratio to the gross raw material demand will not diminish below 85-90 % by the turn of millenary. The establishment of equipment of still increasing unit capacity, the increasing of capacity of the running plants and the erection of new high-capacity alumina plants remain the trend of development. The trends of technical development and economy, will be determined by the up-to-date, high-capacity alumina plants, whereas the smaller-capacity

## 0.4 OVERALL ENERGY SURVEY OF THE BAYER PROCESS

The main components of energy consumption can be recognized as follows:

- External heat input at high temperature is required in the digestion step which would be proportional to the "water equivalent" of digestion slurry and the temperature gap to be covered by external heating.
- A low temperature heat input at the evaporation section must be provided to restore the water balance. The required energy depends on the surplus of water accumulated in the cycle mainly due to wash water entry.
- Potential areas for heat recovery do exist in the process cycle, and it may be assumed that effective heat exchange could strongly improve overall heat economy.

## 0.5 THERMAL PROPERTIES OF PLANT FLUIDS

It is necessary to compute material and heat balances of the whole circuit and the unit operations as well. The following thermal and chemical properties are discussed in details for this purposes:

- solubility of alumina in caustic liquors,
- effects of bauxite composition,
- volume of liquor required for digestion,
- density and specific heat of aluminate liquor,
- calculations with solids and slurries,
- boiling point elevation.

## XVIII.

### 0.6 HEAT TRANSFER IN ALUMINA PLANTS

Surface heat exchangers and flash type heat exchangers are widely used in the Bayer process to decrease the energy consumption.

The methods to calculate heat transfer conditions are presented.

### 0.7 ENERGY AUDITS OF DIGESTION, CLARIFICATION AND PRECIPITATION

Heat recovery in most digestion plant units is performed by a multistep flash system. The heat recovery improves in consequence of increasing the number of flashing steps and dividing the same heat transfer area accordingly into smaller units.

The average heat transfer coefficient determines the efficiency of heat recovery and, by that, the live steam consumption of digestion as well. Heat recovery is not the only benefit of flash cooling. The other important gain is water extraction. The total water separated is a substantial contribution to restore the water balance of the cycle.

Primary aim of the clarification is to separate red mud from aluminate liquor. Red mud discharge for dumping should be made with least losses on solubles /caustic soda and alumina/, achieved by counter-current decantation. The heat content of the last stage underflow discharged to the mud dump constitutes a significant waste heat item of the plant.

The radiation loss caused by free cooling of the aluminate liquor during the time of precipitation constitutes the



most significant part of the total radiation loss of the cycle. Every modification in precipitation technology resulting improved liquor productivity will reduce the unit volume of aluminate liquor and its heat capacity as well. The unit rate of hydrate wash water should be kept as low as possible because it helps to reduce evaporation load.

#### 0.8 EVAPORATION

Live steam consumption in the evaporators is proportional to the amount of water to be removed from the liquor cycle.

Co-current and counter-current evaporation stations, furthermore flash evaporators and thermo-compression are discussed in details.

The reject heat loss to the hot well /which can be one of the highest in the cycle process/ will be proportional to the total water evaporated.

The heat loss to the hot well cannot be eliminated as long as there is a need for special evaporation to restore the water balance in the cycle.

Heat consumptions of digestion and evaporation may substitute each other to some extent because evaporation reduces liquor quantity required in the digestion section and thereby cuts heat consumption of the digesters.

#### 0.9 CALCINATION

In an alumina hydrate calciner plant, high temperature flue gas is generated by the chemical reaction of fuel combustion.

It is worth to consider co-generation of electricity and heat, because this concept holds a significant potential to conserve primary energy.

The primary heat equivalent of electricity generated by condensing turbines is around 12 MJ/kWh, which involves the losses of both the boiler and the condenser. In contrary, back pressure generated electricity needs a primary heat of about 6MJ/kWh. The overall primary energy needed for power generation can be decreased importantly /up to 20-30 %/ by the gradual increase of the back-pressure portion related to the condensing turbines' generated portion.

#### RECOMMENDATIONS

This study serves as a guide to determine and analyse the energy balance of a Bayer alumina plant and its different process stages. The theoretical background of the calculations and the numerical examples presented on the important energy consuming operations can be adapted to other selected plant conditions as well.

All topics of the technical-technological trends of development of the alumina production are focused on energy correlations, too.

Consequently, it is recommended to use the present study as a manual for "energy planning at plant level" of alumina refineries.

The authors hope that this work will help to select most economic ways /technological improvements and energy-saving modifications, completion or substitution of equipment/

to realize energy conservation programmes.

The present study can be treated as a part of UNIDO's comprehensive training programme in industrial energy management, preferably for training of operating personnel at the enterprise level.

## INTRODUCTION

The main task of UNIDO is to accelerate the industrialization of the developing countries as a contribution to their social and economic welfare.

anel

In general UNIDO carries out energy - related activities, but this field became particularly important after the "oil crisis" of 1973-1974. It is necessary to examine the energy/industry interdependence and the energy implications of the target set at the Second UNIDO General Conference on Industrialization held in Lima, Peru in 1975. The Lima target states that developing countries should produce 25 per cent of world industrial output by 2000. It follows that in terms of energy developing countries must increase their output from 1700 Mtoe/yr in 1980 to about 6500 Mtoe/yr in 2000 /from about 34 Mboe/d to about 130 Mboe/d./. So an "energy gap" of about 4800 Mtoe/yr /or some 96 Mboe/d/ would exist between today and 2000. It is reasonable that about one half of the "Lima energy gap" /some 2400 Mtoe/yr should come from NRSE /New Renewable Sources of Energy/, mainly hydropower and biomass, the other half: from petroleum, natural gas and coal. /"Energy Development and Industrialization", UNIDO/OED. 135. 1982./

Industrial activity is directly or indirectly responsible for the use of about 85 % of the total energy consumed in the world. Aluminium industry belongs to the energy intensive industrial sectors.

The following basic questions or issues are to be considered when analyzing energy/industry interdependence:

- No. 1. Which energy sources have now or may have in the future a significant potential for use in industrial production?

- No. 2. Which sectors, sub-sectors, branches or types of industries can be effectively developed on the basis of available energy resources?
- No. 3. What types of capital goods and industrial engineering services will be required to meet the needs of the energy sector of the developing countries?
- No. 4. Which "energy processing" industries can and should be established to process primary fuels and special raw materials into higher grade or new fuels?
- No. 5. What can be done, in terms of "energy management" to expand the application and to increase the efficiency and effectiveness of energy use in industrial systems, plants, processes and products?

The five questions or issues raised above can be translated into the three main aspects and goals indicated below, which can be concisely identified as: "energy for industry", "industry for energy", and "industrial energy management".

1. "Energy for industry" has to do with the development of industrialization patterns appropriate to and consistent with the local patterns of energy availability; it includes development or adaptation of energy-efficient and/or energy appropriate processes and products, it will necessarily include non-conventional processes and products and it also comprises full use of comparative advantages, such as the use of abundant and cheap hydropower for production of aluminium.
2. "Industry for energy" is concerned with industry as a supplier of inputs and services to the energy sector. The

two main types of activities include the production of equipment and special materials for the energy sector /energy resource development and utilization/ and the industrial processing of fuels /"energy processing industry"/.

3. "Industrial energy management" is concerned with the creation of the capability to plan effectively energy production and use, from national level to plant level, in order to ensure maximum self-reliance and efficiency of the local industry in so far as the energy input is concerned.

The energy resources of developing countries are vast and diversified and they are by far more than adequate to ensure the energy inputs required for implementation of the Lima target. The good management required to ensure the transformation of "potential" into "reality" is the critical factor.

The industrial energy management consists of three main areas as follows:

a/ National industrial energy planning expresses the direct and inextricable connection and harmonizing between the national energy planning and industrial planning. For developing countries it is necessary to utilize effectively and to the maximum extent possible the locally available energy resources and this leads in many cases to the intensive use of NRSE.

b/ Energy planning at plant level means to consider and manage the optimization, improvement and control of plant energy balances with special attention to: energy substitution, for lower costs and/or to save foreign currency; "conservation" or savings through increasing energy -

efficiency of processes and equipment, with close energy - monitoring and auditing /energy "accounting"/: preventive maintenance of energy producing equipment and accessories; recovery of waste heat; diversification of sources /to ensure supply/; optimization of operating schedules /to take maximum advantage of "peak and trough" in supply, demand and costs/; etc. usually, it is possible to attain 20 % saving on energy consumed in industry. The first 10 % is normally achieved by simple changes and only the next 10 % requires some investment through changes in processes and equipment.

c/ Energy management: the "MEANS" Industrial energy management must consider, analyse, plan and program actions related to the "MEANS" required, in developing countries, to enable the successful expeditions and effective implementation of the concurrent goals of energy development and utilization as well as those of industrialization. It is necessary to plan and implement actions to ensure "human-ware" and "soft ware" resources needed.

These MEANS include:

- scientific and technological development
- education and training
- adequate financial machinery
- legislative, fiscal and promotional framework.

To reach the Lima target it will be an imperative to train or recycle planners, managers and operators at all levels. The education and training include regular courses, specialized training and "re-cycling programmes".

Recognizing the vital link between energy and industrial development, UNIDO has embarked upon an extensive programme of assistance to the developing countries in the field of industrial planning and management - and in the training of industrial personnel in appropriate principles and techniques.

The UNIDO's "Energy Management" integrated modular training system consists of three training sections /7 modules/ based one upon the other, as follows:

- |                                      |  |
|--------------------------------------|--|
| Section I:<br>Fundamentals           | 1. Fundamentals of thermodynamics<br>2. Fundamentals of combustion engineering<br>3. Fundamentals of electricity<br>4. Fundamentals of control engineering |
| Section II:<br>General aspects       | 5. Rational energy supply<br>6. Rational energy use  |
| Section III:<br>Specific application | 7. Power economy in various industries<br>/E.g. Iron and steel<br>Glass<br>Cement<br><u>Aluminium</u>  |

The main task of the training is to contribute to an actual energy saving as soon and as quickly as possible.

The subjects of modules 1 to 4 are only obligatory for participants who do not have the necessary training background. Modules 5 and 6 form the core of the modular system. All participants are required to attend the lectures held on the subject of these two modules, regardless of their knowledge level and of the industry in which they work. The



subjects of module 7 are intended for participants from specific branches of industry.

The present study is part of UNIDO's comprehensive training programme in industrial energy management, which includes inter alia training of operating personnel at the enterprise level /where the savings ultimately must be realized/.

The authors of this study considered the above mentioned points of view of UNIDO's policy options and training recommendations as far as possible.

The general trends of the development of the world aluminium industry, the raw and auxiliary materials related questions of the bauxite processing and the main directions of the technical development in alumina production, all topics focused on energy correlations, are discussed in the first part of this study. The second part contains the detailed analysis of the energy balance of a Bayer alumina plant , discussing the different process stages and completed by the theoretical background and numerical examples of the important energy consuming operations.

## 1. Expected development of the world aluminium industry

### 1.1 Expected rate of growth

The aluminium industry's typical features are high energy consumption and high investment requirement. The times of inexpensive raw material and low energy prices are over. The trend of the world's primary aluminium production up to the midsixties was exponential /Fig.1./: the growth rate exceeded 10 per cent annually, whereas at present a linear growth rate is experienced, and a 5 per cent annual growth rate can be expected in the next 10-15 years. Forecasts for the expected aluminium production at the turn of the century have some uncertainties: 30-36 million tons, and the maximum is estimated to be 43-53 million tons /1/.

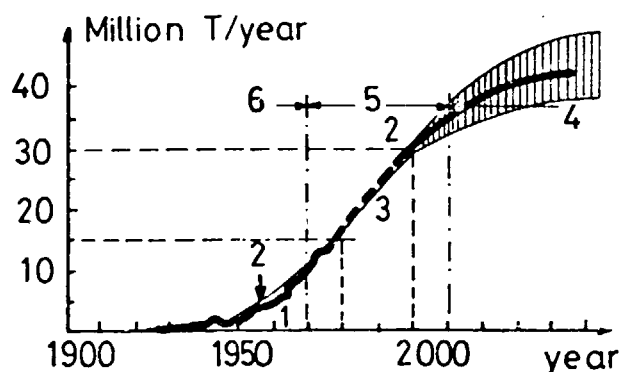


Fig.1. The expected primary aluminium production of the world in 2000. /after Kapolyi, Ref 1/.

1 - production, 2 - fitted curve, 3 - extrapolated curve, 4 - unsaturated, 5 - linear increase, 6 - exponential increase

According to Fitzgerald and Pollio /2/ the demand for finished aluminium goods will rise by about 4-5 % per annum over the next 20 years from around 18 million tons in 1980 to 38 million tons in 2000.

The geographic distribution of production in 1980. is summarized in Table 1. /2/

Table 1. Geographic Distribution of Production, 1980.  
/percentages of world total, /after Fitzgerald and Pollio, Ref. 2./

Area	Bauxite	Alumina	Primary Aluminium
Europe /ind USSR/	20.9	32.6	44.2
Africa	14.0	2.0	2.2
North America	2.4	23.3	36.6
South America	26.1	12.8	2.5
Asia	5.8	7.6	11.7
Australia, Oceania	30.8	21.7	2.8

Demand forecasts for aluminium inputs are given in Table. 2. /2/

Table 2. Demand Forecasts for Aluminium Inputs /million metric tons/ /after Fitzgerald and Pollio, Ref. 2./

	1980. /estimation/	2000. /forecast/
Primary aluminium	16.5	30.5
Secondary aluminium	2.5	7.5
Alumina	34.0	68.0
Bauxite	91.5	187.0

Major trends to note in the aluminium industry are the transfer of alumina production from the developed countries to the bauxite producers, the shift of smelting capacity to low-cost energy sources, particularly to hydropower, and growing significance of Australia and Brazil in the world aluminium market.

The required capacity additions and their estimated capital costs are given in Table 3. /2/ where capital cost data are expressed in billions of 1980 dollars; aluminium demand is forecast to grow at 4.0 % per annum 1980-1985 , 4.5 % 1986-1990 and 5.0 % 1991-2000. Replacement capacity is forecast as 1 % of 1980 installed capacity per year. Scrap production is forecast to rise from 16 % of final demand in 1980 to 20 % in 2000.

Table 3. Capacity and Investment Predictions for Aluminium  
/after Fitzgerald and Pollio, Ref. 2./

	Capacity Additions 1980-1985 million tons	Capital cost billion of 1980 USD	Capacity Additions 1986-2000 million tons	Capital cost billion of 1980 USD
Primary aluminium	4.5	14.0	13.0	40.0
Secondary aluminium	1.0	1.5	5.0	6.5
Alumina	9.5	9.0	27.0	25.0
Bauxite	19.5		73.5	
Total capital expenditure		24.5		71.5

Although the world aluminium production in 1982 reached only 14.200 thousands of short tons lagging behind the capacity of 19.600 tons as can be seen in Table 4. /3/, however, recently both the primary aluminium production and the metal price are increasing already. The secondary production, particularly from old scrap has continued to increase and this tendency will remain unchanged in the next decade. /4/

Table 4. World Aluminium Production and Capacity, 1982.  
thousands of short tons /by K.J. Brondyke,  
Ref. 3./

	Production 1982. /estimate/	Year-end Capacity 1982. /estimate/
United States	3.600	5.480
Canada	1.190	1.360
France	420	490
German Fed. Rep.	780	830
Japan	400	1.180
Norway	700	880
China /Peoples Rep.	Unavail	363
Spain	400	440
United Kingdom	250	310
USSR	2.100	2.400
Other	4.360	5.837
World total	14.200	19.600

According to the present status of the alternative processes /5, 6/ the realization of these technologies can not be expected worldwide on plant scale until 2000. A special difficulty is that "while alternative routes such as the ALCOA- $\text{AlCl}_3$ -Smelting Process, show distinct potential for reducing electrical energy requirements, they offer little chance of reducing overall energy requirements. Furthermore, because of more stringent purity requirements, any gains made may be at the expense of production costs" states K. Grjotheim and B. Welch /6/.

### 1.2 The energy demand of aluminium production

The aluminium production is one of the most energy intensive technologies. The production chain basically consists of the Bayer process and the Hall-Héroult electrolysis. An average of 2.4 tons of bauxite is required to produce 1 ton of alumina and 1.93 ton alumina to produce 1 ton of aluminium.

The total energy requirement of the aluminium production is summarized in Table 5, adopted from the paper of T. Balabanov /7/. Considering average efficiency of thermal power stations /about 30 %/ the total energy demand of 57.78 GJ/ton will result in a primary energy consumption of 193 GJ/ton for electricity.

Table 5. Energy cost per ton of aluminium /all energy units in GJ/ /by T. Balabanov, Ref. 7./

A/ Bauxite to Alumina Production		
Process	Electrical Energy	Fuel Energy /thermal/
Bauxite mining and preparation	0.09	4.2
Bauxite grinding	1.09	-
Bauxite transportation	-	3.1
Lime preparation from limestone	0.08	-
Digestion and steam generation		26.3
Alumina calcination /direct heat/		8.4
Evaporation, pumping, etc.		3.7
Total	1.98	45.7

B/ Alumina - to - Aluminium Production		
Process	Electrical energy	Fuel Energy /thermal/
Hall-Héroult electrolysis	55.8	
Auxiliary use		13.0
Anode baking		2.8
Catode manufacture		1.05
Reheat and holding furnace		8.4
Casting		5.3
Total	55.8	30.55
A+B:	57.78	76.25

According to the calculations of Bielfeldt and Winkhaus /8/ the absolutely lowest energy consumption for alumina plants processing boehmitic or diasporic bauxite should be 7.9 GJ/t  $Al_2O_3$  for the Bayer cycle, power generation and hydroxide calcination. Many plants use 16-24 GJ today. This latter value has been taken into account when calculating the figures of Table 5. /1.93 t alumina / t aluminium/.

Cochran /9/ discussed the energy balance of aluminium from production to application on the example of material and energy flow diagram valid for U.S. production of aluminium cans. Energy savings in end uses are also demonstrated in this paper.

Russel, A.S. /10/ reported already about some good results achieved in energy savings during the last years. The overall energy consumption for primary aluminium production has been decreased between 1972 and 1981 by 8 % in USA /in the field of bauxite mining and shipping 13 %, in alumina processing and shipping 14 %, in Hall-Héroult smelting 6 %



saving was realized/.

The energy decrease in aluminium cans reached 45 % in the same period in the USA with the following distribution: primary metal 5 %, fabrication 9 %, recycling 24 %, container weight 7 % /10/.

In summary it can be concluded that the aluminium industry has quite favourable perspectives and the demand is expected to expand at a more rapid rate than for other basic metals /2/.

### 1.3 Potential of the developing countries

Developing countries have abundant bauxite resources and 95 % of the lowest processing cost category reserves are found in Jamaica, Guinea, Australia, Surinam and Greece. Brasil and Guinea are also very rich in such kinds of bauxite. The aim to build up own processing facilities in developing countries seems to be justified.

The world primary aluminium producing capacity by type of power is presented in Fig. 2.

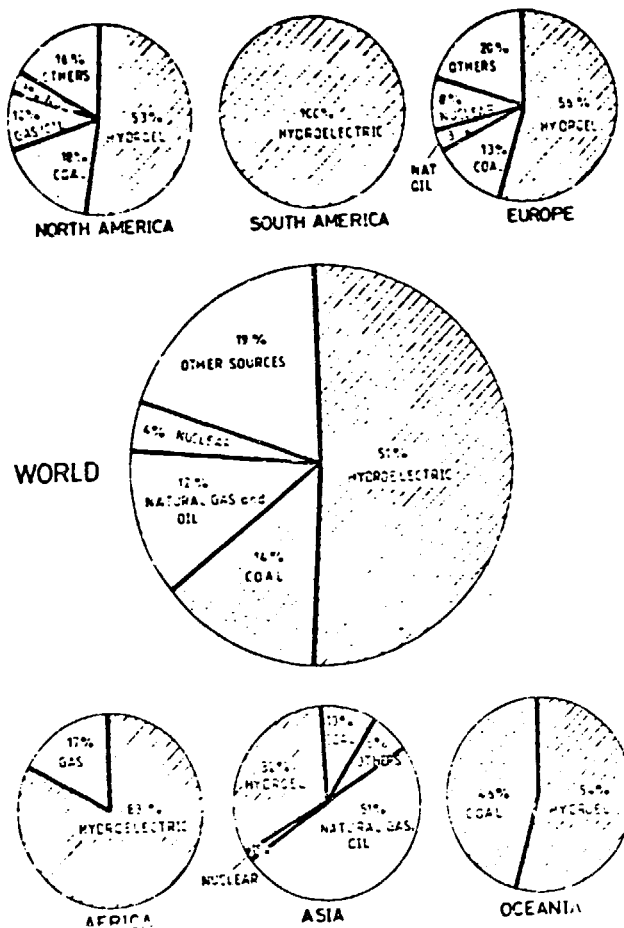


Fig. 2. The world primary aluminium producing capacity by type of power /after Laue, H.J. Ref. 11/

The diagram indicates that more than 50 per cent of energy consumption by the world's aluminium industry is based on hydropower. This trend will become even more dominant in the future. New aluminium smelters will be based in the future on hydroelectric power stations.

iner

y  
ed  
s

ite.  
ng

Hydropower /hydroelectric power generation/ constitutes an extraordinary energy option for developing countries in view of the fact that their potential is of the order of 1.500-2.000 MKW of installed capacity /all developing countries, including centrally planned Asia/. This potential is widely distributed in developing countries and could generate up to 8.600 billion kWh/yr. This energy would be equivalent to 2.800 Mtoe/yr or to 50 Mboe/d in terms of "effective energy".

One can expect an increased share /possibly a major share/ of developing countries in certain energy intensive industries taking advantage of low cost electricity from large hydropower facilities or from thermal generation with use of cheap local fissile or mineral fuels such as flared gas, natural gas, uranium, etc. Correspondingly the aluminium industry is already being shifted to favourable locations in developing countries, a world wide restructuring of this industry has already started.

The total and per capita energy consumption of the industrialized and developing countries between 1981 and 2000 /Fig. 3. source: see ref 11./ shows that the rate of growth is required to be much higher for developing countries than for the developed ones.

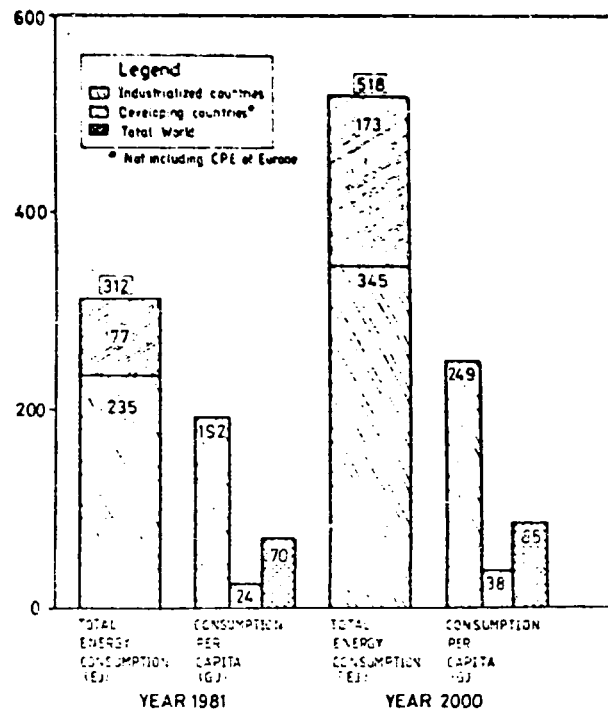


Fig. 3. The total and per capita energy consumption of the industrialized and developing countries between 1981 and 2000

According to the Lima target developing countries should produce 25 per cent of world industrial output in 2000. To realize this aim it is necessary to increase the energy input of the developing countries from 1700 Mtoe/yr in 1980 to about 6500 Mtoe/yr in 2000. This difference /4800 Mtoe/yr/ is called "Lima energy gap." It is reasonable to generate one half of the Lima energy gap /2400 Mto/yr/ from NRSE /new and renewable sources of energy, mainly hydropower and biomass/. The other half from petroleum, natural gas and coal.

This availability of the relatively cheap energy in developing countries will accelerate the development of aluminium industry, the setting up of new alumina refineries and aluminium smelters in these areas.

## 2. World bauxite resources and energetic aspects of their utilization

### 2.1 World bauxite resources

The explored bauxite deposits of the world are increasing faster than the rate of growth of production, however, the distribution of the significant bauxite deposits is not homogenous, their geographical allocation does not match the distribution of the energy-carrier reserves /1/. The specific costs of the ore can be increased significantly as a consequence of the poor infrastructure and the long transportation distance.

The classification system for the world's bauxite resources according to Lotze /13/ is shown in Table 6.

The bauxite resources identified world wide are estimated to be approx. 50 billion metric tons. Their classification by Lotze is given in Table 7. /14/.

ping  
ni-

Table 6. Classification system for bauxite resources  
/after J. Lotze, Ref. 13./

R e s o u r c e s			
Developed		Undeveloped	
Mineable Reserves	Potential Ores	Reserves	Potential Ores
<u>Definitions:</u>			
<u>Resources:</u> Concentration of bauxite in or on the Earth's crust in such form that economic exploration is currently or potentially feasible. Resources = Reserves + Potential Ores.			
<u>Developed Resources:</u> Bauxite deposits/areas currently under exploitation.			
<u>Undeveloped Resources:</u> Known bauxite deposits/areas of bauxite, from which an economical exploitation can be expected in future.			
<u>Reserves:</u> That portion of resources from which bauxite is currently economically exploited under existing conditions, including cost, quality, geologic evidence and technology /category: Mineable Reserves of Developed Resources/ or economical exploitation will be expected in future /category: Reserves of Undeveloped Resources/.			
<u>Potential Ores:</u> That portion of resources in the continuity of known deposits which are insufficiently explored at this time and for which quantitative estimates are based largely on broad knowledge /category: Potential Ores of Developed Resources/ or that portion of subeconomic resources which may become reserves as a result of changes in economic conditions or after further exploration /category: Potential Ores of Undeveloped Resources/.			

Table 7. World bauxite resources, classified according to their state of development /after Lotze, J. Ref. 14./

Country/continent	Identified Resources					Undiscovered resources	
	Developed		Undeveloped		Total	Hypothetical	
	Mineable reserves	Potential ores	Reserves	Potential ores		Speculative	
Australia	1,215	2,175	1,030	1,980	6,400	> 50,000 1 50,000	
Guinea	1,210	250	3,345	13,990	18,795		
Cameroon	-	-	680	1,320	2,000		
other Africa	50	-	720	1,885	2,655		
Africa	1,260	250	4,745	17,195	23,450		
Brazil	620	-	850	3,030	4,500		
Jamaica	1,800	-	-	600	2,400		
Surinam	200	-	200	1,570	1,970		
Guyana	90	250	-	820	1,160		
other America	65	5	295	2,325	2,690		
America	2,775	255	1,345	8,345	12,720		
India	50	-	1,070	1,495	2,615		
Indonesia	40	40	500	500	1,080		
other Asia	35	5	160	790	990		
Asia	125	45	1,730	2,785	4,685		
Europe	805	345	-	325	1,475		
Western World	6,180	3,070	8,850	30,630	48,730		
State trade countr.			not classified		1,960		
World Total					50,690		> 50,000

The identified world bauxite reserves increased from 8 billion tons to about 50 billion tons during the last 10 years. On the other hand the yearly bauxite production is approaching 100 million tons per year only. Consequently, the development of the alumina production will not be restricted by any shortage of bauxite raw material.

The commercial value of a bauxite can be determined on the basis of the costs required for the processing /15, 16/. Analyzing the bauxite quality related processing costs the value of bauxite is basically determined by the costs of replacing the caustic soda losses and by the amount of dry bauxite to be processed /15/

$$V_B = \frac{C - C_{Na_2O}}{Q_B}$$

where  $V_B$  is the commercial value of the bauxite

$C_{Na_2O}$  is the cost of replacing the  $Na_2O$  losses for 1 t of alumina produced and

$Q_B$  is the quantity of bauxite consumed, t/t alumina

The bauxite contaminants can also influence considerably the real value of a bauxite /17/.

## 2.2 Energy consumption in bauxite production

The main steps of the bauxite mining activity are demonstrated in Fig. 4.

State Trade Council.  
World Total  
50,690  
> 50,000



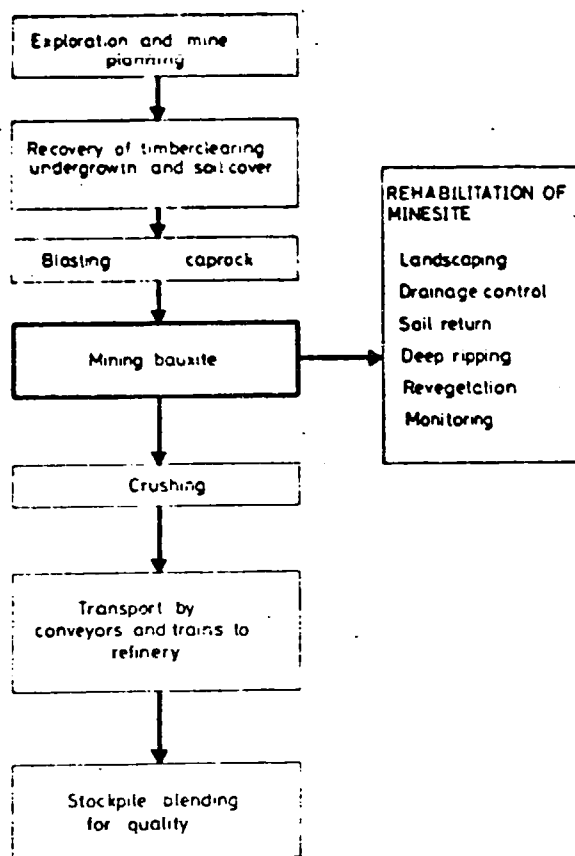


Fig. 4. Main phases of the bauxite mining from exploration to refinery's gate /after ALCOA of AUSTRALIA leaflet/

90 per cent of the world's bauxite resources are of lateritic origin and are covered only by a thin layer of soil which is to be removed and stockpiled prior to open pit mining. The thickness of the soil layer often does not exceed 1 meter. These are mostly gibbsitic type bauxites, excavated by high productivity machinery, which consume 1 or 2 per cent of the energy needed for alumina production. Open cut mining is predominant in the bauxite supply of the world. The exploited areas have to be recultivated by the formerly removed overburden after finishing the mining activity.

Table 8. Unit energy rates in MJ per ton bauxite for open cut surface mining with different cover layer volumes at an output capacity of 400 000 tpy.

Remark: Higher unit rates apply for diesel engine powered shovel loading and trucking, with hydro-electric equipment lower unit energy rates can be achieved

Unit volume of cover layer	Surface stoipping			Open pit mining			Ancilla- ries		Total MJ/t bauxite
	electr.	diesel	total	electr.	diesel	total	electri- city	coal	
0,5 m <sup>3</sup> cover layer t bauxite	-	11.7	11.7	-	18.2	18.2	0.4	0.8	31.1 /high/
	3.2	3.5	6.7	6.2	2.2	8.4	0.4	0.8	16.3 /low/
1,0 "	-	23.4	23.4	-	18.2	18.2	0.6	1.2	43.4 /high/
	6.3	7.0	13.3	6.2	2.2	8.4	0.6	1.2	23.5 /low/
2,0 "	-	47.0	47.0	-	18.2	18.2	1.0	2.0	68.2 /high/
	12.7	14.1	26.8	6.2	2.2	8.4	1.0	2.0	38.2 /low/
3,0 "	-	70.4	70.4	-	18.2	18.2	1.4	2.8	92.8 /high/
	19.0	21.1	40.1	6.2	2.2	8.4	1.4	2.8	52.7 /low/
4,0 "	-	94.0	94.0	-	18.2	18.2	1.8	3.6	117.6 /high/
	25.3	28.2	53.5	6.2	2.2	8.4	1.8	3.6	67.3 /low/
5,0 "	-	117.4	117.4	-	18.2	18.2	2.2	4.4	142.2 /high/
	31.6	35.2	66.8	6.2	2.2	8.4	2.2	4.4	81.8 /low/

Table 9. Unit energy rates in MJ per ton bauxite for underground mining in 200 metres depth and an output capacity of 500 000 tpy.

Remark: High unit rates can be reduced to low ones by substituting compressed air and diesel engine driven drilling and shovel loading with hydro-electric equipment

Water Load /m <sup>3</sup> /min/	Electrical Energy			Diesel Oil Fuel Electricity- Oil coal				Overall Unit Consumption /M /ton bauxite/
	Compressi- on /Comp- ressors/	Transport /Conveyors/	Ventilla- tion /Fans/	Drainage /Pumps/	Main- tenance /Repair Shop/	Loading- Trucking	Heat supply	
1	21.1	18.0	12.7	3.3	10.0	34.0	38.0	137.1 /high/
	7.0	17.0	11.6	3.3	23.5	20.0	40.0	122.4 /low/
10	21.1	18.0	12.7	33.0	10.0	34.0	38.0	166.8 /high/
	7.0	17.0	11.6	33.0	23.5	20.0	40.0	152.1 /low/
80	21.1	18.0	12.7	198.0	10.0	34.0	38.0	331.8 /high/
	7.0	17.0	11.6	198.0	23.5	20.0	40.0	317.1 /low/
300	21.1	18.0	12.7	990.0	10.0	34.0	38.0	1123.8 /high/
	7.0	17.0	11.6	990.0	23.5	20.0	40.0	1103.1 /low/

### 2.3 Utilization of the bauxite reserves

To utilize bauxite deposits infrastructure and transportation facilities, like road, ropeline, railway, seaport are to be installed. Infrastructure is necessary in the case of the local processing, too. Therefore high quality bauxite deposits with developed infrastructure are especially preferred for bauxite mining and processing.

The bauxite cost fob consists of the following elements /and their summarized energy input/: prospecting, exploration, mining, pretreatment, domestic transportation, loading /harbour/, social sector, fiscal burden.

Bauxite cost cif alumina refinery /e.g. in USA or Europe/ includes the costs of shipment, unloading and inland transportation, supplementarily.

Bauxite shipment from Australia to Europe needs about 67 kg fuel oil per ton of bauxite /154 kg fuel oil/t alumina/. Inland transport for a distance of 500 km requires further 40.5 kg Diesel oil. The energy consumption of the transportation can be equal to the total energy consumption of the most up-to-date refinery /approximately 8 GJ/t alumina/.

Consequently, although the existing alumina plants in industrialized countries need imported bauxite from the developing countries even in the future and the higher level of the bauxite price can be used for the accelerated industrialization /including aluminium industry/ of the bauxite producer developing countries, it is clear that alumina plants will be located most frequently in close proximity of mining areas.

Bauxite testing laboratories have an important role in the economic utilization of the resources /19/.

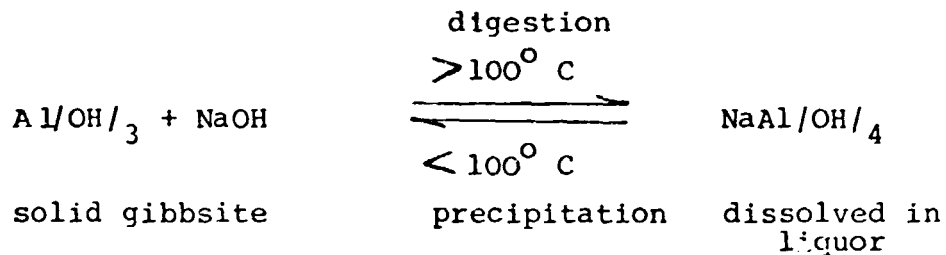
### 3. Main Trends of the Technical Development of the Bayer Process

#### 3.1 Characteristics of the Process

At present more than 90 % of the world's alumina is produced by the Bayer process, providing a high purity final product.

Alumina production is a beneficiation /refining/ process separating the  $Al_2O_3$  content of bauxite from the other accompanying oxides. This alumina is suitable for electrolysis in a cryolite melt.

The industrial practice of the Bayer technology is based on the following reversible reaction



The Bayer process consists essentially of digesting the crushed and ground bauxite with strong caustic soda solution at temperatures above  $100^\circ \text{ C}$  /for gibbsitic bauxites  $100-140^\circ \text{ C}$ , for boehmitic and diasporic bauxites  $200-250^\circ \text{ C}$ /. After separation from the residue /red mud/ and cooling the dissolved alumina is seeded with crystallites of trihydrate whereupon precipitation takes place. The precipitated trihydrate is filtered and calcined at about

1200° C. Fig. 5. shows the flow-chart of processing gibbsitic bauxites. It can be seen that the Bayer process for extracting alumina from bauxite is a closed-loop process.

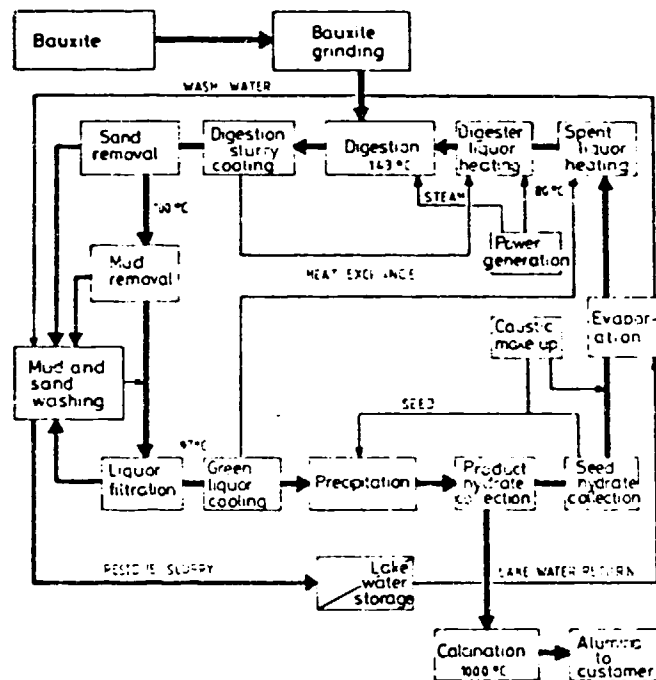
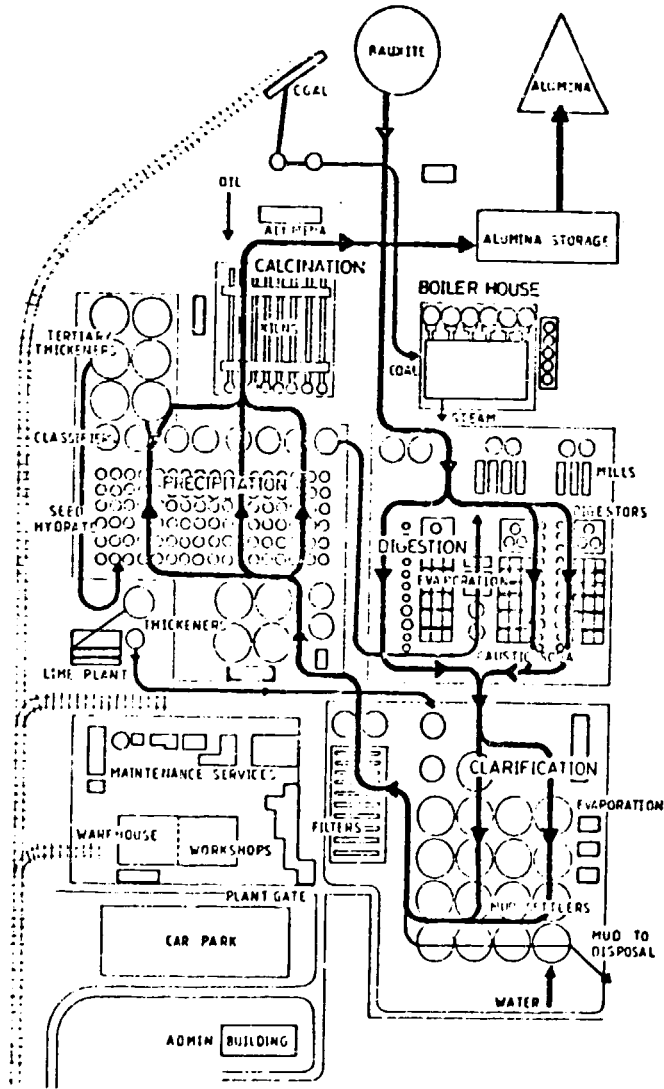


Fig. 5. Block-diagram of the Bayer process using low-temperature digestion /after ALCOA of Australia's leaflet/

The layout of the world's largest capacity alumina refinery at Gladstone, Australia /Fig. 6./ demonstrates the up-to-date replacement of a giant alumina plant applying modul system and optimizing the length of the piping-lines, and network, saving investment costs and production costs /energy!/ as well.

itic



e-

ry

Fig. 6. Layout of the Gladstone alumina plant  
/after a leaflet of Queensland Alumina/

### 3.2 Determining factors of the technical development

The trends of technical and technological development have to be determined by setting out from the increase of production. It became evident nowadays that a moderate rate, 3 to 4 % yearly increase in production can be expected. Based on this optimistic forecast the expected world alumina production and bauxite demand can be seen in Fig. 7.

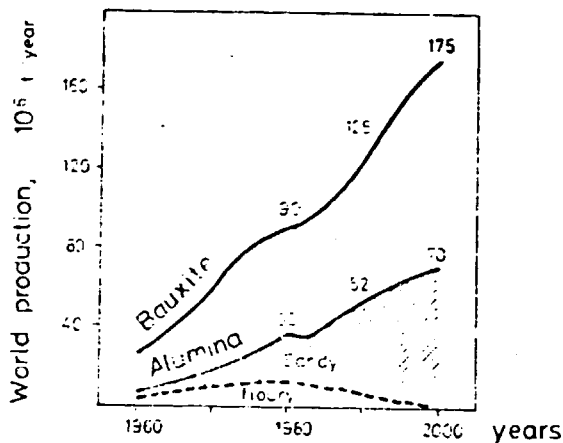


Fig. 7. Expected world production of bauxite and alumina

As far as the quality of alumina to be produced is concerned, apart from the expectable increase in demand for the chemical purity it can be established unequivocally that the production of fluorspar alumina keeps gradually diminishing. The production of sandy alumina is performed not only in the newly established plants, but switching over to this kind of product has started recently in some plants which produced previously fluorspar alumina although their position could be located on the descending branch of "lifetime". In connection



with this and in order to decrease energy consumption both in Europe and overseas it is striven commonly for the production of sandy alumina hydrate by the use of higher caustic soda concentration which condition would permit very attractive expansion of capacity of the alumina plants using "American" low caustic soda process /20/. Economic considerations seem to motivate some allowance on the expense of sandy-type granulometry and the production of a coarser intermediate alumina in the future which would still meet the requirement of metallurgy and that of the dry gas scrubbing.

Bauxite is the main raw material for the alumina production at present and its ratio to the gross raw material demand will not diminish below 85-90 % by the turn of millinary. The prospected bauxite reserves of the world come to about  $50 \cdot 10^9$  tons, the estimated resources are even larger, therefore the bauxite raw material would be at disposal to satisfy the expected growth of alumina production for a long time. Industrial scale processing of indigenous non-bauxitic raw materials in individual countries can not be expected in the near future except for nepheline and alunite due to high energy consumption and investment costs /6/.

Owing to the technological development, up-to-date alumina plants are less and less sensitive to the quality of bauxite. Mineralogical composition of some characteristic bauxite samples can be found in Table 1. It becomes evident from this that the quality of the European carstic bauxites is far more disadvantageous, their silica content is about twice as high as that of lateritic bauxites dominating world production. The comparative advantages of domestic bauxite raw material in the European countries do not show up in general due to the high costs of underground mining sometimes below the carstic water table. Thus the disadvantages resulting

from the lower-grade raw material have to be counterbalanced by the development of technology. 90-95 % of the bauxite will be most probably further on processed by the Bayer process therefore it is basically required to further develop both the procedures and equipment pertaining to the Bayer process.

The distribution of total alumina producing capacity as a function of the capacity of the individual plants corresponding to the state of 1980 and that predicted for 2000 are shown in Fig. 8.

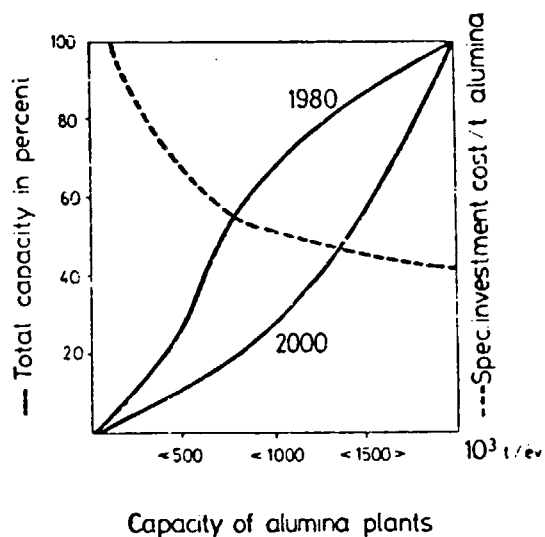


Fig. 8. Total capacity in percent and specific investment cost as a function of the plant size

The specific investment costs indicate that the smallest economic new project is a 500.000-600.000 tpy capacity unit which is established by the so-called "line capacity" i.e. the capacity of certain production trains /digester series,

set of red mud settlers and washers/. The establishment of equipment of still increasing unit capacity, the increasing of capacity of the running plants and the erection of new high-capacity alumina plants remain the trend of development. It ensues from the above mentioned that the trends of technical development of the alumina production and the economy, too, will be determined by the up-to-date, high-capacity alumina plants, whereas the smaller-capacity plants will be able to compete with them merely by a permanent modernisation of the technology.

Table 10. Mineralogical composition of some characteristic bauxites

Component in mineral, %	Australian bx	Guinean bx	Jamaican bx	Hungarian "Iszka" bx
Al <sub>2</sub> O <sub>3</sub> in Gibbsite	40.7	39.1	39.0	12.0
Boehmite	6.6	1.4	4.4	31.9
Diaspore	0.3	0.8	0.2	-
Kaolinite	4.6	2.2	0.2	5.5
Goethite	0.3	2.6	3.3	0.6
Hematite	0.1	0.2	0.2	0.2
Total	52.6	46.3	47.3	50.2
Fe <sub>2</sub> O <sub>3</sub> in Goethite	2.5	9.1	11.9	5.0
Hematite	10.8	12.1	7.9	15.2
Total	13.3	21.2	19.8	20.2
SiO <sub>2</sub> in Kaolinite	5.0	2.6	0.2	6.1
Quartz	-	-	0.4	-
Total	5.0	2.6	0.6	6.1
TiO <sub>2</sub> in Anatase	1.9	1.1	2.1	2.0
Rutile	0.7	1.2	0.5	0.6
Total	2.6	2.3	2.6	2.6
L. O. I.	24.5	25.7	26.1	19.2
CaO	0.05	0.08	0.3	0.8
MgO	0.03	0.03	0.1	0.4

Fig. 9. shows the characteristic cost estimate of the alumina production and the distribution of energy consumption for an European alumina plant.

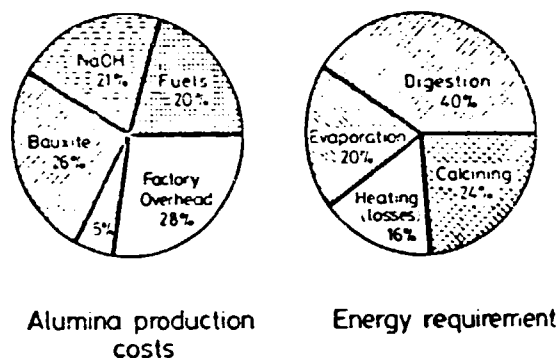


Fig. 9. Structure of production costs and energy consumption

Though the distribution of production costs of the overseas plants deviates to some extent, e.g. less costs for caustic soda due to less NaOH consumption, higher factory overhead due to interest rates, yet it is of universal validity that the cost for bauxite, energy and NaOH accounts for 50-70 % of the total production cost. The most important tasks of the technical development are therefore the following: greatest economy measures relative to the consumption of bauxite /maximum  $\text{Al}_2\text{O}_3$ -recovery/, energy /application of energy-saving technology/ and NaOH /application of methods for the regeneration of caustic soda/.

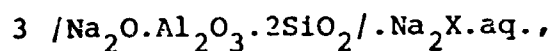
The energy structure shown in Fig. 9. is characteristic mainly for European alumina plants practicing high-temperature digestion, however, the structure is applicable to all. For the reduction of energy consumption of North-

American alumina plants producing sandy alumina and being erected before the energy crisis Donaldson /4/ pointed out the following three directions:

- retrofitting existing plants by additional or more efficient heat recovery equipment,
- converting energy supply from expensive oil or natural gas to lower cost coal,
- developing process modifications in order to reduce energy consumption.

It is obvious that the development of up-to-date energy-saving equipment is a direct method for decreasing the energy consumption at digestion, evaporation and calcination. Chin /22/ points out that it is decisively important to adjust the technology to the energy supply, where according to the analysis of Láng and Veres /23/ that circuit promises basic energy economy which demands the least heat for digestion and the greatest one for evaporation. Bielfeldt and Winkhaus /8/ consider the reduction of energy costs the most important task in alumina production in the 80'-es. In their opinion the present energy consumption of 12-14 GJ/t  $Al_2O_3$  can be reduced to about 8 GJ by suitable measures. Decisive importance is assigned to liquor efficiency. Technological development may serve the reduction of energy consumption primarily by increasing the efficiency of the circuit, adjusting technology to the nature of raw material and by optimizing the concentration conditions.

The bauxite requirement of the Bayer process is determined by the alumina yield whereas NaOH consumption basically depends on  $Na_2O$  content bound in sodium-aluminium-hydrosilicates due to the reactive silica content. The former may be characterised by the formula below:



where  $\text{X} = 2\text{OH}^-, 2\text{AlO}_2^-, \text{CO}_3^{--}, \text{SO}_4^{--}, 2\text{Cl}^-$ , etc. anions.

Certain caustic soda losses are due to the formation of sodium-titanates from the  $\text{TiO}_2$  content of bauxite.

In Fig. 10. the expected alumina recovery, bauxite consumption and NaOH consumption appearing as "bound losses" are plotted for the case of a bauxite with 50 % alumina and variable silica content.

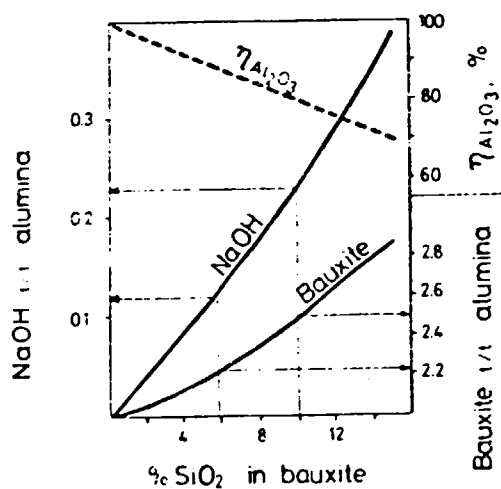


Fig. 10. Alumina yield after digestion, silica related bound NaOH losses and specific bauxite consumption as function of the  $\text{SiO}_2$  content on processing a bauxite with 50 %  $\text{Al}_2\text{O}_3$ .

Alumina recovery has been calculated from the following relation:

$$\frac{\text{Al}_2\text{O}_3 - \text{SiO}_2}{\text{Al}_2\text{O}_3} ,$$

whereas the NaOH losses have been calculated as 0.9 times the  $\text{SiO}_2$  content.

It is clear from the figure that increasing the  $\text{SiO}_2$  content from 6 % to 10 % the specific bauxite consumption increases only about 10 %, however, bound NaOH losses increase almost 100 %. When considering the fact that the prices of NaOH and alumina may be taken equal it is obvious that the applicability of the Bayer process to higher silica containing bauxites is primarily limited by the extent of NaOH consumption. At the same time the Bayer technology permits to increase alumina recovery up to the elimination of undigested losses. Further increase of alumina recovery necessitates the application of a special technology /e.g. formation of iron-containing hydrogarnets /24/ or the complex processing of red mud.

A review about the recent advances and prospects in alumina technology was published by Perry and Russel /25/.

It is clear that all of the important technical-technological developments influence the energy consumption, too. Direct effects can be achieved by upgrading the heat recovery equipment, while technological improvement affects mostly via increasing the efficiency of the circuit. Sometimes technology and equipment form a complex unity, as e.g. in tube digestion.

The wide range of possibilities to save energy by technological development will be discussed in the following sections.

### 3.3 Flowsheet modifications, optimization of the concentration

To characterize the alumina processing technology, to illustrate the changes in the sodium aluminate liquor concentrations and to demonstrate the efficiency of the process cycle the data of the Ajka plant /Hungary/ are shown in the  $\text{Na}_2\text{O}-\text{Al}_2\text{O}_3-\text{H}_2\text{O}$  system in Fig. 11. for the 1958 to 1980 period.

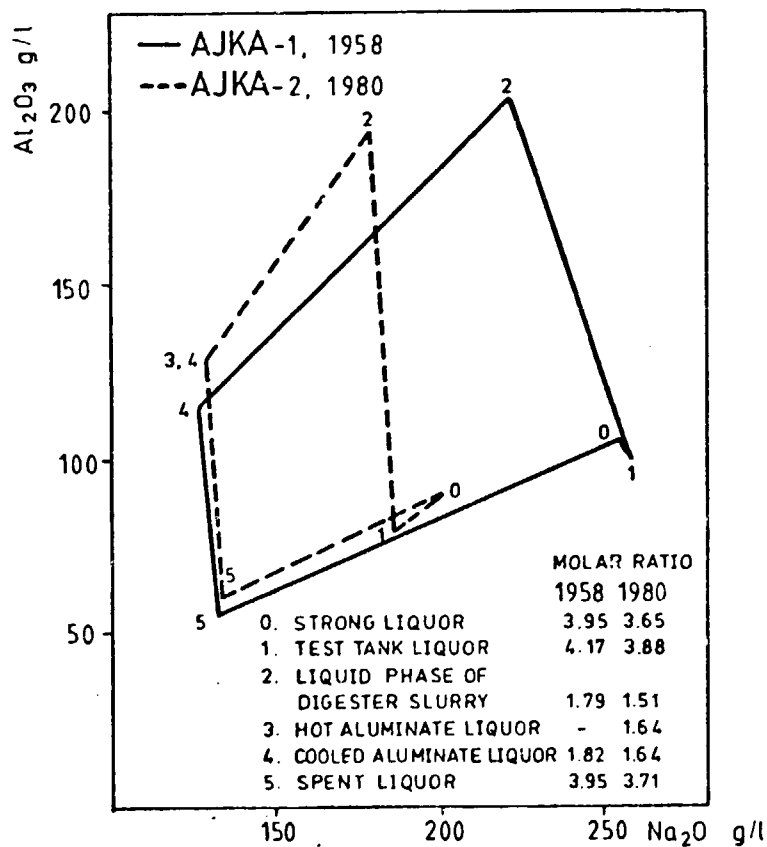


Fig. 11. Bayer cycle in the  $\text{Na}_2\text{O}-\text{Al}_2\text{O}_3-\text{H}_2\text{O}$  system for the Ajka Alumina Plant, Hungary /after Tóth, Vörös and Zámbo, Ref. 26/



The decrease of the digestion concentration and  $\text{Na}_2\text{O}$  to  $\text{Al}_2\text{O}_3$  molar ratio is striking, indicating a significant increase in the efficiency of the cycle, since essentially the same amount of  $\text{Al}_2\text{O}_3$  per cycle can be extracted by and separated from the same volume of sodium aluminate liquor with much less evaporation.

The steam energy requirements of the alumina production broken down according to the main consumption purposes, the resources for their satisfaction, the enthalpy /I/ and the temperature /T/ of the consumed steam are shown in an I-T diagram. Fig. 12. shows the heat contents of the liquor circulated and the steam consumed for producing 1 ton of alumina in Ajka in 1980 and 1959, respectively.

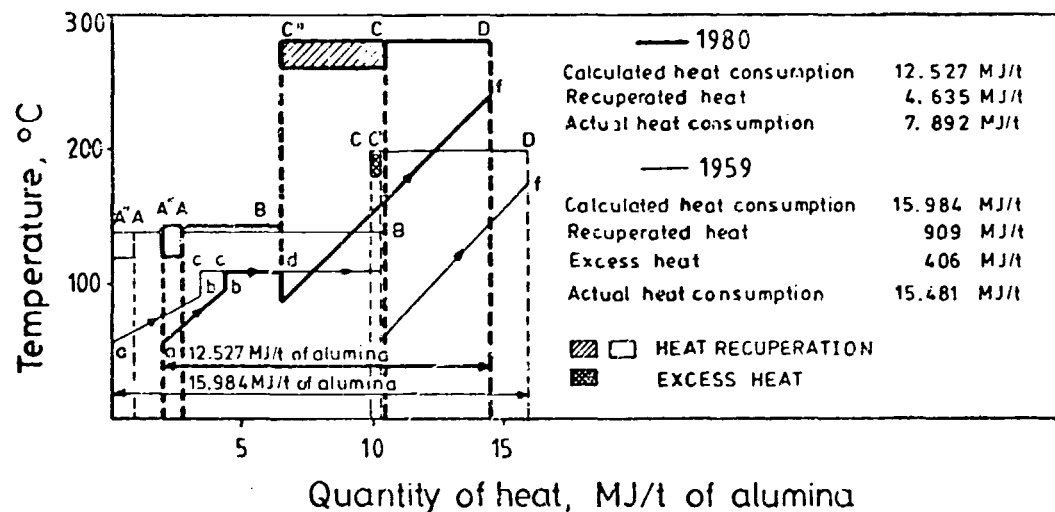


Fig. 12. I-T Diagram for the Bayer cycle of the Ajka Alumina Plant, Hungary /after Tóth, Vörös and Zámbo, Ref. 26/

Symbols applied in the said Figure:

Requirements:

- ab - heat demand of red mud wash water + slurry preheating;  
 cd - heat demand of evaporation  
 ef - heat demand of digestion

Resources:

- AB - steam consumption at low pressure  
 CD - steam consumption at high pressure  
 A"B - total calculated heat consumption at low pressure  
 C"D - total calculated heat consumption at high pressure

Heat balance

- AA' - heat balance surplus at low pressure  
 CC' - heat balance surplus at high pressure  
 A"A - heat recuperation at low pressure  
 C"C - heat recuperation at high pressure

Efficiency of heat recuperation at low pressure:

$$\frac{A"A}{A"B} \cdot 100 \quad / \omega_k /$$

Efficiency of heat recuperation at high pressure:

$$\frac{C"C}{C"D} \cdot 100 \quad / \omega_n /$$

The data characterizing the Ajka Alumina Plant in 1980 compared with those of 1959 in Fig. 12. show a significant decrease of the steam consumption of evaporation with much increase of the digestion steam demand.

### 3.4 Tube Digestion

#### 3.4.1 Development and general characteristics of the tube digestion

The tube reactor has been proposed first in 1927 by Müller and Hiller /27/ for the digestion of diasporic bauxites, however the industrial realisation has been postponed. Renewed laboratory tests have been carried out only in the 50's and 60's in Czechoslovakia, FRG and Hungary. The pioneer work of B.Lányi /28/ related to the principal possibilities and kinetics should be mentioned here. The first operating plant was built by VAW in FRG and the extremely good results were published by Bielfeldt and his coworkers in 1967-1968 /29, 30/. The temperature of digestion could be increased up to 300° C using tube-in-tube heat exchanger /tube digester/ and molten salt as a heat transfer medium.

According to the data published the rate of dissolution of  $Al_2O_3$  from bauxite was increased extraordinarily /10 times at least/ because of the turbulent stream, consequently, the required reactor volume could be decreased from 2 m<sup>3</sup>/t  $Al_2O_3$ /day to 0.1 m<sup>3</sup>/t  $Al_2O_3$ /day. By increasing the temperature the amount of flashed water can be high enough that evaporation can be omitted. Owing to the piston like stream of the slurry in a tube

digester the uneven holding time /which is always disturbing the digestion in autoclave series/ can be avoided, consequently, the undigested losses of  $\text{Al}_2\text{O}_3$  can be minimized. Increasing the digestion temperature by  $10^\circ\text{C}$  the volume of the slurry to be treated can be reduced by 5 %, what results in a cut back of energy consumption and a proportional increase in the efficiency of the circuit. Due to the higher digestion temperature the settling properties of the produced red mud improve because the minerals of the red mud are more regularly crystallized. Since the underflow concentration is higher the dissolved NaOH and alumina losses are smaller. The investment costs of a tube digester are only 60 to 80 % of an autoclave series of similar throughput. Further arguments for a tube digester are its flexibility and that it can be cleaned chemically and that the saving in energy consumption is 20 to 40 %. Introducing the tube digestion the problem of a cheap digester is reduced to the problem of a cheap heat-exchanger.

#### 3.4.2 Development and characteristics of the Hungarian tube digester

After the laboratory experiments by B. Lányi /28/ the industrial realization started in Hungary in 1966 at the Almásfüzitő Alumina Plant using plant scale heat-exchanger units. ALUTERV designed a pilot plant tube digester between 1969 and 1971 and it was installed at the Mosonmagyaróvár Alumina Plant /MOTIM/ in 1972-1973. It processed  $50-60\text{ m}^3$ /hour slurry, had been heated by steam and the maximum digestion temperature reached  $260^\circ\text{C}$ . This equipment was tested from 1974 to 1980 helping to design the final process technology and in 1980-1981 the old autoclave series could be replaced by a tube digester.

Multi-stream operation is the most important feature of the Hungarian tube digester, what means that in one tube several /at least 3/ tubes serve to heat up the slurry. This Hungarian version is patented /31/. A theoretical flow-sheet of the equipment is presented is Fig. 13.

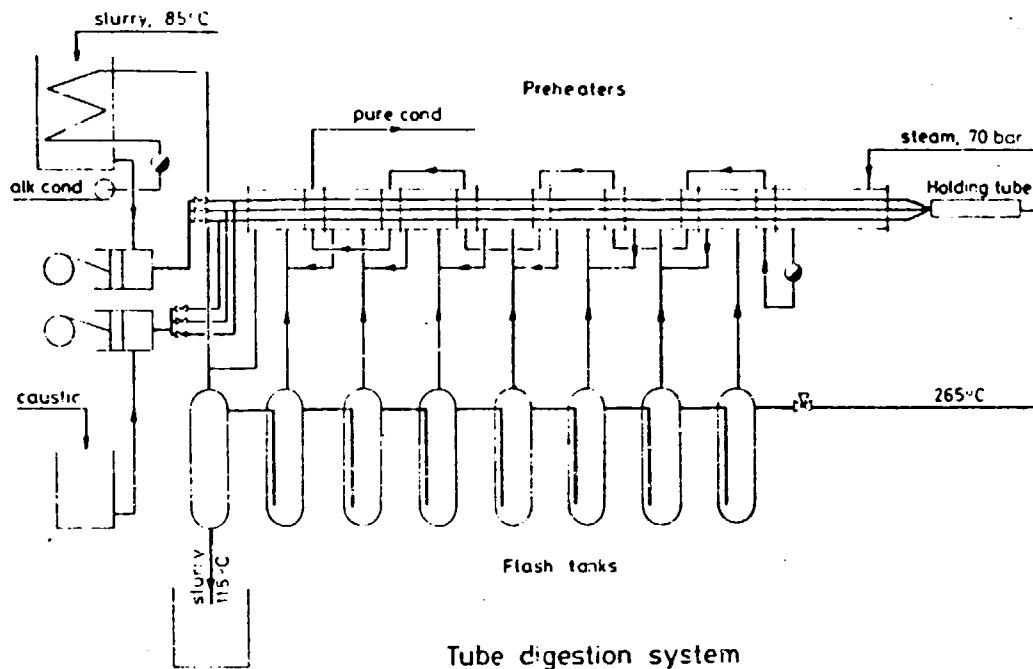


Fig. 13. Hungarian tube digester system /after Tóth, Vörös and Zámbo, Ref. 26/

It is an essential feature of this technology that the pipes can transport either digester liquor or bauxite slurry, and these flows can be interchanged cyclically, so, that the digester liquor cleans the scalings from the pipes continuously. At the final temperature of digestion the three flows join, thus the bauxite is digested by the full quantity of the liquor. This solution ensures a closer approach to the equilibrium A/C ratio which means higher

$\text{Al}_2\text{O}_3$  saturation and simultaneously the digestion of  $\text{Al}_2\text{O}_3$  minerals is more efficient, consequently the undigested losses are reduced.

### 3.4.3 Experiences from pilot plant tests

The mineralogical phase composition of the Halimba bauxite, which has been processed in the tube digester is given in Table 11.

Table 11. Typical composition of the bauxite from Halimba processed by tube digestion

$\text{Al}_2\text{O}_3$ % in gibbsite	13.1	$\text{Fe}_2\text{O}_3$ % in goethite	2.6
in boehmite	31.9	in hematite	20.3
in diaspore	0.3	Total	22.9
in kaolinite	5.0	$\text{SiO}_2$ % in kaolinite	5.9
in hematite	0.4	$\text{TiO}_2$ % /anatase+rutile/	2.7
Total	50.7	L.O.I. %	15.3

The raw material is a medium quality boehmitic-hematitic type ore. Fig. 14. shows the digestion kinetics of this boehmite expressed in  $\text{Al}_2\text{O}_3$ .

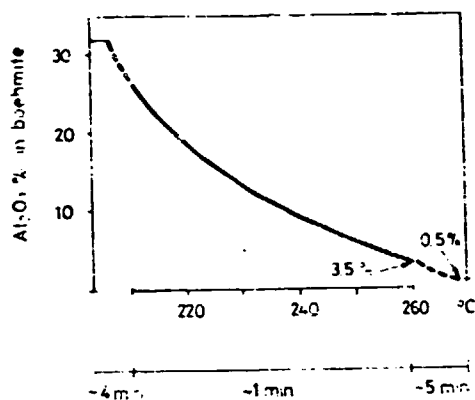


Fig. 14. Kinetics of boehmite dissolution in the Hungarian pilot tube digester.

The diagram explains that during the 5 minutes holding time between 210 and 260° C 70 % of the boehmite was dissolved in 1 minute, while 20 % at lower temperatures and only about 10 % in the dwelling pipe.

These data verify that the turbulent stream increases very much the rate of reaction.

In Fig. 15. the heat transfer coefficients of the tube digester and that of an up to date system consisting of preheaters and an autoclave line are compared.

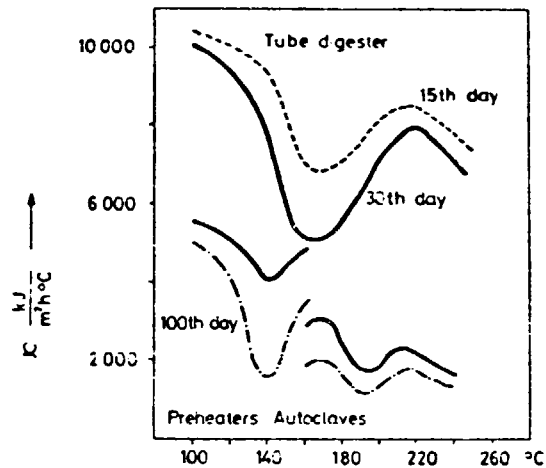


Fig. 15. Comparison of heat transfer coefficients measured in the Hungarian pilot tube digester and an up-to-date system consisting of preheaters plus autoclave line, respectively.

On the basis of this diagram it is evident that the heat transfer coefficient of the tube digester is twice as large as that of the traditional autoclaves even if the tubes are cleaned only after 30 days /by acid/. This diagram gives the reason why the energy consumption of the tube digester is 20-30 % lower than that of the autoclaves.

Also the scales were examined thoroughly, including their formation, composition and solubility. Fig. 16. gives a comparison between the  $\text{TiO}_2$  content of the scalings and the heat transfer coefficient before cleaning the tube.



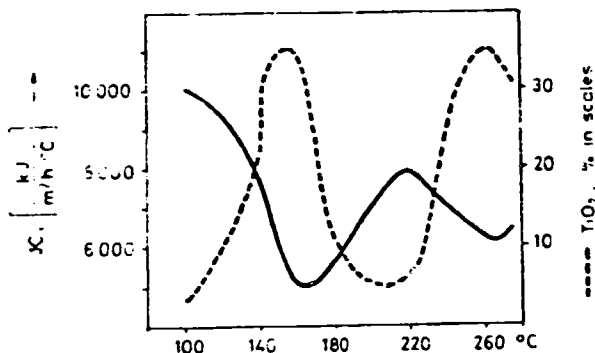


Fig. 16. Relation between the heat transfer coefficients measured in the Hungarian pilot tube digester after a cycle of 30 days and the  $TiO_2$  content of the scalings.

It can be observed that the heat transfer coefficient is inversely proportional to the  $TiO_2$  content of the scaling. It should be mentioned here, that the scales contain Ca- and Mg-titanates [33] which conduct heat very poorly and these compounds are formed at much lower temperatures [140-170° C] in a tube digester than in autoclaves. This fact proves that the turbulent stream helps to dissolve anatase and the formation of undissoluble titanates. Fig. 17. illustrates the effect of acidic treatment.

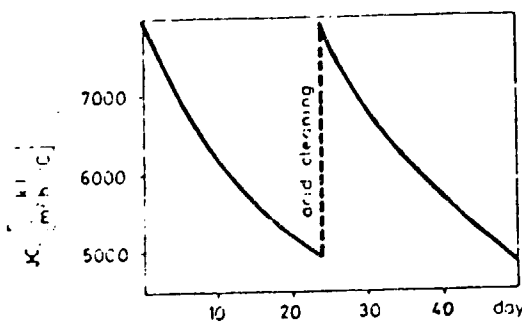


Fig. 17. Variation of the heat transfer coefficient proving the effectiveness of the acid cleaning.

As seen in this figure, cleaning by a special acid mixture occurred after each 24 days operation. A special acid mixture and an inhibitor ingredient has been established which removes the scales in 2-4 hours and the surface of the tube gets metal clean so it can be taken into operation immediately, the original heat transfer coefficient being restored.

#### 3.4.4 Construction of the Hungarian tube digester and outlooks for the future

The advantageous results of pilot plant tests were followed by the start up of the 10 t/h tube digester /also triple tube/ at MOTIM early May 1982. The digestion temperature is  $260 \pm 5^{\circ}$  C, the holding time 12 minutes, the interval heated by living steam extends about  $45^{\circ}$  C only. The start up was trouble-free and the equipment runs at the designed parameters. The predicted average steam consumption is 1.5 t/t alumina /1.38 - 1.62 t/t alumina/ at  $260^{\circ}$  C and higher digestion temperatures.

According to our opinion tube digestion will become widespread among monohydrate bauxite digesters both when new installations will be erected, and at the replacement of physically and technically worn autoclave series. The raising of the digestion temperature over  $260^{\circ}$  C is not feasible but only by the application of tube reactors where the heat transferring medium can be organic or inorganic compound. The higher temperature region opens new potentials to develop further the Bayer technology.

Recently the tube digester has been proved for processing diasporic bauxites in FRG /32/.

### 3.5 Bauxite digestion with catalytic additives

#### 3.5.1 Catalyzers and their effects

Beside tube digestion there is an other successful invention, namely the application of catalytic additives. This had been proved also on industrial scale. The process helps to realize the hydrothermal transformation of goethite into hematite in the 220 to 250° C temperature range of digestion applied at present. The worldwide patented processes /34/ of the Hungarian Aluminium Corporation apply CaO and different anions /Cl<sup>-</sup>, SO<sub>4</sub><sup>-</sup>/ or CaO and different cations /Mn<sup>++</sup>, Fe<sup>++</sup>/ or iron-containing hydrogarnet:

$A_3B_2/SiO_4/_{3-x}[/OH/_4]_x$ , where A=Ca<sup>++</sup> and/or Mg<sup>++</sup> and/or Mn<sup>++</sup> and/or Fe<sup>++</sup>; B = Al<sup>+++</sup> and/or Fe<sup>++</sup>;  
as additives to catalyze the process.

The typical technological parameters and the success of this process were discussed in earlier publications /35, 36, 37/. The benefits of catalyzing additives over pure CaO additive are the following: the transformation of goethite into hematite occurs much faster, at about 20 to 30° C lower temperature and about 20-30 % lower CaO addition and even in the case of the most stable goethite it can be achieved reliably at not higher than 240° C using the existing autoclave lines. The application of iron-hydrogarnet catalyzer was proven to be the most economical solution, consequently, it has been introduced in the Hungarian alumina plants. The preparation and dosage of the catalyzer is a know how of the Hungarian Aluminium Corporation.

### 3.5.2 Typical results of catalyzed digestion in Hungarian alumina plants

The catalyzed digestion technology has been applied since 1979 in the Ajka Plant and since 1980 in the Almásfüzitő Plant. The technological and economic benefits are considerable.

Fig. 18. shows the increase in recovery /2.5 %/ and in A/C ratio attained by catalyzed digestion for a Hungarian goethitic bauxite.

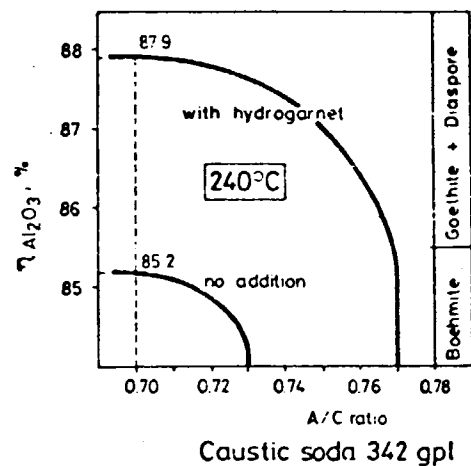


Fig. 18. Digestion of Hungarian goethitic bauxite without and with additive.

In this instance 6 to 10 % higher amount of Al<sub>2</sub>O<sub>3</sub> can be dissolved by a unit volume of liquor and this brings improvement in the circuit efficiency and reduces the steam consumption of the digestion proportionally. It is evident that the application of the hydrogarnet catalyzer reduces the bound NaOH losses similarly as does the CaO addition, but with a lower CaO consumption, because by the incorpora-

tion of  $\text{Fe}^{+++}$  into the hydrogarnet structure, its  $\text{SiO}_2$  content increases and its  $\text{Al}_2\text{O}_3$  content decreases.

A considerable improvement can be observed in separability, filterability and settling capacity of red mud. This improvement is considerable even if the bauxite contains very little amount of goethite. As a consequence of the introduction of catalyzed digestion at the Ajka and Almásfüzitő Alumina Plants fine dispersed iron minerals, chiefly goethite and some hematite, were recrystallized and the  $\text{Fe}_2\text{O}_3$  content of the aluminate liquor sank to 10 to 15 mg/l without control filtration - as it is shown in Fig. 19. - and as a result of that the  $\text{Fe}_2\text{O}_3$  content of the alumina produced is constantly below 0.03 %.

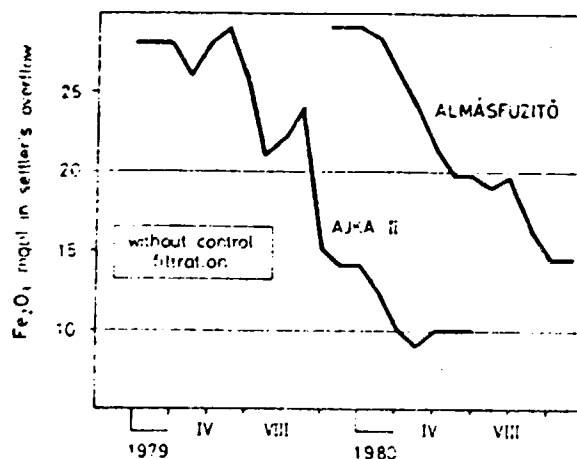


Fig. 19. Decrease of  $\text{Fe}_2\text{O}_3$  content in the aluminate liquor /without control filtration/ after introducing digestion with additives into the production of Hungarian alumina plants.

The increase of solid content in the underflow of the red mud washers allows to increase their capacity and reduce the dissolved caustic soda and alumina losses by 50 %. At the Almásfüzitő Alumina Plant 10 kg/t alumina savings could be attained out of soluble NaOH losses.

Fig. 20. illustrates the increase of the solid content in the underflow of the last washer after the introduction of catalyzed digestion.

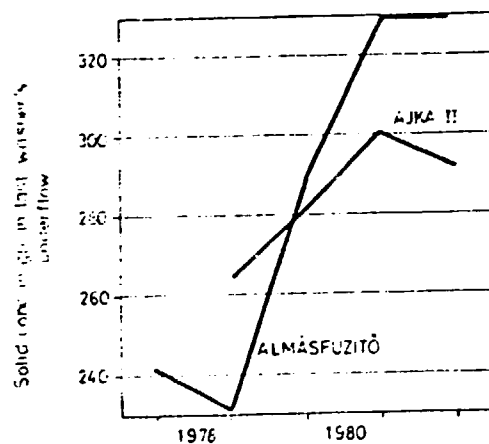


Fig. 20. Increase of solid concentration in the cone of the last washer in Hungarian alumina plants as a consequence of applying digestion with catalytic additives.

In Fig. 21. the decrease of free  $\text{Na}_2\text{O}$  content of the last washer is plotted versus time in the same period.

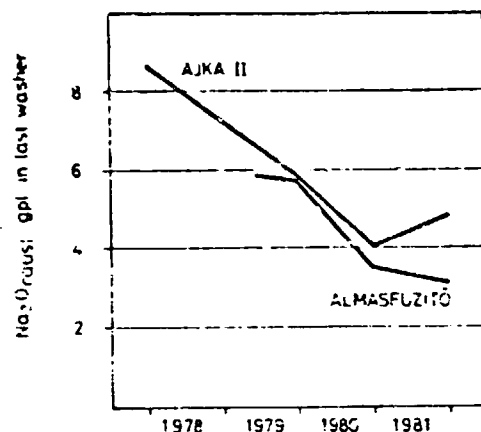


Fig. 21. Decrease of free  $\text{Na}_2\text{O}$  content in the last washer in Hungarian alumina plants as a consequence of applying catalytic additives during digestion.

Fig. 21. shows that the  $\text{Na}_2\text{O}$  content of the liquor which was disposed to the red mud pond, was reduced to the half in the period under survey.

The amount of settling aids could be reduced by 30 to 50 % owing to the favourable phase composition of the red mud.

It must be underlined here that the goethite content of bauxite which is processed at the Ajka Alumina Plant corresponds only to about 1-2 %  $\text{Fe}_2\text{O}_3$ , however, the improvements are several times larger than was expected on the basis of the goethite-hematite ratio. The only disadvantage which was observed upon the realization of goethite-hematite conversion is the increase of Zn-content of the aluminate liquor.

The mineralogical and textural composition of Jamaican goethitic bauxites is similar to that of the Hungarian ones so on the basis of model experiments and that of the results of the Hungarian plant operation it can be supposed with high confidence that the application of these processes to Jamaican bauxites could lead to similarly considerable advantages.

### 3.5.3 Application field of the Hungarian digestion technology with catalytic additives

Relying on the results presented above and the laboratory and plant experiences it can be stated that these processes may be applied for any bauxite /even for those containing little or no goethite/ with high technical and economical efficiency.

This statement was controlled by laboratory experiments with bauxite samples from Australia and Guinea.

The phase compositions of the bauxite and the corresponding red mud gained without and with hydrogarnet catalyzed digestion from an Australian sample are summarized in Table 12. and those from a Guinean bauxite in Table 13. It can be read out of these data that even the very stable aluminogothite of the Guinean bauxite could be converted into hematite and in this way the  $\text{Al}_2\text{O}_3$  content of red mud reduced from 15.8 % to 9.5 % and the alumina recovery of digestion increased by 5 %.



Table 12. Phase composition of an Australian bauxite and the red muds gained therefrom at 235° C without additives and applying hydrogarnet catalyzer /Na<sub>2</sub>CO<sub>3</sub> caust. 360 gpl, A/C = 0.7/

Component	Bauxite	Red mud without additives	Red mud with catalyzer
Al <sub>2</sub> O <sub>3</sub> % in gibbsite	40.7	-	-
boehmite	6.6	3.2	1.9
diaspore	0.3	0.9	0.4
kaolinite	4.6	-	-
goethite	0.3	0.9	0.4
hematite	0.1	0.3	0.3
Na-Al-hydrosilicates	-	12.7	11.6
Ca-Al-hydrosilicates	-	0.2	1.2
Total	52.6	18.2	15.8
Fe <sub>2</sub> O <sub>3</sub> % in goethite	2.5	7.0	1.8
hematite	10.8	34.3	34.9
Total	13.3	41.3	36.7
SiO <sub>2</sub> % in kaolinite	5.0	-	-
Na-Al-hydrosilicates	-	14.9	11.6
Ca-Al-hydrosilicates	-	-	2.0
Total	5.0	14.9	13.6
TiO <sub>2</sub> % in anatase	1.9	-	-
rutile	0.7	-	-
Na-titanate	-	7.9	-
Ca-titanate	-	-	6.8
Total	2.6	7.9	6.8
L.O.I. %	24.5	5.6	5.1
CaO %	0.1	0.3	6.8
MgO %	0.02	0.05	0.05
Na <sub>2</sub> O %	-	11.3	5.8
Na <sub>2</sub> O/SiO <sub>2</sub> molar ratio in red mud		0.73	0.41
Bound caustic soda losses, NaOH kg/t alumina		100.2	56.3
CaO consumption, kg/t alumina		-	52.8
Al <sub>2</sub> O <sub>3</sub> recovery, %		89.0	89.2
Bauxite consumption t/t alumina		2.13	2.12

**Table 13.** Phase composition of a Guinean bauxite and the red muds gained therefrom at 235° C without additives and applying hydrogarnet catalyzer /Na<sub>2</sub>CO<sub>3</sub> caust. 360 gpl, A/C = 0.7/

Component	Bauxite	Red mud without additives	Red mud with catalyzer
Al <sub>2</sub> O <sub>3</sub> % in gibbsite	39.1	-	-
boehmite	1.4	1.0	0.4
diaspore	0.8	1.2	0.7
kaolinite	2.2	-	-
goethite	2.6	7.1	0.3
hematite	0.2	0.5	0.4
Na-Al-hydrosilicates	-	6.0	5.3
Ca-Al-hydrosilicates	-	-	2.4
Total	46.3	15.8	9.5
Fe <sub>2</sub> O <sub>3</sub> % in goethite	9.1	24.7	2.3
hematite	12.1	33.0	55.2
Total	21.2	57.7	57.5
SiO <sub>2</sub> % in kaolinite	2.6	-	-
Na-Al-hydrosilicates	-	7.1	6.2
Ca-Al-hydrosilicates	-	-	0.9
Total	2.6	7.1	7.1
TiO <sub>2</sub> % in anatase	1.9	-	-
rutile	0.7	-	-
Na-titanate	-	7.1	-
Ca-titanate	-	-	6.5
Total	2.6	7.1	6.5
L.O.I. %	24.5	5.0	4.8
CaO %	0.05	0.2	8.6
MgO %	0.03	0.1	0.1
Na <sub>2</sub> O %	-	5.3	4.3
Na <sub>2</sub> O/SiO <sub>2</sub> molar ratio in red mud		0.72	0.59
Bound caustic soda losses, NaOH kg/t alumina		63	49
CaO consumption kg/t alumina		-	74
Al <sub>2</sub> O <sub>3</sub> recovery, %		87.5	92.4
Bauxite consumption t/t alumina		2.47	2.34

The mineralogical composition of differently obtained red muds are shown in Fig. 22.

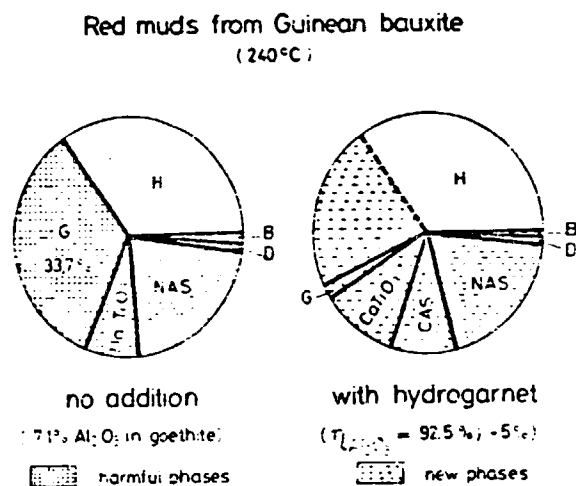


Fig. 22. Comparison of the phase compositions of the respective red muds obtained from a Guinean bauxite sample without additives and using catalyzed digestion.

The proportion of goethite and  $\text{Na}_2\text{TiO}_3$  which hinder the separability of the red mud extremely, could be reduced from 42 % to 2 % by application of catalyzed digestion.

A higher A/C ratio, good clarity of the aluminate liquor without control filtration and better separability and washability of red mud, reduction of bound and dissolved losses of caustic soda and alumina can be achieved in all cases.

### 3.6 Two-stage digestion of diasporic bauxites

#### 3.6.1 Digestibility of diasporic bauxites

The diasporic bauxites are processed by the Bayer process, too. The process technology has to be modified in order to compensate the disadvantageous technological character of diasporic bauxites as compared to the boehmitic ones. These are the following: less favourable digestibility, lower equilibrium solubility, abrasive character.

The digestion with lime addition has been developed to enhance the total dissolution of the diasporic content /38, 39, 40, 41, 42/. Referred to dry bauxite an amount of 3-4 % CaO is generally added. Though the process mechanism of CaO is not cleared so far, in most cases diasporic can be dissolved at 240-250° C.

Tikhonov and Lapin /43/, as well as Mercier and Noble /44/ compared the main technological parameters of processing different quality bauxites. Tikhonov and co-workers /45/ determined the equilibrium solubility of diasporic of the bauxite from North-Ural. The dissolution from diasporic into the unit volume was found to be less by 15-20 % as compared to boehmite. In order to reduce this effect higher digestion temperature and higher caustic concentration is suggested.

For the processing of diasporic bauxite abrasion resistant equipments and pipelines are required.

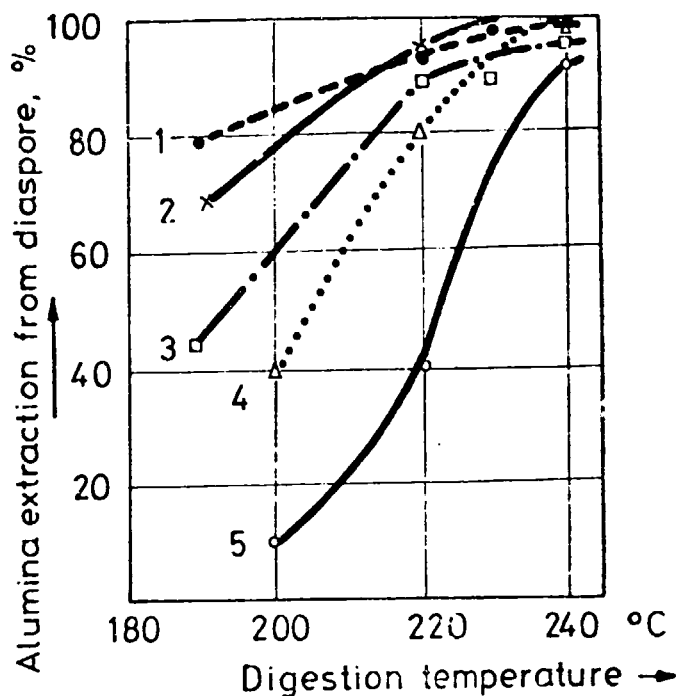
In the following the technological peculiarities of diasporic bauxites connected with their individualism and heterotypism, moreover the new technological processes developed in ALUTERV-FKI /Hungary/ will be presented.

Technological studies were carried out on diasporic bauxites from Greece /Parnasse/ and Vietnam /Lang Son/. The results obtained were compared with that of Beneslavsky, Tikhonov and Jasunin /38/, as well as Tikhonov and co-workers /45/. Chemical composition of the bauxite samples are listed in Table 14.

Table 14. Chemical compositions of bauxite samples

Component %	No.1.	No. 2.	No.3.	No.4.	No.5.
Fe <sub>2</sub> O <sub>3</sub>	26.5	24.2	20.1	21.0	25.6
SiO <sub>2</sub>	2.3	1.82	3.9	4.6	7.3
Al <sub>2</sub> O <sub>3</sub>	54.7	54.6	59.9	56.0	50.3
TiO <sub>2</sub>	3.1	2.1	2.9	2.6	3.1
CaO	1.2	2.4	0.15	1.5	0.1
L.O.I.	13.0	12.8	11.7	13.1	12.5
No 1.	Halimba /Hungary/				
No. 2.	North-Ural /Soviet Union/				
No. 3.	Bihar /Rumania/				
No. 4.	Parnasse /Greece/				
No. 5.	Lang Son /Vietnam/				

The digestibility of different diasporic bauxites is shown in Fig. 23.



1. Gupiansk, China
2. North Ural, USSR
3. Bihar, Rumania
4. Parnasse, Greece
5. Lang Son, Vietnam

$\text{Na}_2\text{O}_c = 200 \text{ gpl}$ ; 3% CaO addition;  
Digestion time 1.5 hrs

Fig. 23. Digestibility of diasporic bauxites.

It is obvious from the figure that the diaspore from Gupiansk and North-Ural deposits can be digested with lime already at 220-240° C, however, the diaspore from the Lang Son deposit is very difficult to digest and even at 240° C only 90-92 % can be dissolved. Medium digestibility is found with Rumanian /Bihar/ and Greek /Parnasse/ bauxites. The diagram clearly shows the individualism of the different diaspore minerals. The undigested  $\text{Al}_2\text{O}_3$  content, however corresponds to the

diaspore fraction with strong  $\text{OH}^-$  bond characteristic of the heterotypism of the given diaspore. It can be stated that though the solubility of individual diasporic bauxites digested with lime addition may approach the solubility of the boehmitic bauxites, the more perfectly crystallized diaspore would incompletely dissolve even at higher temperatures.

In some bauxites the diaspore particles are covered with an iron layer consisting of goethite and/or hematite reducing the alumina yield. This phenomenon is characteristic for the bauxite particles from Vietnam /Lang Son/. For the digestion of such grains it is necessary to break /by grinding/ or to dissolve the iron layer.

Characteristic digestion curves of diasporic bauxites from Lang Son and Parnasse are compared in Fig. 24.

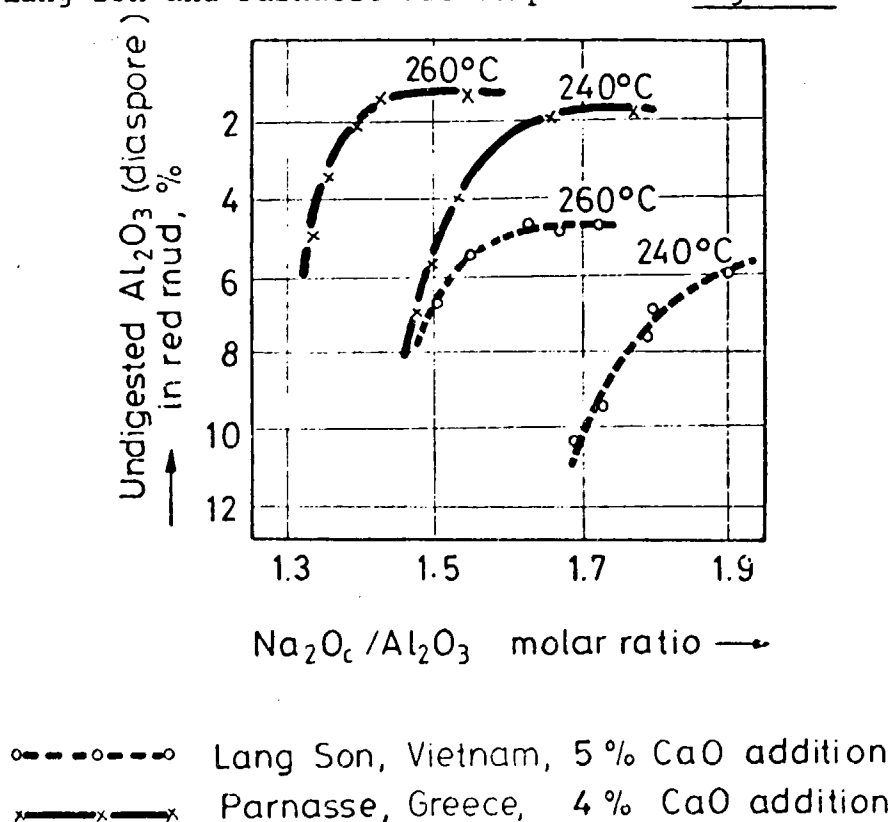


Fig. 24. Digestibility curves of diasporic bauxites

The digestion experiments were carried out at 240 and 260° C, with digestion liquor of 200 gpl Na<sub>2</sub>O caustic concentration and with lime addition.

According to the given data 5 % Al<sub>2</sub>O<sub>3</sub> /diaspore/ remained undigested in the red mud of the Vietnamese bauxite at 260° C, moreover the digestion of the Greek bauxite could be realised with the same amount of liquor and similar molar ratio, however, at a temperature lower by 20° C.

The scanning electron micrographs of the Parnasse and Lang Son bauxites showed that while the first has a strongly dispersed structure, the second is composed of lamellar plane blocks. The difference in morphology highly affects the reactivity as shown in Fig. 24.

In order to increase the digestibility of diasporic bauxites, as well as to decrease the molar ratio after digestion /i.e. increasing of the soluble alumina content in unit volume of liquor/ in Hungary the new method, using catalyst /34/, has been applied to diasporic bauxites, too.

Advantages of the process are shown in Fig. 25. using the example of Lang Son diasporic bauxite which is very difficult to digest. Due to the effect of the catalyst the alumina yield approached the theoretical limit - there is nearly no undissolved fraction - and at the same time the amount of the soluble diaspore in the unit volume of liquor increased considerably.



The mineralogical compositions of bauxites from Lang Son and Parnasse, as well as the obtained red muds are given in Table 15. By the use of catalyst the dissolution of iron crust around the individual grains on one hand and the digestion of the crystalline diasporite on the other hand can be achieved. The similarity of technological behaviour of the goethite and diasporite minerals has been justified.

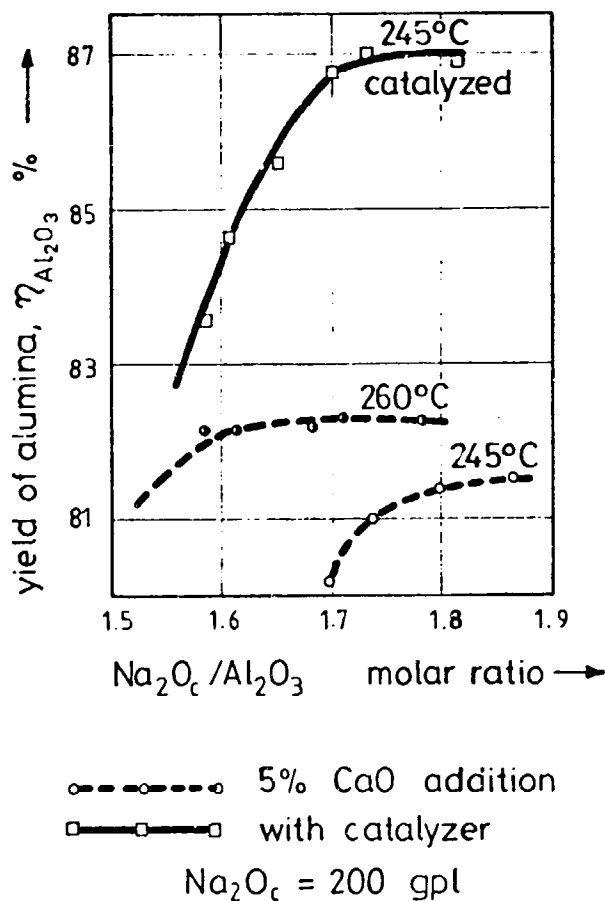


Fig. 25. Digestibility curves of the Lang Son bauxite /Vietnam/

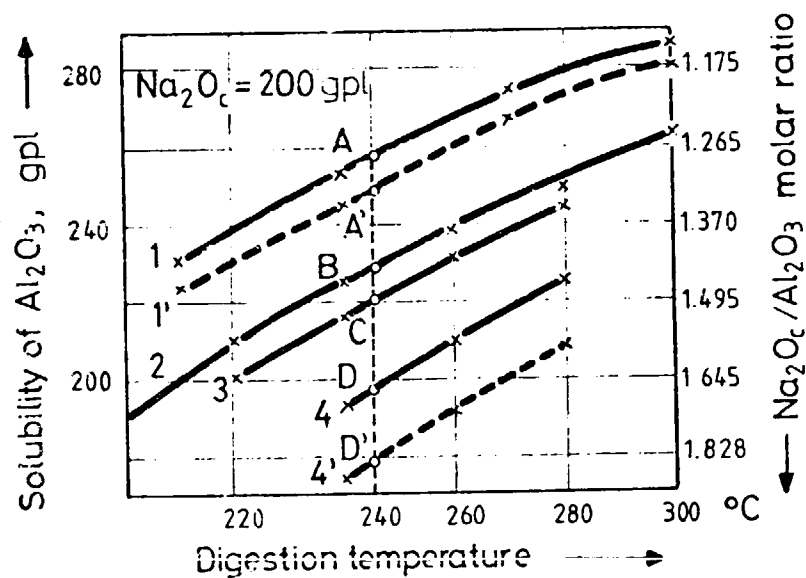
**Table 15. Mineralogical compositions of bauxites and their characteristic red muds**

Component, %	Bauxites		Red muds formed at 245° C		
	Lang Son	Parnasse	Lang Son	Parnasse	
Al <sub>2</sub> O <sub>3</sub> in	gibbsite	2.5	-	-	-
	boehmite	2.8	17.2	-	1.1
	diaspore	38.2	35.0	0.7	0.5
	corundum	0.3	-	0.3	-
	kaolinite	4.7	3.8	-	-
	chamosite	1.2	-	-	-
	goethite	0.6	-	-	-
	NAS	-	-	9.9	5.3
	CAS	-	-	2.1	4.3
Total	50.3	56.0	13.0	11.2	
SiO <sub>2</sub> in	kaolinite	5.5	4.5	-	-
	chamosite	1.1	-	-	-
	quartz	0.7	0.1	-	-
	NAS	-	-	11.6	6.2
	CAS	-	-	1.0	3.4
Total	7.3	4.6	12.6	9.6	
Fe <sub>2</sub> O <sub>3</sub> in	hematite	15.1	18.5	40.0	46.6
	goethite	7.6	2.5	4.0	-
	maghemite	0.7	-	-	-
	chamosite	2.2	-	-	-
Total	25.6	21.0	44.0	46.6	
TiO <sub>2</sub> in	anatase	2.0	0.9	-	-
	rutile	1.1	1.7	-	-
	CaTiO <sub>3</sub>	-	-	5.7	5.7
	Total	3.1	2.6	5.7	5.7
CaO in	calcite	0.1	1.5	-	2.0
	CaTiO <sub>3</sub>	-	-	2.3	3.1
	CAS	-	-	3.7	7.1
	Total	0.1	1.5	6.0	12.2
NAS = Na-Al-silicates; CAS = Ca-Al-silicates					

### 3.6.2 Equilibrium solubility of diasporic bauxites and two-stage digestion technology

Because of the individualism of diasporic bauxites, they have not only highly different digestibility /Fig.23./, but a diversity in equilibrium solubility, too.

In Fig. 26. the equilibrium solubilities of Lang Son and Parnasse bauxites, as well as those of the diasporic North-Ural /45/ and the boehmitic Halimba, Hungary /46/ are compared.



1. Boehmitic bauxite from Halimba, Hungary
  2. North Ural, USSR
  3. Parnasse, Greece
  4. Lang Son, Vietnam
- } Diasporic bauxites

x—x—x—x Equilibrium solubility  
 x---x---x Solubility achieved at plant conditions

Fig. 26. Equilibrium solubility of diasporic bauxites compared to that of a boehmitic one.

Using a liquor concentration of 200 gpl  $\text{Na}_2\text{O}$  the alumina content dissolved in unit volume is less by 38 gpl for the diasporic of the Parnasse bauxite and by 60 gpl for the diasporic of the Lang Son bauxite as compared to the data of the boehmitic Halimba bauxite. The low equilibrium solubility of the diasporic is one of the greatest technological problems as compared to the boehmitic bauxites. This results in a significant decrease of the efficiency of the process circuit, as well as the increase of steam consumption and investment costs. In order to eliminate this disadvantage in ALUTERV-FKI /Hungary/ institute a two-stage technology has been developed. In this process boehmitic bauxite is added to the slurry coming from the digestion of diasporic bauxite /47/. This slurry is saturated for diasporic, however, unsaturated for boehmite. By the addition of undigested boehmite /in slurry/ the equilibrium solubility of boehmite can be approached. The characteristic concentrations at  $245^\circ\text{C}$  are represented by the points A, B, C and D on Fig. 26. However, the equilibrium concentration cannot be achieved in practice. One has to calculate with the concentrations corresponding to points A' and D' respectively, taking into account the accuracy of the actual control system and the shape of the characteristic digestion curve.

If the Vietnamese bauxite is digested with the technology using catalyst /Fig. 25./ the concentration corresponding to point D can be achieved in practice, too. Let us assume that as an example the diasporic Lang Son and the boehmitic Halimba bauxites in equal proportions are processed together. The principal scheme of the process is shown in Fig. 27.

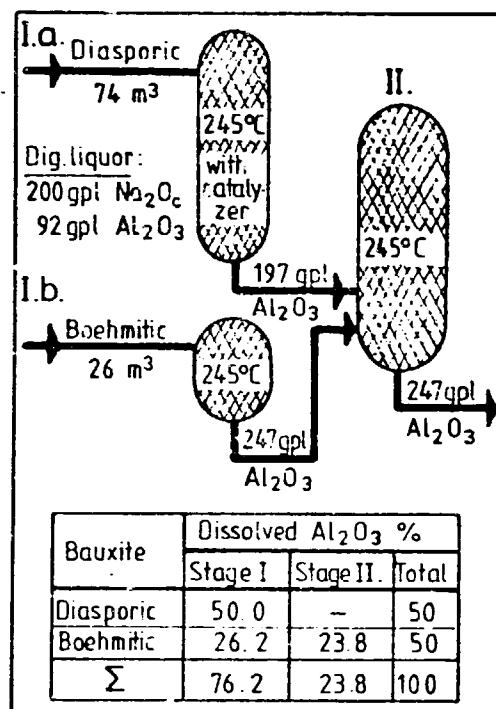


Fig. 27. Two-stage digestion for processing diasporic and boehmitic bauxites.

In the processing stage of the diasporic bauxite 74 % of the digesting liquor is used and  $197 - 92 = 105$  gpl  $\text{Al}_2\text{O}_3$  is dissolved. On digesting the boehmitic bauxite  $247 - 92 = 155$  gpl alumina can be dissolved but almost half the amount of boehmitic bauxite remains yet undigested and gets into the second stage, and is united with the diasporic stream. Here the liquor of the diasporic slurry is saturated with boehmite, and  $247 - 197 = 50$  gpl  $\text{Al}_2\text{O}_3$  may be dissolved. As a result the entire digestion can be realized under the technological parameters characteristic for the boehmitic bauxite. Minimum excess equipment is required.

Instead of boehmitic bauxite one could also use advantageously fairly digestable diasporic bauxite, an ore with low diasporic content and even gibbsitic bauxite, however, the technology must always be optimized according to the given bauxite supply. It frequently occurs that within a given bauxite deposit the boehmitic bauxite, the easily digestable diasporic bauxite and the more crystalline diasporic ore can be found. In this case the selective mining is the only solution to be taken.

It is of high importance to protect the equipments against the abrasive effect of diasporic bauxites. The hardness varying in wide ranges is also due to their individualism. For that reason abrasion resistant digesters, pumps and pipelines are of primary importance. In favour of digestibility, especially in the case of oolitic grains, due care should be taken of the proper grinding and the control of grain size distribution. In the course of the design work and running the Tulcea Alumina Plant ALUTERV-FKI had successfully solved those problems and acquired projecting, technological and manufacturing experiences on the basis of which the technological and mechanical solutions for the processing of any given diasporic bauxite can be provided. Recently tube digester can be recommended for processing diasporic bauxites /32, 48/.

The results mentioned above are summarized regarding the tube digestion and digesting with catalytic additives in the paper of Solymár and Steiner /49/, for the processing diasporic bauxites in the paper of Solymár and Ferenczi /50/.

### 3.7 Recent trends in the precipitation

One of the most important fields of the technological development is the precipitation. The main aim can be formulated to produce coarse, "sandy" alumina hydrate at as high caustic soda concentration as possible. An increase in alkali concentration from 170 to 250 gpl  $\text{Na}_2\text{CO}_3$  would result in a 50 % decrease of liquor requirement for the same production. Increasing caustic soda concentration from 180 to 230 gpl  $\text{Na}_2\text{CO}_3$  the total energy consumption would be decreased by about 15 %. The liquor productivity reaches about 80 gpl in the European refineries while in the American ones only 40-50 gpl can be achieved. The quite big difference is due to the different caustic soda concentrations /250-260 gpl and 180 gpl, respectively/. Therefore the actual trends in the precipitation technology are:

- to produce the same quality sandy type alumina at an elevated caustic soda concentration in the American plants /increasing liquor productivity and saving energy/
- to produce sandy alumina at the actual high caustic soda concentration without decreasing liquor productivity in European plants /fluory to sandy alumina conversion/.

The conversion has been carried out in two plants already, namely at Tomakoma /Nippon Light Metals/ /51/ and at Gove /Alusuisse/ /52, 53/.

As a consequence of the conversion the capacity of the Gove plant increased by 10 %- 15 % at the formerly used caustic soda concentrations of 250-260 gpl  $\text{Na}_2\text{CO}_3$  /54/. The basis of the process is to separate the phases of agglomeration and growth. Fine seed is fed continuously

to an agglomeration stage operating at  $66^{\circ}$ - $77^{\circ}$  C and at a rate which controls the supersaturation to seed surface area ratio in the range of 7-16 gm/m<sup>2</sup>. Under these conditions agglomeration is completed in 6 hours. The slurry is then cooled by  $15^{\circ}$ - $20^{\circ}$  C and fed to growth precipitators to which coarse secondary seed is also added. Seed densities of 400 gpl are maintained in this stage and residence times range from 40-80 hours. Critical process conditions in the suppression of fines generation in the growth stage is the maintenance of high seed charges and ensuring that cooling steps do not exceed  $15^{\circ}$  C -  $20^{\circ}$  C. Alumina produced by this method has 5 % - 8 % minus 45 micrometer.

Liquor productivity is affected by alumina solubility which is increasing in the presence of impurities.

The solubility can be increased by 20 % compared to pure liquor. Intensive cleaning of the circuit could be a very effective means to improve the liquor productivity. The effect of the different contaminants is very variable. A small amount of some organic fractions can extremely inhibit precipitation. In this way one can understand the efforts being made to realize the intensive purification of the liquor.

The studied methods are the following /37, 55, 56, 57, 58/:

- Precipitation of oxalate - organic mixtures in fluidized bed columns.
- Precipitation of oxalate in packed spray trickle columns.
- Precipitation of oxalate from destabilised spent liquor.
- Precipitation of Bayer organics from deeply evaporated spent liquor /with soda salt, and to be calcined/.
- Liquor calcination with added bauxite or alumina hydrate.
- Liquor oxidation by air or oxygen.



- Liquor ozonation.
- Renoval by barium salt precipitation.
- Renoval by magnezium-salts.

There are different methods partially used in the plants, however, a definitive, cheap method is not available yet.

It seems to be reasonable to combine the organics removal /e.g. wet air oxidation/ with an effective reduction of the sodium carbonate /37/.

In the field of precipitation a very intensive, further R and D activity is required.

### 3.8 Reduction of caustic soda losses

#### 3.8.1 Distribution of the NaOH losses within the Bayer process

Fig. 28. illustrates the distribution of NaOH losses characteristic for the Hungarian Bayer plants.

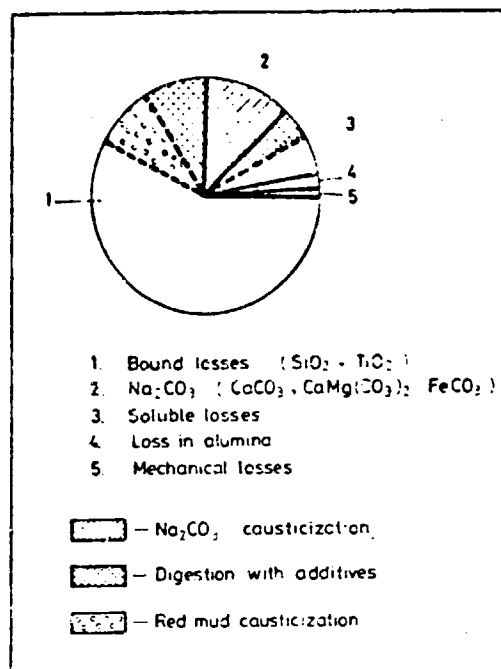
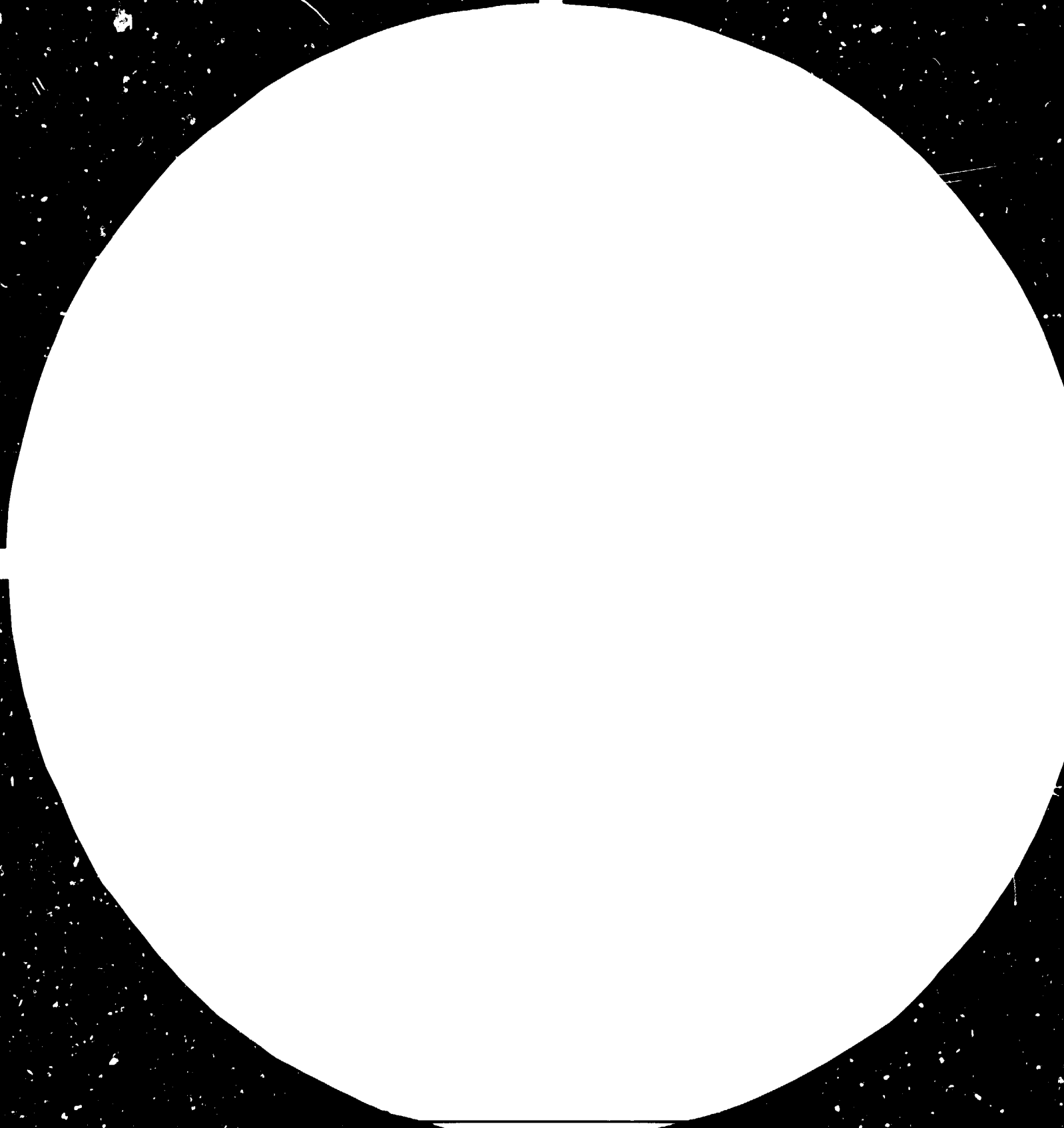


Fig. 28. Relative magnitude of the contributions to NaOH losses and their diminution.

According to this 75 % of the total losses is due to the so called bound-loss. The second most important seems to be the salt-loss which is a consequence of the decausticization effect of impurities, first of all of carbonates present in the bauxite. Certain Hungarian bauxites contain calcite, dolomite and siderite impurities in considerable percentages, therefore the monitoring and control of soda level as well as the separation of soda salts is rather important [60].

The effects of measures carried out with the aim to diminish the various NaOH losses are also marked on Fig. 28. The soda is kept in equilibrium in the cycle by causticization at the washer line. Bound NaO<sub>2</sub> is regenerated partly by

84.03.27  
AD.85.03





28



32



36



## MICROSCOPY RESOLUTION TEST CHART

NATIONAL BUREAU OF STANDARDS  
STANDARD REFERENCE MATERIAL 1963-A  
APRIL 1963 EDITION

means of the digestion with additives and partly by causticizing the mud phase in course of the complex causticization. Losses in solution removed together with the red mud were also diminished by about 50 % as a result of the digestion technology using additives and of the improved settling of the mud due to the goethite-hematite transformation. In order to achieve further decrease in the NaOH losses first of all the bound  $\text{NaO}_2$  content must be regained in higher proportion.

It must be mentioned, that the absolute magnitude of NaOH losses and the relative importance of loss-sources depends on the quality of bauxite processed and on the technology applied in a particular plant. E.g. in the Gove alumina plant the bound loss amounts only to 54 % and the dissolved loss merely to 38 % /61/. The appropriate measures for caustic soda regeneration must be determined in each case through the analysis of the distribution of losses.

In what follows the methods will be described applicable to decrease the NaOH losses.

### 3.8.2 Digestion of bauxite using catalysing additives

Addition of burnt lime was first carried out on commercial scale for the digestion of diasporic bauxite /40/. This has been followed recently by the digestion of goethitic bauxite using additives in order to achieve hydrothermal transformation of goethite to hematite.

Fig. 29. shows the  $\text{Na}_2\text{O}/\text{SiO}_2$  weight ratio and digestion yield attainable in red mud by means of digestion using additives in dependence of the CaO content of the resulting red mud.

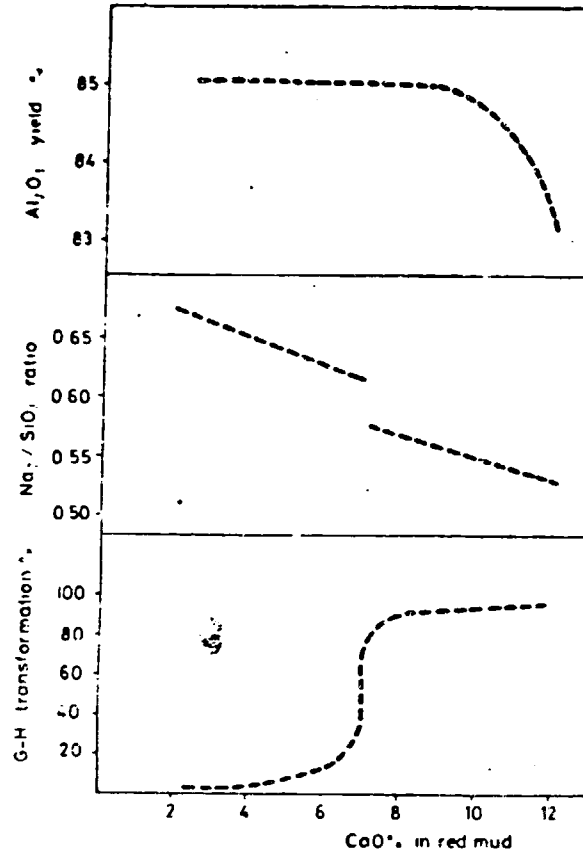


Fig. 29. Alumina yield, bound  $\text{Na}_2\text{O}$  in red mud and the efficiency of goethite-hematite transformation in dependence from the  $\text{CaO}$  content in the red mud during digestion using additives /There was 5,5 %  $\text{Fe}_2\text{O}_3$  in the bauxite in the form of goethite/.

It becomes clear that the variation of the  $\text{Na}_2\text{O}/\text{SiO}_2$  ratio is described by a discontinuous function. When the  $\text{CaO}$  content of red mud reaches 7 % the goethite-hematite transformation becomes complete and the released  $\text{Fe}^{3+}$  ions forming iron-hydrogarnet reduce abruptly the bound  $\text{Na}_2\text{O}$  loss. In the given example, with due regard to the  $\text{Al}_2\text{O}_3$

yield the quantity of catalyzing additive must be adjusted to provide for 8-9 % /7-10 %/ CaO in the red mud. Thus digestion using additives, besides other important advantages, renders possible the regeneration of about 15 % bound  $\text{Na}_2\text{O}$  from the red mud as well as the significant diminution of dissolved losses.

### 3.8.3 Causticization of soda on the washer line

Especially when processing a bauxite with higher carbonate content / / it became a common practice in the European alumina plants to causticize the soda on the washer line /62, 63/. The regeneration of soda within the cycle, e.g. in the overflow of the 3. washer requires theoretically 0.7 kg CaO/kg NaOH and the burnt lime consumption does not exceed in practice the value of 1 kg/kg NaOH.

In Fig. 30. the efficiency of soda causticization and the magnitude of  $\text{Al}_2\text{O}_3$  loss are plotted as a function of the caustic  $\text{Na}_2\text{O}$  concentration in the liquor to be causticized.

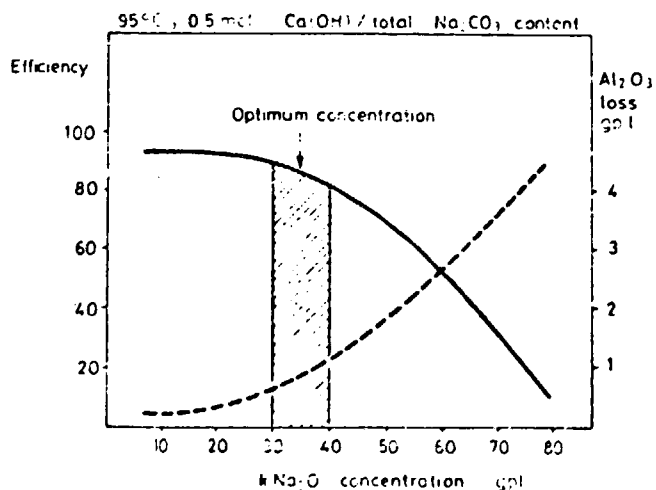


Fig. 30. Efficiency of causticization at the Dorr line and loss of  $\text{Al}_2\text{O}_3$  versus caustic concentration.



The optimal range of concentration seems to be 30-40 gpl. Naturally, it is reasonable to carry out the soda causticization in such a way that the soda salt separated from the evaporated strong liquor should be dissolved also in the overflow to be causticized.

#### 3.8.4 Causticization of red mud

Hungarian alumina plants, because of the higher  $\text{SiO}_2$  of the bauxite processed, have applied the causticization of red mud by means of burnt lime [54, 65] even on plant scale in order to diminish the bound caustic soda losses. If good quality burnt lime or lime slurry are used and the causticized red mud is carefully filtered and washed the procedure provides for the regeneration of the major portion of bound  $\text{Na}_2\text{O}$ .

The efficiency of red mud causticization, the percentage of regenerated NaOH are plotted in Fig. 31. versus the temperature for the case of 3 mole CaO/mole Na<sub>2</sub>O addition.

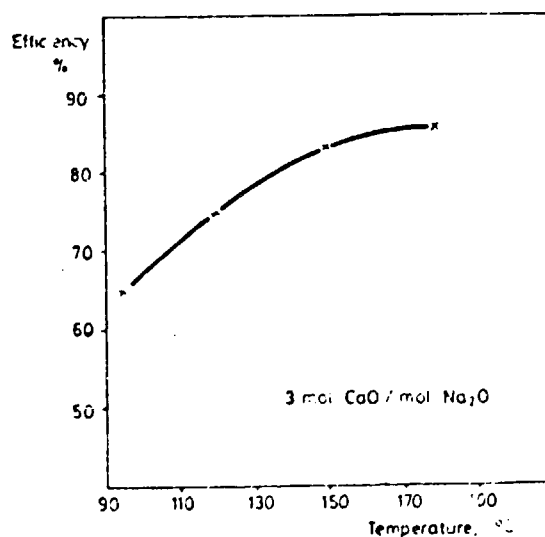
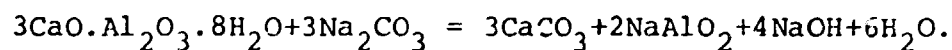


Fig. 31. The efficiency of red mud causticization as a function of the temperature of treatment.

It can be seen that when the treatment is carried out under pressure, in autoclaves, the efficiency of causticization can be augmented up to 85 %. Recently the causticization of red mud was stopped in the Hungarian alumina plants because of the lack of labour and the adequate filtering capacity, respectively. In order to diminish significantly and economically the NaOH losses a new method had been developed with the essential feature that the causticization of red mud is not a separated operation but it is accomplished within the Bayer circuit in integration with the soda regeneration. This procedure is known and patented under the term "complex causticization" /No. 593/82 request for Hungarian patent, 1982. 02. 20/.

### 3.8.5 Complex causticization

Complex causticization is based on the fact that in a certain concentration and temperature range not the hydrogarnet type  $3\text{CaO} \cdot \text{Al}_2\text{O}_3 \cdot k\text{SiO}_2$  /6-2k/  $\text{H}_2\text{O}$  compound is formed from the sodium aluminate solution but a calcium aluminate without silica of the composition:  $3\text{CaO} \cdot \text{Al}_2\text{O}_3 \cdot 8\text{H}_2\text{O}$ . The latter is much more reactive and can be regenerated quantitatively by  $\text{Na}_2\text{CO}_3$  according to the following equation:



In Fig. 32. it can be seen clearly that the red mud produced in the course of digestion with an additive /"sample a"/ contained relatively small amount of CAS.

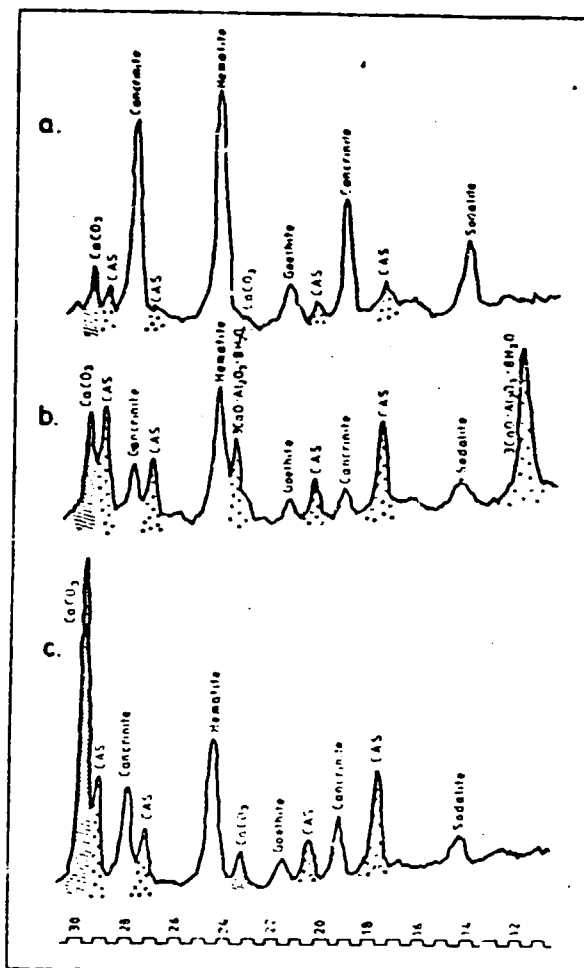
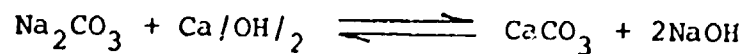


Fig. 32. Typical phase transformations occurring during complex causticization.

Adding to this mud /to the cone of a member of the washer line/  $\text{Ca}/\text{OH}/_2$  it reacts with the  $\text{Al}_2\text{O}_3$  of the solution according to the above reaction, the excess  $\text{Ca}/\text{OH}/_2$  causticizes the  $\text{Na}_2\text{CO}_3$  component of the solution following the well known



equation, while the  $\text{Ca}/\text{OH}/_2$  added in further excess

transforms the sodium-aluminium-hydro-silicate present in the red mud into hydrogarnet /CAS/ where the value of K is approximately 1.5. In the red mud treated in this manner /"sample b"/ high amounts of  $3\text{CaO}\cdot\text{Al}_2\text{O}_3\cdot 8\text{H}_2\text{O}$  and CAS can be detected as illustrated by Fig. 32. The  $\text{Al}_2\text{O}_3$  content of the CAS is recovered by the soda salt separated at an other point of the circuit /at the evaporation of liquor/ and at the same time NaOH forms from the soda. The corresponding red mud /"sample c" in Fig. 32./ does not contain any CAS but a considerable amount of  $\text{CaCO}_3$  can be detected.

A simplified flow sheet of complex causticization is reproduced in Fig. 33.

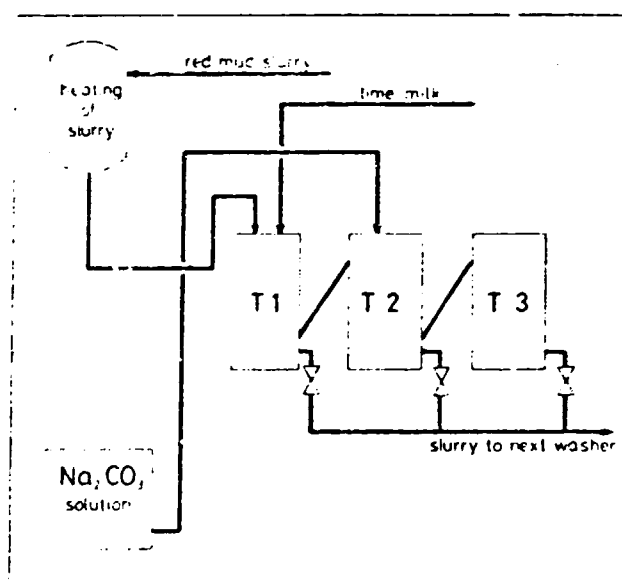


Fig. 33. Flow sheet of the complex causticization.

The procedure is executed between two units of the washer line, reasonably by treating the cone mud of the 3-rd or 4th washer /in fact a fraction of the mud/. The lime slurry is added to tank T1, in tank T2 the preliminarily precipitated  $\text{Al}_2\text{O}_3$  will be regenerated by means of soda solution, in tank T3 the soda eventually in excess is causticized by  $\text{Ca}(\text{OH})_2$  and then the slurry fed into the next washer. It is advantageous to use a longer tank series, composed from several reactors.

Fig. 34. demonstrates the commercial results gained by complex causticization.

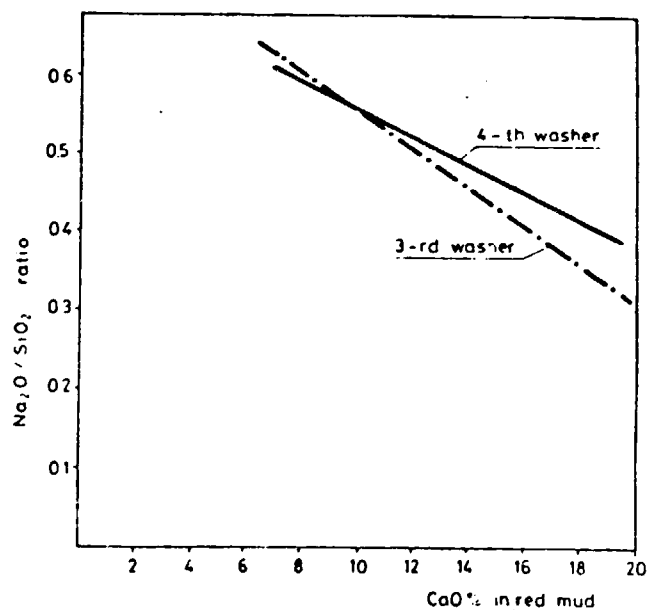


Fig. 34. The change of  $\text{Na}_2\text{O}/\text{SiO}_2$  ratio in red mud versus  $\text{CaO}$  content during complex causticization.

The  $\text{Na}_2\text{O}/\text{SiO}_2$  weight ratio of the red mud is plotted in dependence from the CaO content in the treated material. It can be seen that the procedure provides for the regeneration of 30-40 %  $\text{Na}_2\text{O}$  bound in the red mud. The consumption of burnt lime amounts to about 2 kg CaO/kg regenerated NaOH. Table 16. offers plant data for the phase composition of the processed bauxite and the red mud produced thereof.

The benefits of the procedure can be assured even in the case of red mud washer lines terminated by filters and if necessary the soda can be supplied from external sources.

### 3.8.6 Comparison of the methods for regenerating NaOH

Fig. 35. gives the specific CaO demand of the different procedures for regenerating NaOH.

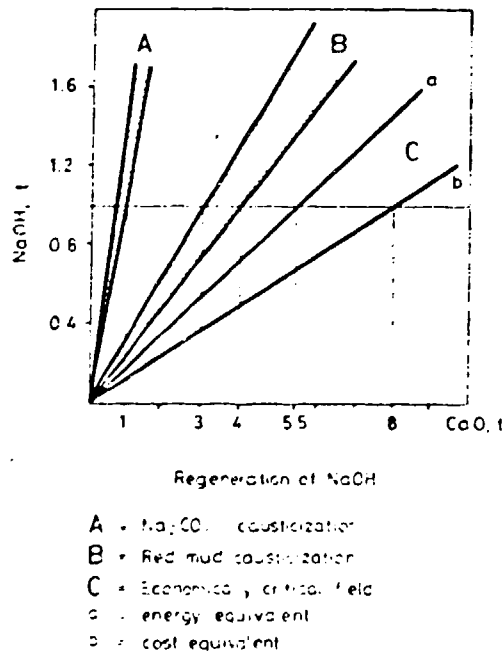


Fig. 35. Specific CaO consumption in various treatments for the regeneration of NaOH.

Table 16. Phase composition of bauxite and of its characteristic red mud

	Bauxite	Mud 1. /without additi- ves/	Mud 2. /with additi- ves/	Mud 3. /after causti- cization	Mud 4. /last washer/
<b>Al<sub>2</sub>O<sub>3</sub> % in</b>					
gibbsite	17.2	-	-	-	-
boehmite	27.0	0.5	-	-	-
diaspore	0.5	0.6	-	-	-
goethite	0.4	0.8	-	-	-
hematite	0.2	0.4	0.4	0.4	0.4
kaolinite	5.0	-	-	-	-
sodalite	-	5.5	3.8	2.2	3.4
cancrinite	-	7.3	6.9	1.8	5.8
CAS	-	-	2.2	7.6	3.4
Total	50.3	15.1	13.3	12.0	13.0
<b>SiO<sub>2</sub> % in</b>					
kaolinite	5.9	-	-	-	-
sodalite	-	5.5	4.2	2.2	3.4
cancrinite	-	7.3	6.9	1.8	5.8
CAS	-	-	1.0	6.0	2.5
Total	5.9	12.8	12.1	10.0	11.7
<b>Fe<sub>2</sub>O<sub>3</sub> % in</b>					
hematite	16.7	36.2	44.2	35.5	42.4
goethite	5.5	12.1	1.3	1.1	1.3
Total	22.2	48.3	45.5	36.6	43.7
<b>TiO<sub>2</sub> % in</b>					
anatase	1.7	-	-	-	-
rutile	0.8	-	-	-	-
Ca-titanates	-	2.0	4.4	3.5	4.2
Na-titanates	-	2.5	-	-	-
Ca/Mg;Al/titanates	-	0.7	0.7	0.6	0.7
Total	2.5	5.2	5.1	4.1	4.9
<b>CaO % in</b>					
dolomite	0.4	-	-	-	-
calcite	0.4	-	-	5.1	1.5
Ca-titanates	-	1.4	3.1	2.5	3.0
CAS	-	-	4.0	11.6	5.2
Ca/Mg;Al/titanates	-	0.3	0.4	0.4	0.4
Total	0.8	1.7	7.5	19.6	10.1
MgO %	0.4	0.8	0.7	0.6	0.7
Na <sub>2</sub> O %	-	8.9	7.3	3.3	6.5
Na <sub>2</sub> O/SiO <sub>2</sub> molar r.	-	0.68	0.59	0.33	0.54
Loss on ignition	17.0	7.0	6.5	12.5	7.7

Causticized red mud /Sample No3/ 20 % of the total red mud.

For comparison the curves representing the price equivalent of lime and NaOH, respectively, /8 kg CaO = 1 kg NaOH/, as well as the energy equivalent for these two raw materials /5.5 kg CaO = 1 kg NaOH/ are plotted, too. The latter represent the very amount of products for which the same quantity of primary energy is needed in production /taking into account the efficiency of electrical energy production and the 3:1 share of costs in NaCl electrolysis between NaOH and Cl<sub>2</sub>/.

According to this figure even the independent causticization of red mud seems to be justified /3-4 kg CaO/kg regenerated NaOH/, however, complex causticization seems to be prominently economic because it appears between the fields "A" and "B" /1-3 kg CaO/kg regenerated NaOH/ and the coupled investment and operation costs are very low.

The enhanced regeneration of NaOH can be identified as an extremely important development target in order to diminish production costs and indirectly energy consumption in alumina plants.

Soda causticization on the washer line is without doubts economic and essentially important to maintain equilibrium in the circuit. In particular cases the causticization of red mud can be justified, too.

The complex causticization process developed recently in Hungary permits to decrease bound NaOH losses by 20-40 % very economically and using low investments.



### 3.9 Energy consumption of the different stages of the Bayer process

A medium level alumina plant consumes about 16 GJ energy per ton of alumina produced. The distribution of the energy consumption among the main process stages is represented in the Fig. 36.

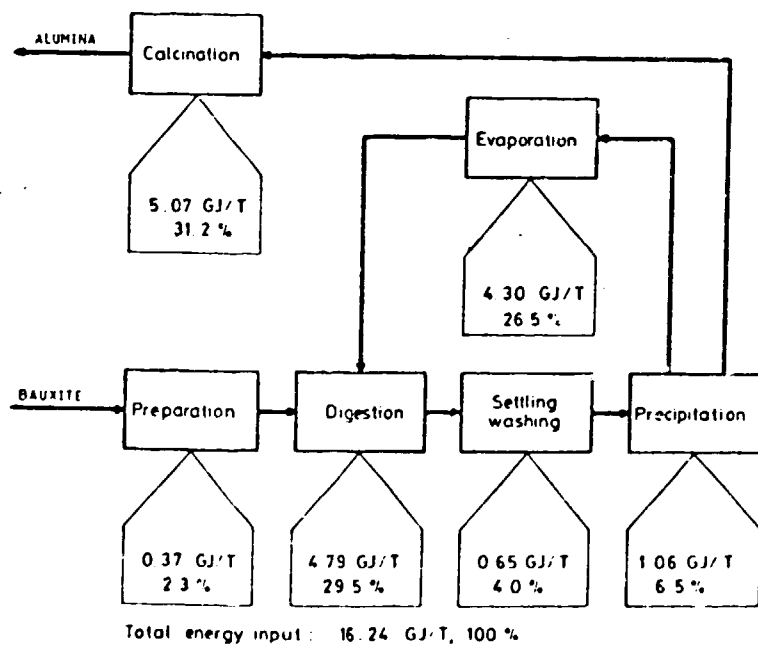


Fig. 36. Distribution of energy consumption in a medium level alumina plant among the process stages.

A very important part of the total energy input is required nowadays to compensate radiation and waste heat losses of hydrate cycle. The distribution of these losses is demonstrated in Fig. 37.

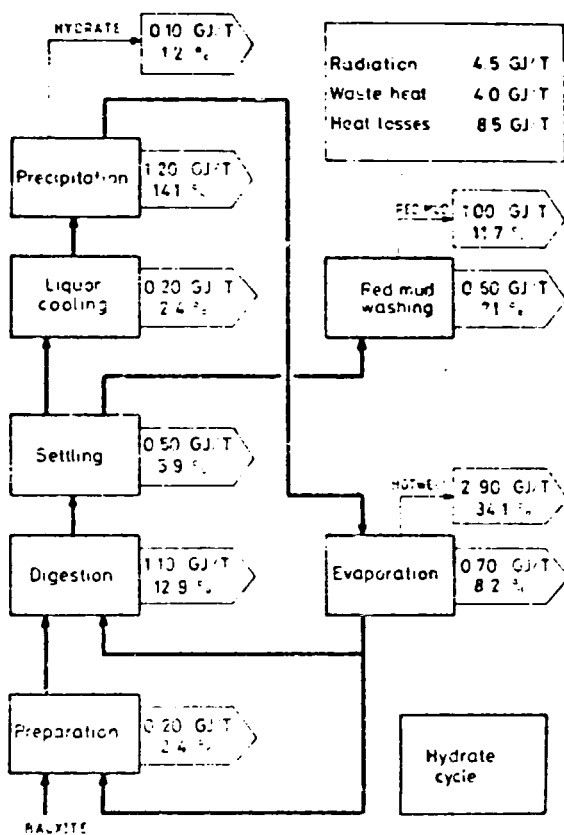


Fig. 37. Radiation and waste heat losses of the alumina hydrate manufacturing.

In the former sections of this study some technological possibilities were discussed resulting in energy saving in the process. As further significant means are to be mentioned the application of special chemicals /flocclulants

and dewatering aids / 59/ and the computerized process control /66/.

A quite large amount of the wash water can be saved applying effective synthetic flocculants in the red mud settling and washing line, which decreases the quantity of water to be evaporated. The use of dewatering aids in hydrate filtration drops the moisture content of the hydrate before the calcination by 2-3 %. It is a practical experience that for each percent moisture in the hydrate about 45 MJ/ton is required for evaporating and superheating of the vapour to the stack temperature /67/.

The computerized process control enables to approach very closely the optimum parameters avoiding overconsumption of energy due to oversized material flow-rates.

In Fig. 38. the total energy consumption of the Bayer alumina plants is given for different stages of development /8/. The theoretical minimum /curve 1./ can be found quite far from the actual plant values, even in the case of an up-to-date refinery /curve 2./. It can be mentioned as well, that sometimes the bauxite transportation /e.g. from Australia to Mid-Europe/ needs as high energy consumption as the total demand of the whole circuit under optimal conditions.

The diagram justifies the actuality and possibility of the energy saving actions.

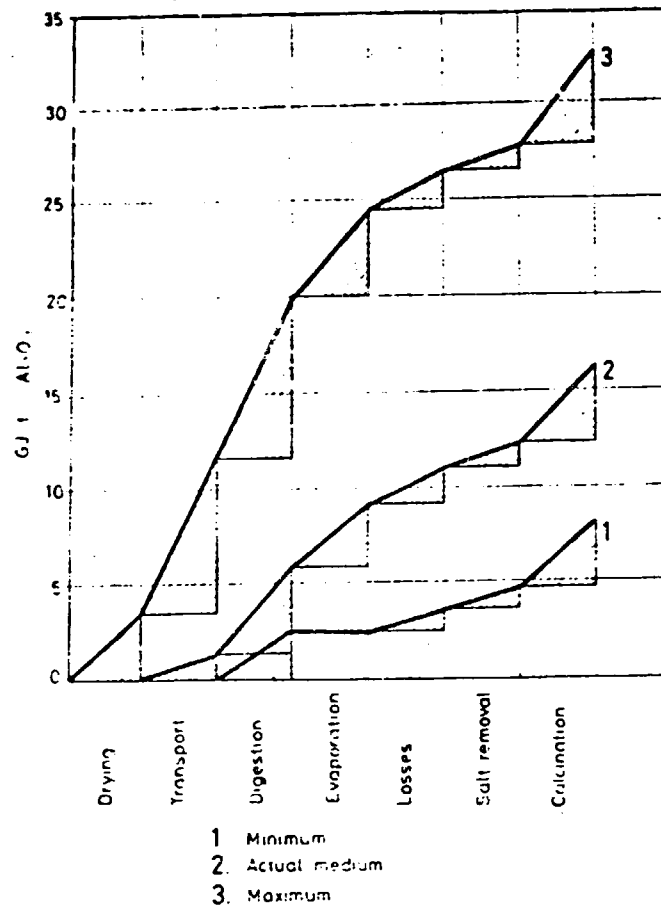


Fig. 38. Energy consumption of the Bayer alumina plant  
/after Bielfeldt, Ref. 8./

In the second part /following sections/ of this study those methods will be discussed in details which can be used to determine energy balance of the different process stages and the ways for saving energy will be showed.

#### 4. Overall energy survey of the Bayer process

The energy demand in the alumina plant may be investigated in three main areas: heat used in the Bayer cycle for alumina hydrate production; heat energy needed to calcine alumina; and electrical energy to drive pumps, agitators and other processes equipment.

The fuel fired calciner kiln is a well known equipment in other industries than alumina production too, so calcination of alumina is a unit operation without many very special features. The application of electrical energy for providing shaft power and the energy efficiency of pumps, fans, compressors and even tank mixers or ball mills are more or less well understood and generally belong to practical areas in the chemical and metallurgical industries.

Production of alumina hydrate, on the other hand, has many special features and should be discussed in some depth to get a thorough understanding of the material and energy flow rates involved.

The Bayer process is of cyclic nature that should be described shortly: A continuously circulating caustic soda solution dissolves alumina from bauxite while being heated - /digestion/ - and after solid residues, called red mud, have been removed - /clarification/ - alumina precipitates on cooling - /precipitation/ -. The liquor is diluted in the course of this process by water associated with the bauxite, and water used to recover chemicals by washing of red mud and alumina hydrate, while water contained in the discharged red mud and alumina hydrate leaves the cycle.

The net amount of water added to the process liquor must be removed by evaporation, and the fresh liquor starts anew going round the cycle. Fig. 39. illustrates the simplified process description:

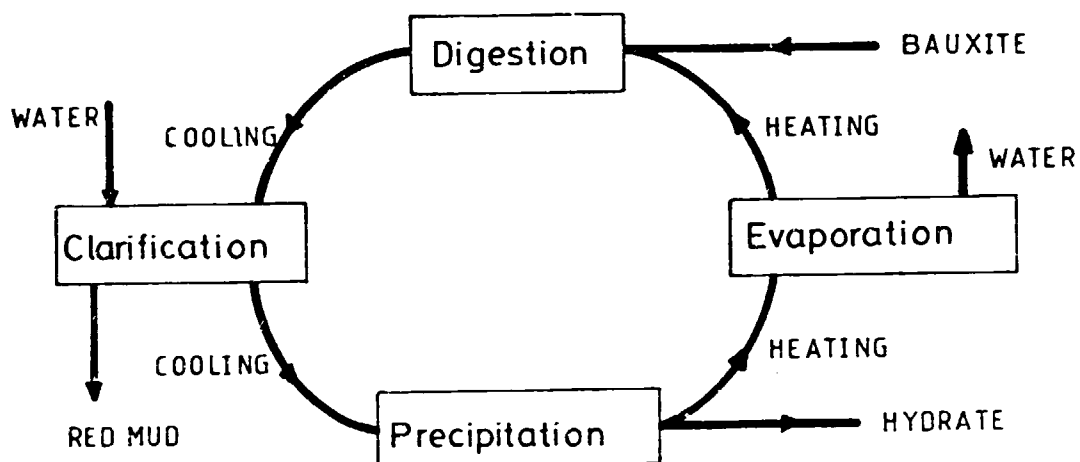


Fig. 39. The Bayer cycle /by Donaldson, Ref. 20/

In order to show the process cycle from an engineering point of view Fig. 40. may prove useful. The T-Q diagram shows the heat flow rates involved to produce a quantity of alumina hydrate adequate for one ton of calcined alumina, and the changing temperatures of the process fluids during one full cycle.

While following the course of changes within the process cycle, some characteristics of the T-Q diagram may be mentioned.

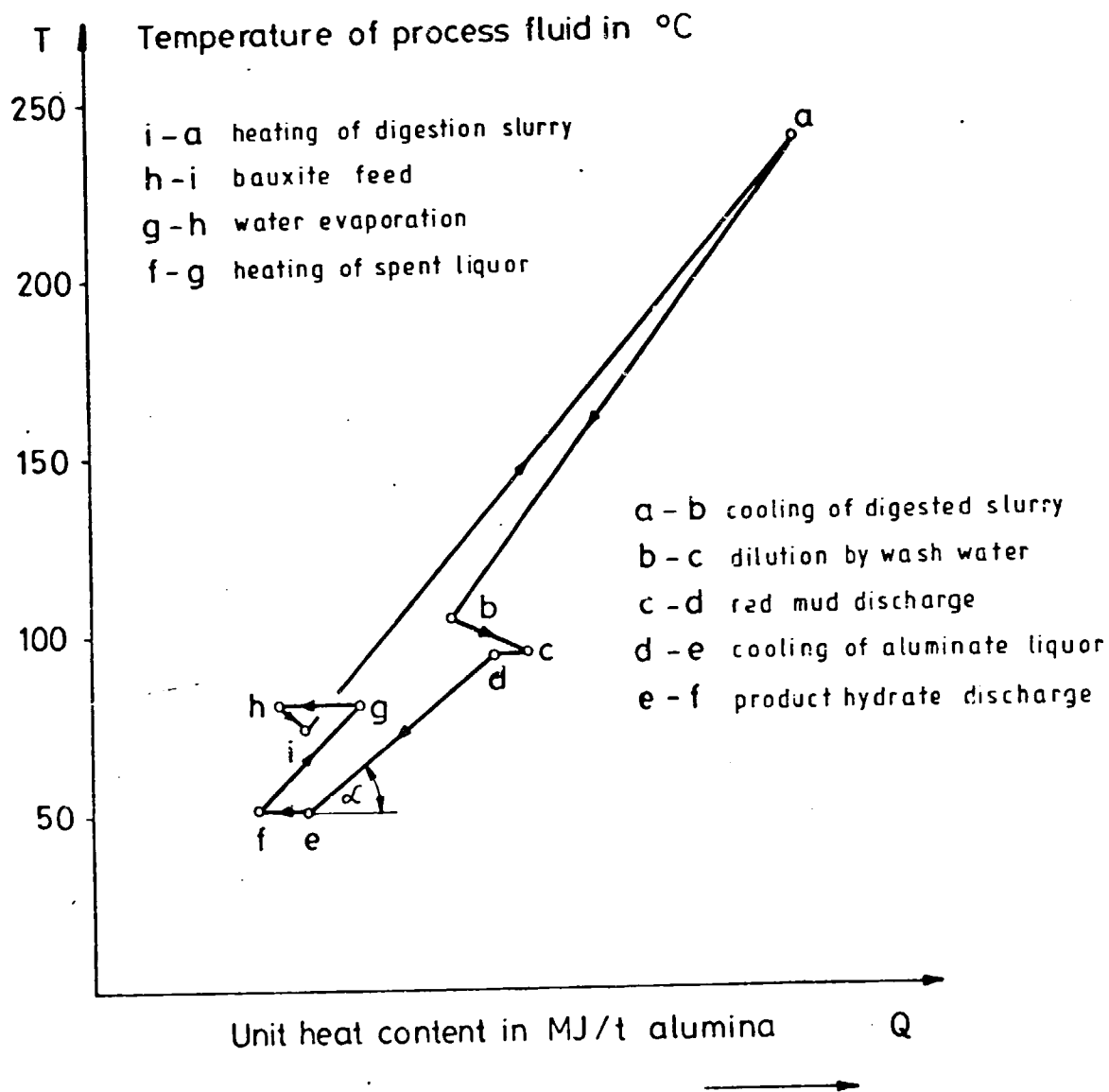


Fig. 40. T-Q diagram of the process

Point "a" represents the condition of the process fluid at the end of digestion, having reached the highest temperature of the cycle. Cooling proceeds from "a" to "b" /along a straight line with a temperature drop  $T_a - T_b$  and/

along a straight line with a temperature drop  $T_a - T_b$  and an associated heat loss of:  $\Delta Q_{a,b} = 4.1868 \times W_a / T_b - T_a /$  MJ/t.  $W_{a,b}$  is a process variable expressing the heat capacity of the fluid in terms of "water equivalent", which is to say that the process fluid of known unit mass  $M_a / t / t /$  and specific heat  $q_a / MJ / t, ^\circ C /$  has the same heat capacity as  $W$  tons of water, as  $q_w = 4.1868 / MJ / t, ^\circ C /$ , so

$$\Delta Q_{a,b} = q_a \times M_a / T_b - T_a / = 4.1868 \times W_a / T_b - T_a /$$

It may be noted that since the final temperature  $T_b$  of the cooling process is smaller than the initial temperature  $T_a$ ,  $\Delta Q_{a,b}$  will be a negative value, so line a-b goes to the left, indicating a diminishing heat content.

At point "b" diluting water is added. Line b-c goes to the right indicating an increase in heat content of  $\Delta Q_{b,c} = 4.1868 \times W_w / T_w - T_o /$ , where  $W_w$  and  $T_w$  are the water equivalent of the diluting liquid and its temperature, while  $T_o$  is the temperature of environment. The temperature in point "c" can be determined by applying the mixing rule:

$$W_b \times T_b + W_w \times T_w = (W_b + W_w) / T_c$$

$$\text{where from } T_c = \frac{W_b \times T_b + W_w \times T_w}{W_b + W_w} \times c$$

The change c-d comes from red mud discharge, and the associated loss on heat content is

$$\Delta Q_{d,c} = 4.1868 \times W_{rm} / T_c - T_o / \quad / MJ / t /$$

Alumina liquor cooling is illustrated by line d-c. its slope is less than that of line a-b. The tangent of the



slope is smaller because the heat capacity of aluminate liquor  $W_a$  is larger than that of digested slurry  $W_d$ . For aluminate liquor cooling:  $\tan \alpha = \frac{T_e - T_d}{\Delta Q_{d,e}} = \frac{1}{4.1868 \times W_d}$

because

$$\Delta Q_{d,e} = 4.1868 \times W_d / T_e - T_d / \text{ /MJ/t/}$$

The heat content reduction caused by product hydrate discharge at 50 °C is shown by line e-f.

Heating of spent liquor starts at "f" and terminates at "g". The heat content of the liquor is increased as the final temperature  $T_g$  at point "g" is higher than the initial temperature  $T_f$ .

Water evaporation at  $T_g = 80$  °C means a loss of heat content of  $\Delta Q_h = 4.1868 \times W_{ev} / T_o - T_h /$ , where  $W_{ev}$  is the unit rate of water evaporated in t/t, and  $T_o$  is the temperature of the environment.

Bauxite feed causes a change in temperature and heat content shown as line h-i, which can be computed by the same logic as in case of adding wash water, whown by line b-c.

The heating of digestion slurry is represented by line i-a. Theoretically, the line should run parallel to line a-b because the same heat capacities are involved both in heating and in cooling of digestion slurry.

When, however, radiation losses are taken into account, any slope would become flatter than the one computed from the heat capacity of the process fluid alone. It looks as

if the heat capacity would be greater than it really is. An examination of the Bayer cycle in the Q-T diagram reveals two potential areas for heat recovery. The cooling line a-b could be coupled in heat exchange to the heating line starting from point "i" towards point "a". It appears that heating from "i" to "a" requires more heat than can be gained from cooling between "a" and "b":

$$\Delta Q_{ia} > \Delta Q_{ab}$$

Consequently, to reach the final digestion temperature  $T_a$  an external heat supply is required.

The second potential situation for heat recovery is between alumina cooling d-e and spent liquor heating f-g. Unfortunately, the heat extracted by cooling can only partly be used to spent liquor heating because of the need for a temperature difference in heat exchange. So only one portion "x" of  $Q_{de}$  the total depletion in heat content of aluminate liquor could be utilized to the end of heating up spent liquor by a heat amount  $Q_{fg} = x Q_{de}$ , while the remaining  $(1-x)Q_{de}$  would be lost to the environment by free cooling.

The main components of energy consumption can be recognized from the qualitative survey of the process:

- 1/ External heat input at high temperature is required in the digestion step which would be proportional to the "water equivalent" of digestion slurry and the temperature gap to be covered by external heating.
- 2/ A low temperature heat input at the evaporation section must be provided to restore the water balance. The required energy depends on the surplus of water gathered

in the cycle mainly due to wash water entry.

3/ Potential areas for heat recovery do exist in the process cycle, and it may be assumed that effective heat exchange could strongly improve overall heat economy.

Special attention will be paid to the points mentioned above in a detailed survey, in the course of which every major unit operation of the process will be dealt with to some depth.

Before dealing with the characteristic unit operations, the chemistry of bauxite digestion and heat transfer fundamentals and specialities are investigated in order to build a solid basis for calculations that are used in energy accounts of the alumina plant.

These general sections are regarded to be important practical guides to deal with a variety of individual problems unique for each given plant and process flow sheet, raw material composition, etc. Case examples involving numerical computations are presented to serve as a guide for action in other applications of the method and procedure.

## 5. Thermal properties of plant fluids

### 5.1 Solubility of alumina in caustic liquors

A thorough understanding of what happens in the process of bauxite digestion is necessary to compute material and heat balances of the operation.

Extraction of alumina from bauxite is governed by the solubility in caustic soda solutions. The limit of alumina solubility is expressed by its saturation concentration which depends essentially on the temperature and on the prevailing caustic soda concentration in the digester unit, as expressed by the relation:

$$C_A = \frac{C_N}{3.903 + 0.0000316T^2 - 0.019271T - \frac{0.243 \cdot C_N}{T - 52}} \text{ kp/m}^3$$

where:

- $C_A$  is the saturation concentration in  $\text{kp Al}_2\text{O}_3/\text{m}^3$
- $C_N$  is the caustic soda concentration in  $\text{kp Na}_2\text{O}/\text{m}^3$   
/expressed as  $\text{Na}_2\text{O}/$
- $T$  is the temperature of digestion in  $^\circ\text{C}$

The relation may be used for monohydrate extraction in the 160 to 280  $^\circ\text{C}$  temperature range. Table 17 gives  $C_A/C_N$  limits for different caustic concentrations and extraction temperatures as computed from the above equation.

Table 17. Saturation  $C_A/C_N$  ratios

$\text{kp Na}_2\text{O}/\text{m}^3$	140	160	180	200	220
180 $^\circ\text{C}$	0.85	0.87	0.90	0.93	0.97
200 $^\circ\text{C}$	0.93	0.95	0.99	1.02	1.05
222 $^\circ\text{C}$	1.01	1.04	1.08	1.11	1.15
240 $^\circ\text{C}$	1.09	1.12	1.15	1.19	1.22
260 $^\circ\text{C}$	1.15	1.19	1.22	1.25	1.30
280 $^\circ\text{C}$	1.20	1.23	1.27	1.30	1.33

### 5.2 Effects of bauxite composition

The silica content in the bauxite also dissolves in caustic liquors and reacts with alumina and with caustic soda to form a sodium-aluminium-hydrosilicate which precipitates and reports to the red mud. This procedure must also be taken into account in order to get the actually required liquor volumes for bauxite digestion.

Unfortunately, no universally applicable relation can be formulated. Bauxite and red mud compositions are decisive in deriving a useful relation applicable for the given circumstances. A case example might serve well for better understanding.

The average bauxite composition /by weight per cent/ used during the period under investigation must be known. In the numerical example to be presented, bauxite composition was as shown in Table 18.

Table 18. Average bauxite composition

Al <sub>2</sub> O <sub>3</sub> content	50.0 weight per cent
SiO <sub>2</sub> content	5.0 weight per cent
Fe <sub>2</sub> O <sub>3</sub> content	24.0 weight per cent
TiO <sub>2</sub> content	2.5 weight per cent
CaO content	0.5 weight per cent
Other elements	0.5 weight per cent
Loss on ignition	17.5 weight per cent
<hr/>	
Dry bauxite	100.0 weight per cent
Moisture	17.0 weight per cent
<hr/>	
Wet bauxite	117.0 weight per cent

A second important information comes from the analysis of red mud. Again, the average composition of red mud determined over the period under examination will serve as an example in Table 19.

Table 19. Average red mud composition

Al <sub>2</sub> O <sub>3</sub> content	11.6 weight per cent
SiO <sub>2</sub> content	11.0 weight per cent
Fe <sub>2</sub> O <sub>3</sub> content	52.8 weight per cent
TiO <sub>2</sub> content	5.5 weight per cent
CaO content	1.1 weight per cent
Na <sub>2</sub> O content	8.1 weight per cent
Other elements	1.1 weight per cent
Loss on ignition	8.8 weight per cent
Dry red mud	100.0 weight per cent

From Tables 18 and 19 the weight ratios of dry solids of red mud and bauxite can be derived on the assumption that iron did not react in the digestion process.

$$\frac{M_{\text{red mud}}}{M_{\text{bauxite}}} = \frac{\text{Fe}_2\text{O}_3 \text{ \% in bauxite}}{\text{Fe}_2\text{O}_3 \text{ \% in red mud}} = \frac{24.0}{52.9} = 0.4545$$

Another important result of the bauxite and red mud analysis is the formulation of the sodalite structure. In the investigated case the insoluble portion of alumina in bauxite and the soda losses due to TiO<sub>2</sub> reaction were also taken into account, and so a sodalite composition of

1.33 . Na<sub>2</sub>O . Al<sub>2</sub>O<sub>3</sub> . 2SiO<sub>2</sub> is assumed for further calculations. The molecular weights involved are: 62 for Na<sub>2</sub>O, 102 for Al<sub>2</sub>O<sub>3</sub>, and 60.1 for SiO<sub>2</sub>. So each ton of

SiO<sub>2</sub> will capture

$$102/120.0 = 0.85 \text{ tons of Al}_2\text{O}_3 \text{ and}$$

1.33 x 62/120.2 = 0.69 tons of Na<sub>2</sub>O in the sodalite compound.

Now the extractable alumina from one ton of dry bauxite can be expressed:

$$X_{\text{Al extr.}} = X_{\text{Al total}} - X_{\text{Al insol.}} - \frac{102}{120.2} X_{\text{SiO}_2} =$$

$$= 0.50 - 0.01 - 0.85 \times 0.05 = 0.448 \text{ t/t bauxite.}$$

Soda losses by SiO<sub>2</sub> and TiO<sub>2</sub> reaction per ton of dry bauxite:

$$N_{\text{loss}} = \frac{82.5}{120.2} X_{\text{SiO}_2} + 0.1 X_{\text{TiO}_2} =$$

$$= 0.686 \times 0.05 + 0.1 \times 0.025 = 0.0368 \text{ t/t /ex-}$$

pressed as Na<sub>2</sub>O/.

All these details were only to show the effects of the bauxite composition, and the individual method followed to deal with any special case of given bauxite and red mud.

### 5.3 Volume of liquor required for digestion

The digestion process should be run to get a final C<sub>A</sub>/C<sub>N</sub> ratio in the digester discharge that is close to the saturation C<sub>A</sub>/C<sub>N</sub> ratio for given digestion temperature and caustic concentration of the extraction liquor.

Close to saturation  $C_A/C_N$  means, in good plant practice, that actual  $C_A/C_N$  ratios of the digester blow-off are about 92-96 per cent of the saturation ratio for given conditions. Overcharge of liquor feed will lower the final extraction  $C_A/C_N$  ratio resulting in higher heat consumption.

The volume of digestion liquor can be expressed as required to produce one ton of alumina:

$$V_{EL} = M_B \frac{X_{AL, \text{ extr.}} + \frac{C_A}{C_N} \times N_{\text{loss}}}{\frac{C_A}{C_N} C_{NL} + C_{AL}} \quad /m^3/t/$$

where:

$M_B$  is the unit mass of dry bauxite

$C_{NL}$  is the caustic soda concentration of the liquor  
/in  $Na_2O$ /

$C_{AL}$  is the alumina concentration of the liquor

In order to give a case example, the above variables will be quantified. At an energy audit the unit mass of dry bauxite was  $M_B = 2.306$  t/t. The extractable alumina was determined to be  $X_{AL, \text{ extr.}} = 0.448$  t/t bauxite, so the actually extracted mass rate of alumina is

$$A_{\text{extr.}} = M_B X_{AL, \text{ extr.}} = 2.306 \times 0.448 = 1.033 \text{ t.}$$

This is an acceptable figure because the 3.3 per cent surplus of extracted alumina would cover losses in the course of further processing. Computing now the actual liquor volume needed for that bauxite gives:



$$V_{EL} = 2.306 \frac{0.448 + 1.134 \times 0.0368}{1.134 \times 0.200 - 0.089} = 8.195 \text{ m}^3/\text{t}$$

The extraction liquor concentrations in this case were:

$$C_{NL} = 0.200 \text{ kp/m}^3 \text{ and } C_{AL} = 0.089 \text{ kp/m}^3.$$

The  $C_A/C_N$  ratio in blow-off was  $C_A/C_N = 1.134$ . Since the digestion temperature was  $240^\circ\text{C}$ , this  $C_A/C_N$  ratio is roughly 90 per cent of the saturation  $C_A/C_N$ , as may be checked in Table 17.

By relying on the equation for alumina saturation concentration, the unit rate of extraction liquor volume may be calculated for a given bauxite quality /composition/ and for different conditions of extraction temperature and caustic concentration/. The remarkable outcome of such calculations referring to the bauxite quality of the case example are shown in Table 20.

Table 20. Unit extraction liquor volumes /m<sup>3</sup>/t/

kp Na <sub>2</sub> O/m <sup>3</sup>	140	160	180	200	220
180 °C	19.49	16.28	13.55	11.46	9.66
200 °C	16.38	13.78	11.34	9.74	8.43
220 °C	14.14	11.78	9.84	8.48	7.29
240 °C	12.47	10.45	8.91	7.61	6.67
260 °C	11.46	9.51	8.15	7.08	6.08
280 °C	10.74	9.06	7.68	6.69	5.89

When the unit volume of  $7.61 \text{ m}^3/\text{t}$  for  $200 \text{ kp Na}_2\text{O}/\text{m}^3$  extraction liquor concentration and  $240^\circ\text{C}$  digestion temperature is compared to  $8.195 \text{ m}^3/\text{t}$  as found in the case example, a liquor overcharge of 8 per cent occurs.

#### 5.4 Density and specific heat of aluminate liquor

Concentration readings of process liquors constitute a large portion of useful data available in the plant. Many calculations of the energy audit are based on concentration data. Volume rates can mostly be derived from them.

The energy scrutiny aims at establishing heat flow rates of process liquors where to specific weights and heats of fluids are required. Based on various plant and laboratory measurements, equations are used expressing the dependance of weight and heat capacity on caustic soda and alumina concentrations. For any liquor of known volume  $V_L$  and composition  $C_{NL}, C_{AL}$  the weight is:

$$M_L = V_L + 0.0011355 \times C_{NL} + 0.0009395 \times C_{AL} \quad /t/$$

When using unit rate of liquor volume  $\text{m}^3/\text{t}$  and substituting caustic concentration  $C_{NL}$  and alumina concentration  $C_{AL}$  in  $\text{kp}/\text{m}^3$ , the resulting  $M_L$  is the unit mass rate in  $\text{t}/\text{t}$ .

The heat capacity is expressed by the so-called water equivalent. The water equivalent  $W$  can be used in thermal calculations as if dealing with as many tons of water.

$$W_L = M_L - 0.000645 \times C_{NL} - 0.000667 \times C_{AL}$$

$$\text{or } W_L = V_L + 4.905 \times 10^{-4} \times C_{NL} + 2.725 \times 10^{-4} \times C_{AL}$$

Since the specific heat of water is  $q_w = 4.1868 \text{ MJ/t, } ^\circ\text{C}$ , the required heat input for raising the temperature of a liquor of known volume  $V_L$  and concentration  $C_{NL}$  an  $C_{AL}$  from an initial temperature  $T_{L1}$  up to  $T_{L2}$  will be in MJ:

$$Q_L = 4.1868/V_L + 4.905 \times 10^{-4} \times C_{NL} + 2.725 \times 10^{-4} \times C_{AL} / (T_{L2} - T_{L1})$$

### 5.5 Calculations with solids and slurries

All dry solids occurring in the mass and energy balances /like dry bauxite, red mud, alumina hydrate and alumina/ are considered to have the same specific weight and heat capacity.

With a specific weight  $\rho_s = 3 \text{ t/m}^3$ , the relationship between unit mass and volume of solids is

$$M_s = \rho_s \times V_s = 3 \times V_s \quad \text{t/t} \quad \text{or.}$$

$$V_s = M_s / \rho_s = M_s / 3 \quad \text{m}^3/\text{t.}$$

The water equivalent of these solids is computed by

$$W_s = 0.2 \times M_s \quad \text{t/t, a statement expressing that}$$

the heat capacity of the solid is equal to that of a water quantity 20 per cent of the solids weight.

When dealing with slurries, weights and heat capacities of the participating liquids and solids are added to attain the total weight and heat capacities.

### 5.6 Boiling point elevation

The boiling point elevation is also an occurrence experienced with caustic soda liquors which has mostly detrimental effect on heat transfer processes.

The boiling point elevation is the temperature difference between the boiling temperatures of caustic solution and that of water under the same pressure. Independent of the alumina content, it is a function only of the caustic soda concentration and the boiling temperature /or pressure/:

$$\Delta T_{b2} = \frac{T}{100}^2 \cdot 0.375 \frac{C_{NL}}{100} - 0.06 \frac{C_{NL}}{100}^2 + \frac{T}{100} \cdot 1.266 \frac{C_{NL}}{100} - 0.204 \frac{C_{NL}}{100}^2 + 1.092 \frac{C_{NL}}{100}^2 + 0.798 \frac{C_{NL}}{100}$$

At an extraction temperature of  $T = 240^\circ\text{C}$  and a caustic soda concentration of  $C_{NL} = 200 \text{ kp/m}^3$  the boiling point elevation is:

$$T_{b1} = 2.94 + 4.12 + 4.37 + 1.60 = 13.03^\circ\text{C}$$

The vapour flashed from expanding caustic liquors will at first be superheated by  $\Delta T_b$ , but condensing at a heat exchanger surface at its saturation temperature will be that less than the temperature of the expanded liquor. This portion of the overall temperature difference between the cooling flashed liquor and the liquid on the heated side of a surface heat exchanger will be lost for effective heat transfer.

6. Heat transfer in alumina plants

6.1 Surface heat exchangers

Surface heat exchange plays an important role in the heat economy of the Bayer process.

Looking at the lower part of Fig. 41 it becomes clear that the amount of heat lost by the cooling liquid stream  $W_1$  is equal to that gained by the heating liquid  $W_2$ :

$$Q = W_1 / T_1' - T_1'' / = W_2 / T_2'' - T_2' /$$

where  $W_1$  and  $W_2$  are water equivalents of the flow rates of the two participating liquids.

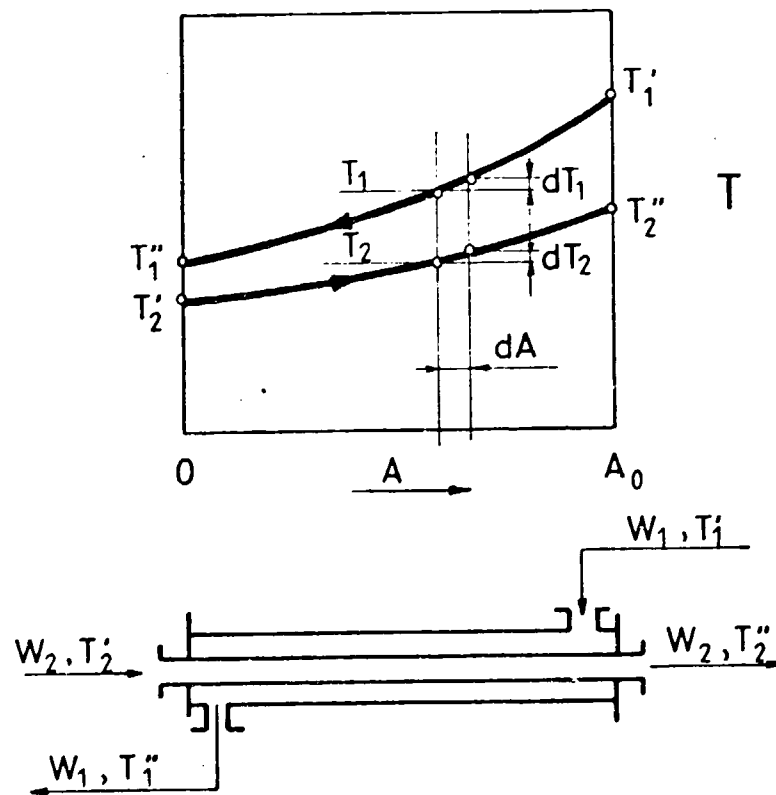


Fig. 41. Surface heat exchangers

With an overall heat transfer coefficient "k" the basic equation of heat transmission through a differential part dA of the wall surface A<sub>0</sub> separating the cooling and heating fluid streams is

$$dQ = k \times dA / T_1 - T_2 /$$

Where  $/T_1 - T_2/$  is the local temperature difference at the surface section dA. The differential equations for both the cooling stream  $/W_1, T_1/$  and the heating stream  $/W_2, T_2/$  are

$$W_1 \times dT_1 = k /T_1 - T_2/ dA \quad \text{and}$$

$$W_2 \times dT_2 = k /T_1 - T_2/ dA \quad \text{or, rearranged:}$$

$$\frac{kA}{W_1} \times T_1 - \frac{kA}{W_1} \times T_2 - \frac{dT_1}{dA} = 0 \quad \text{and}$$

$$\frac{kA}{W_2} \times T_1 - \frac{kA}{W_2} \times T_2 - \frac{dT_2}{dA} = 0$$

The integration of the above system of differential equations with the boundary conditions

$$T_1 = T_1'' \quad \text{and} \quad T_2 = T_2'' \quad \text{at} \quad A = 0, \quad \text{and}$$

$$T_1 = T_1' \quad \text{and} \quad T_2 = T_2' \quad \text{at} \quad A = A_0$$

results in

$$\frac{T_2'' - T_2'}{T_1' - T_2'} = \frac{1 - e^{-/1-W_1/W_2/ kA_0/W_1}}{W_2 - e^{-/1-W_1/W_2/ kA_0/W_1} W_1}$$

an expression for the efficiency of counter-current heat exchange. Mostly denoted by  $\Phi$ :

$$\Phi = \frac{T_2'' - T_2'}{T_1' - T_2'} \quad \text{it expresses percentage of final}$$

temperature approach of heating stream to the highest temperature of the cooling medium. /Would be 100 per cent when  $T_2'' = T_1'$ /

The efficiency of counter current surface heat exchange depends on two process variables. One of them is the ratio of the heat capacities of the participating liquids expressed as the ratio of their water equivalents:

$W_2/W_1$  i.e. ratio of heating to cooling heat capacities.

The second is the specific heat transmission capacity of the cooling stream:  $kA_0/W_1$ . High heat transfer coefficient  $k$  and large heat exchange surfaces  $A_0$  will improve efficiency.

Fig. 42 gives a quantitative information about results of relevant calculations.

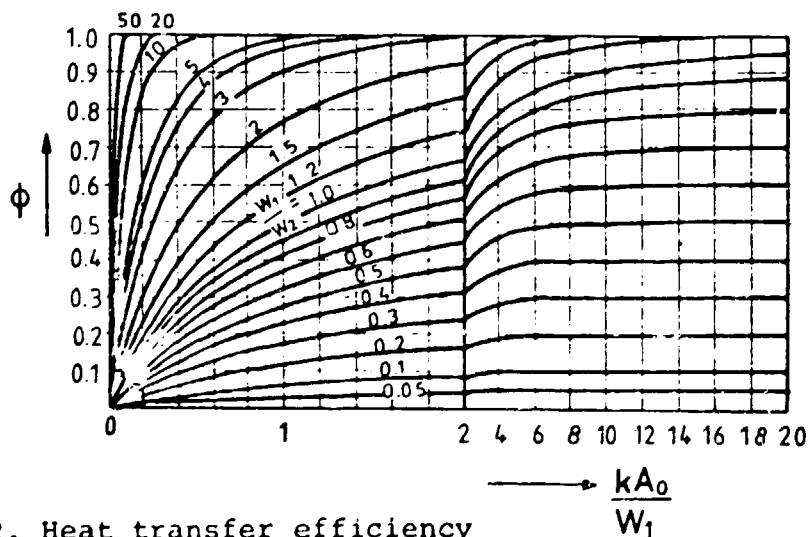


Fig. 42. Heat transfer efficiency





On the shell side of any exchanger section, vapour condensation will occur at the saturation-temperature determined by the vapour pressure of that section. In any section, of the heat exchanger the conditions will be similar to those shown in Fig. 44.

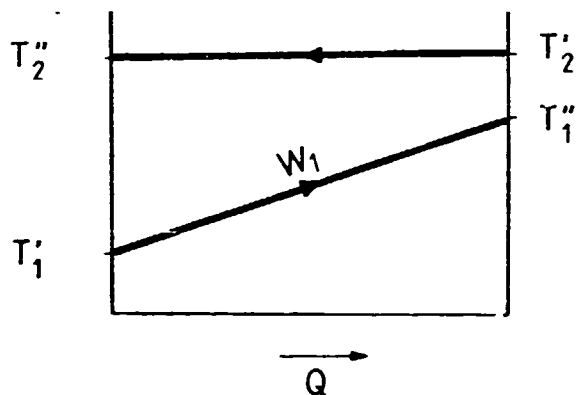


Fig. 44. Q-T diagram of heat transmission

The heat rate transmitted through the heating surface is raising the temperature of the passing liquid stream:

$$Q = k \times A \frac{T_1'' - T_1'}{\ln \frac{T_2'' - T_1'}{T_2'' - T_1'}} = W_1 / T_1'' - T_1' /$$

rearrangement leads to

$$\ln \frac{T_2'' - T_1'}{T_2'' - T_1''} = \frac{kA}{W_1} \quad \text{or} \quad \frac{T_2'' - T_1'}{T_2'' - T_1''} = e^{kA/W_1}$$

By introducing

$$T_2'' - T_1'' = (T_2'' - T_1') / (T_1'' - T_1') \quad \text{and rearranging:}$$

$$\begin{aligned} e^{\frac{1}{kA/W_1}} &= \frac{T_2'' - T_1' / - T_1'' - T_1' /}{T_2'' - T_1'} = \\ &= 1 - \frac{T_2'' - T_1'}{T_2'' - T_2'} = 1 - \frac{1}{\phi} \end{aligned}$$

The efficiency turns out to be

$$\phi = 1 - \frac{1}{e^{kA/W_1}}$$

and the heat transfer coefficient:

$$K = \frac{W}{A} \ln \frac{\phi}{\phi-1}$$

So there are very convenient expressions to calculate heat transfer conditions in a shell-and-tube heat exchanger used to condense flashed vapours.

The condensation temperature  $T_2' = T_2''$  will of course be lower than the temperature of the liquor the vapour has been flashed out from. The difference is the elevation of boiling point due to the caustic soda content of the liquor.

### 6.3 Multistep flash heat recovery

Heat recovery in most digestion plant units is performed by a multistep flash system. Heat capacities of process streams flash-cooled on the one side and heated on the

other are equal, when condensed vapours are flashed parallel to the process slurry, as mostly done. When  $W_1 = W_2$  the slopes of cooling and heating lines in a Q/T-diagram will run parallel to each other as shown in Fig. 45.

$$T_2' - T_2'' = T_1'' - T_1' = \sum_{i=1}^n (\Delta T_i)$$

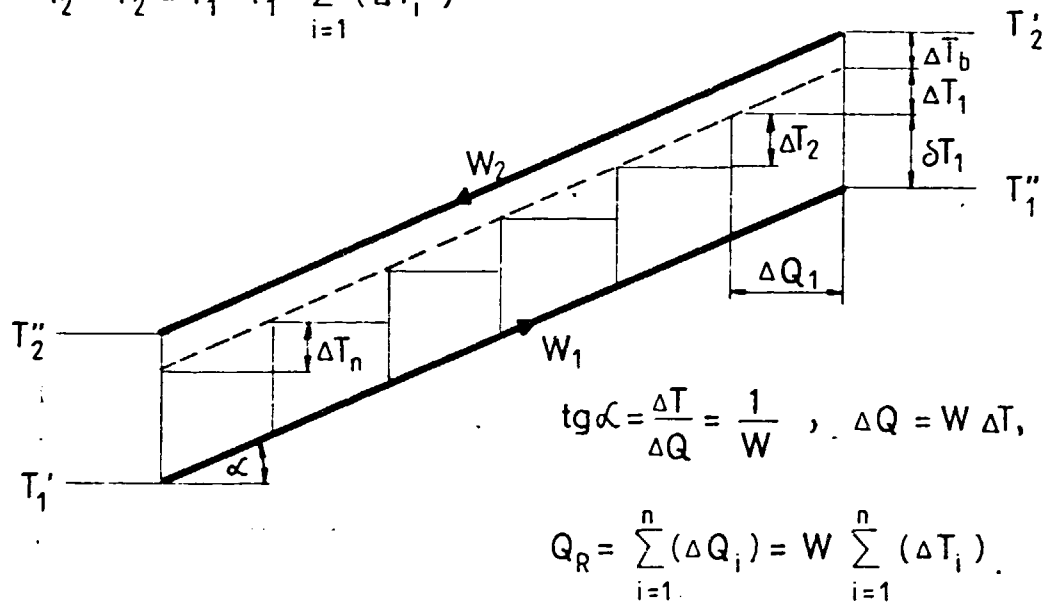


Fig. 45. Q/T diagram of flash heat recovery

A dotted line running at a distance of  $\Delta T_b$  under the line of cooling slurry  $W_2$  is the temperature available for heat transfer, much like as if water would be flashed from a temperature  $T_2' - \Delta T_b$  down to  $T_2'' - \Delta T_b$ .

The temperature drop in one flashing step is

$$\Delta T_1 = \frac{T_2' - T_2''}{n}$$

The approach temperature gap in each stage can be calculated as

$$\delta T_i = \frac{\Delta T_i}{e^{kA/W_{-1}}}$$

It becomes obvious that the number of flashing steps "n" and the specific heat transfer capacity "kA/W" will definitely influence the final approach temperature difference as expressed in the equation

$$T_2' - T_1'' = \Delta T_b + \frac{T_2' - T_1' - \Delta T_b}{e^{\frac{1}{kA/W}} - 1} \cdot \frac{1}{e^{\frac{1}{kA/W}} - 1}$$

The number of applied flashing steps will strongly influence heat recovery even with the same W, k, and total A engaged.

A case example may best illustrate how heat recovery improves in consequence of increasing the number of flashing steps and dividing the same heat transfer area accordingly into smaller units.

The data used in the calculations are:

$$T_1' = 95 \text{ }^\circ\text{C}, T_2' = 230 \text{ }^\circ\text{C}, \Delta T_b = 12 \text{ }^\circ\text{C}$$

$$W_1 = 244 \text{ MJ/h, }^\circ\text{C}, k = 6.28 \text{ MJ/m}^2\text{,h,}^\circ\text{C}$$

$$A_{\text{total}} = 146.7 \text{ m}^2$$

The results are given in Table 21.

Table 21. Number of flashing steps and heat recovery

Variables	8	16	32	64	Units
$A_i$	18.34	9.17	4.58	2.29	$m^2$
$kA_i/W$	0.47	0.24	0.12	0.06	-
$e^{kA_i/W-1}$	0.603	0.266	0.125	0.06	-
$T_2'' - T_1''$	45.8	41.6	33.9	36.3	$^{\circ}C$
$T_1''$	184.2	188.4	196.1	203.7	$^{\circ}C$
$\Phi$	0.661	0.692	0.749	0.805	-
n	8	16	32	64	

7. Energy audits of digestion, clarification and precipitation

7.1 Digestion

The basic information for the mass balance of digestion comes from the concentration readings of the digestion liquor  $/C_{NEL}, C_{AEL}/$ , from the  $C_A/C_N$  ratio in digester blow-off and from bauxite and red mud composition as detailed earlier.

The unit volume of digestion liquor can be calculated as

$$V_{EL} = M_B \frac{X_{Al \text{ extr.}} + \frac{C_A}{C_N} \times N_{\text{loss}}}{\frac{C_A}{C_N} \times C_{NEL} + C_{AEL}} \quad m^3/t$$

and the unit mass rate and water equivalent

$$M_{EL} = V_{EL} / 1 + 0.0011355 \times C_{NEL} + 0.0009395 C_{AEL} \quad \cdot t/t$$

$$W_{EL} = M_{EL} / 1 - 0.000645 \times C_{NEL} + 0.000667 \times C_{AEL} / \text{Mcal/h, } ^\circ\text{C}$$

The unit mass flow and water equivalent of the bauxite feed is

$$M_{BW} = /1 + W/ M_B \quad /t/t/$$

$$W_{BW} = 0.2 \times M_B + 1.0 \times W \times M_B \quad /Mcal/t, ^\circ\text{C}/$$

where  $M_{BW}$  and  $M_B$  stand for wet and dry bauxites.

The unit heat capacity of the extraction slurry feed will be:

$$W_{DIG} = W_{EL} + W_{BW} \quad /Mcal/t, ^\circ\text{C}/$$

The resulting mass of pregnant liquor can be computed from the mass balance of the extraction step:

$$M_{pr} = /M_{EL} + M_{BW}/ - M_{rm} \quad /t/t/$$

wherein the unit mass of red mud is calculated from the iron content of bauxite and red mud:

$$M_{rm} = M_B \frac{Fe_{bx}}{Fe_{rm}} \quad /t/t/$$

The term "pregnant liquor" denotes here the liquid phase of the extracted slurry at the end of digestion and before flashing.

The alumina content brought into the process by the digestion liquor would be replenished by the alumina extracted from bauxite, whereas the caustic soda content carried by

the digestion liquor would be diminished due to the sodalite reaction:

$$A = V_{EL} \times C_{AEL} + M_B \times X_{AL} \text{ extr.} \quad t/t$$

$$N = V_{EL} \times C_{NEL} - M_B \times N_{\text{loss}} \quad t/t$$

The liquid of the original digestion liquor would be diluted by the water entering from bauxite moisture and, from the difference of H<sub>2</sub>O bound in bauxite and red mud crystal lattices respectively:

$$M_{W \text{ DIG}} = WxM_B + X_{\text{ign.loss bx}} - \frac{Fe_{bx}}{Fe_{rm}} \times X_{\text{ign.loss rm}} / xM_B$$

On the other hand, a considerable amount of water would leave the digested slurry by the flash cooling.

The water vapour flashed in any step is directly proportional to the water equivalent of flashing slurry  $W_{Ei}$ , to its temperature drop in the expansion  $/T_{Ei} - T_{E/i+1}/$ , and inversely proportional to the latent heat

$/h_{E''/i+1} - h_{E'/i+1}/$  at a saturation temperature of  $T_{E/i+1}^{-\Delta T_b}$ :

$$M_{E/i+1} = \frac{W_{Ei} / T_{Ei} - T_{E/i+1}}{h_{E''/i+1} - h_{E'/i+1}}$$

The situation mostly experienced is shown in Fig. 46, where condensed vapour  $M_{E1}$  through  $M_{E7}$  are flashed in parallel lines with the expanding slurry, so that the full amount of flashing fluid does not change. The vapours that left the flashing slurry stream in the course of repeated ex-

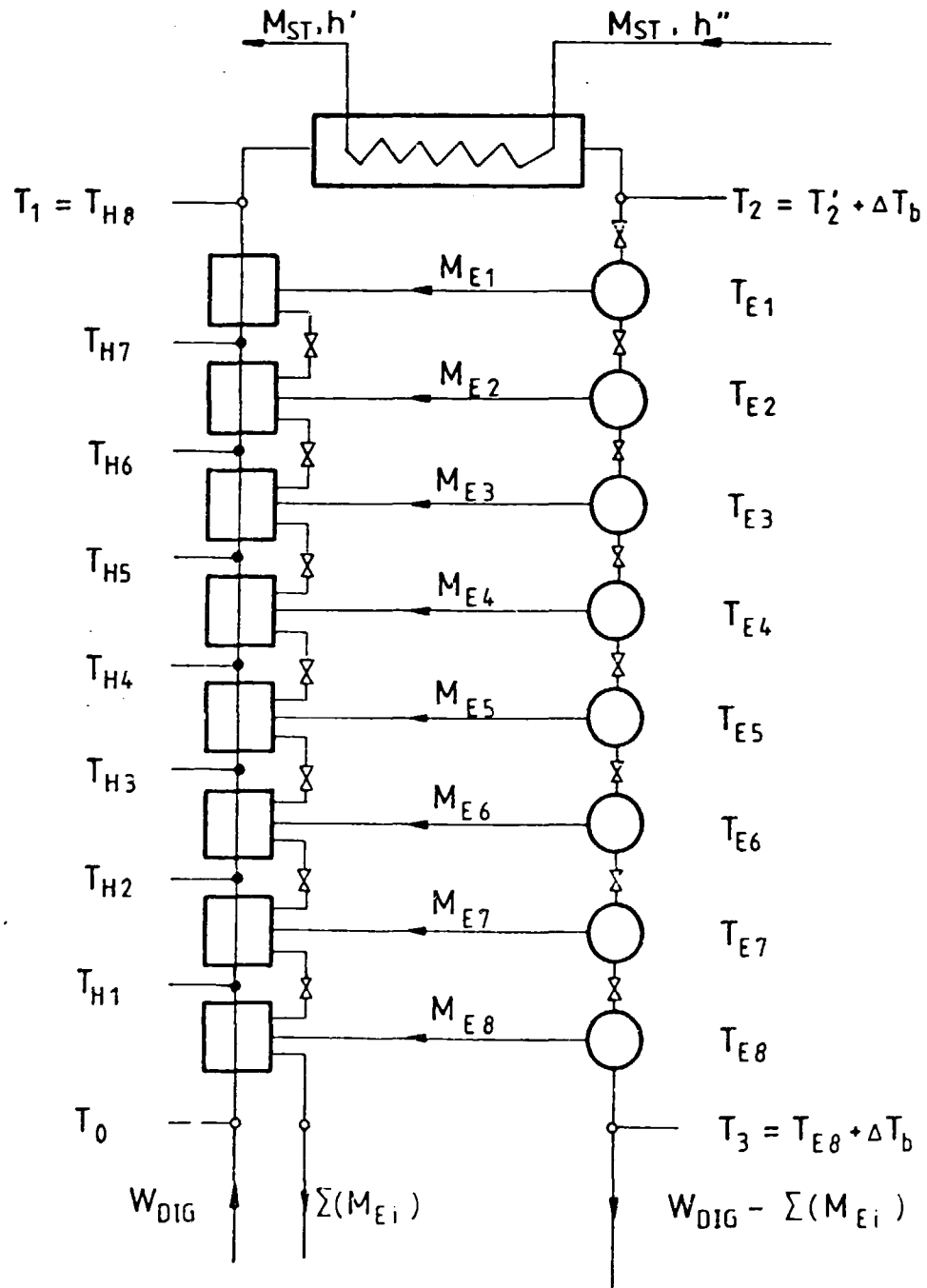


Fig. 46. Flow sheet of digestion



pansions are conducted to the heat exchangers and continue to expand as proceeding to ever lower pressures. So the vapours missing from the slurry side are accumulating in the parallel condensate stream. The heat balance of the whole heat recovery section can be set up then according to Fig. 47.

Heat delivered by flash cooling:

$$4.1868/W_{DIG} \times T_2 - /W_{DIG} - \sum/M_{Ei}/T_3 - \sum/M_{Ei}/x/T_3 \Delta T_b //$$

Heat gained in the heating line:

$$Q_{HR} = 4.1868 W_{DIG} /T_1 - T_0/ \quad /MJ/t/$$

The difference between the two gives the radiation loss of the heat recovery section  $/Q_{LR}/$ .

When analysing this heat loss in the T-Q diagram, the slope of the heating line  $T_0 - T_1$  appears to be flatter than that of the cooling line  $T_2 - T_3$  as shows in Fig. 47.

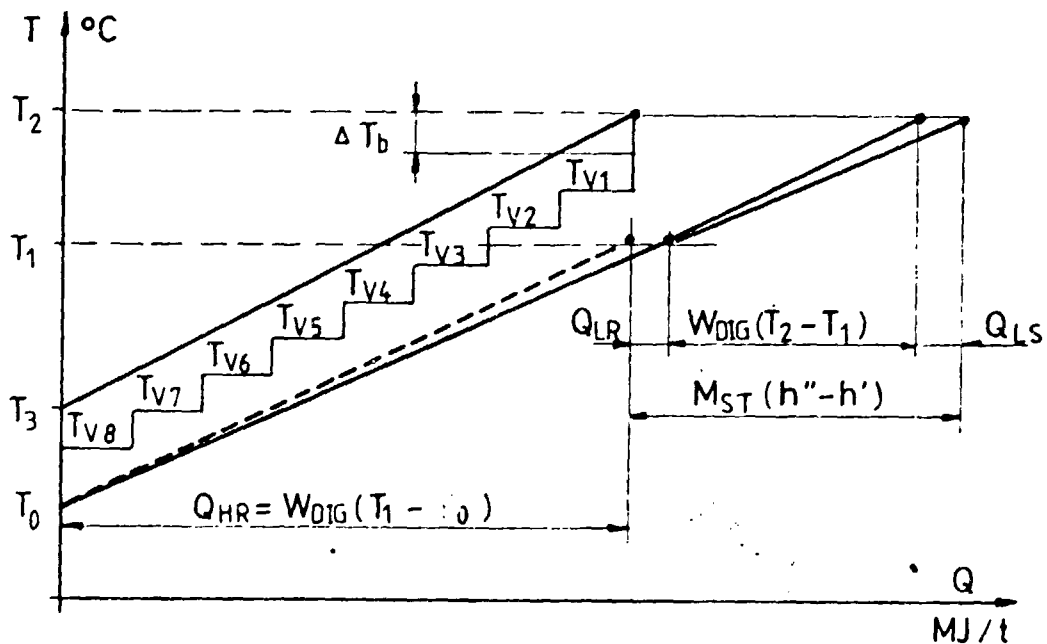


Fig. 47. T-Q diagram of digestion

In the section heated by live steam, the temperature of the digestion slurry reaches its final  $T_2$  temperature. The main part of alumina is thought to get dissolved here, a reaction absorbing energy, and further heat loss by radiation must be reckoned with in this section, too. So the heat delivered by the condensing live steam

$$Q_{ST} = M_{ST} / h'' - h' / \text{ in } / \text{MJ/t/} \text{ will always be more}$$

than required for raising the temperature of the process fluid from  $T_1$  to  $T_2$ . The difference may be accounted for reaction heat and reaction loss which flattens the heating line as compared to the ideal slope expressed by

$$\frac{T}{Q} = \tan \alpha = \frac{1}{4.1868 \times W_{DIG}}$$

In Fig. 47 this part of heat loss is given as  $Q_{LS}$ . The heat supply of live steam has to compensate for all heat losses as shown in the graph. From temperature measurements of flashing vapours  $/T_{v1}$  through  $T_{v8}/$  and corresponding slurry temperature readings of heating slurry stream between  $T_0$  and  $T_1$  the mean logarithmic temperature difference can be computed as described earlier. By taking the heat flow rates  $/W_{DIG}/$  and the corresponding heat transfer areas  $/A_r/$  the heat transfer coefficient for each stage can be established.

A term for average heat transfer coefficient of the entire heat recovery section may be calculated according to

$$K_R = \frac{\sum /A_i \cdot K_i/}{\sum /A_i/}$$

The average heat transfer coefficient is an important result of the energy audit, because it determines the efficiency of heat recovery and, by that, the live steam consumption of digestion as well.

Heat recovery is but one benefit of flash cooling. The other important gain is water extraction. The total water separated  $\Sigma/M_{Ei}$  is a substantial contribution to restore the water balance of the cycle.

## 7.2 Clarification

Primary aim of this operation is to separate red mud from aluminate liquor. Red mud discharge for dumping should be made with least losses on solubles /caustic soda and alumina/, achieved by counter-current decantation.

Sedimentation in thickeners is mostly applied. Fig. 48 shows a series consisting of one thickener and five wash settlers: a frequent arrangement used in alumina plants.

The digested and flash-cooled slurry enters as feed  $V_F$  and mixes with overflow of the first washer /stage 2/  $V_{O2}$ . Diluted aluminate liquor leaves as thickener overflow  $V_{O1}$ .

At the other end of the washer series, wash water  $V_w$  enters the last washer /stage 6/ wherefrom  $V_{u6}$  discharges to red mud dumping.

The energy balance concentrates on unit heat flow rates which come into and go out from the process unit. The difference between the two appears as heat loss radiated to the environment. The heat content of the last stage under-

flow discharged to the mud dump constitutes a significant waste heat item of the plant.

To quantify the heat balance, a mass balance is set up first. Readings of solids concentrations  $/C_s/$  may be used to calculate unit underflow volumes  $/V_u/$ .

Any volume of slurry consists of a liquid and a solid portion:

$$V = V_L + V_S$$

with the mass  $/M_s/$  and the specific weight  $/\rho_s/$  of the solids content known:  $V_S = M_s / \rho_s$ , and solids concentration  $/C_s/$  can be

expressed by

$$C_s = \frac{M_s}{V_L + V_S} = \frac{M_s}{V_L + M_s / \rho_s} \quad /t/m^3/$$

or rearranged:

$$M_s = \frac{V_L}{1 - C_s / \rho_s} \cdot C_s \quad /t/$$

$$\text{and } V_L = \frac{1 - C_s / \rho_s}{C_s} \cdot M_s \quad /m^3/$$

The last expression is very helpful to calculate the underflow volumes of the settlers. The unit mass of solids moving down through every settler is the red mud calculated to be:

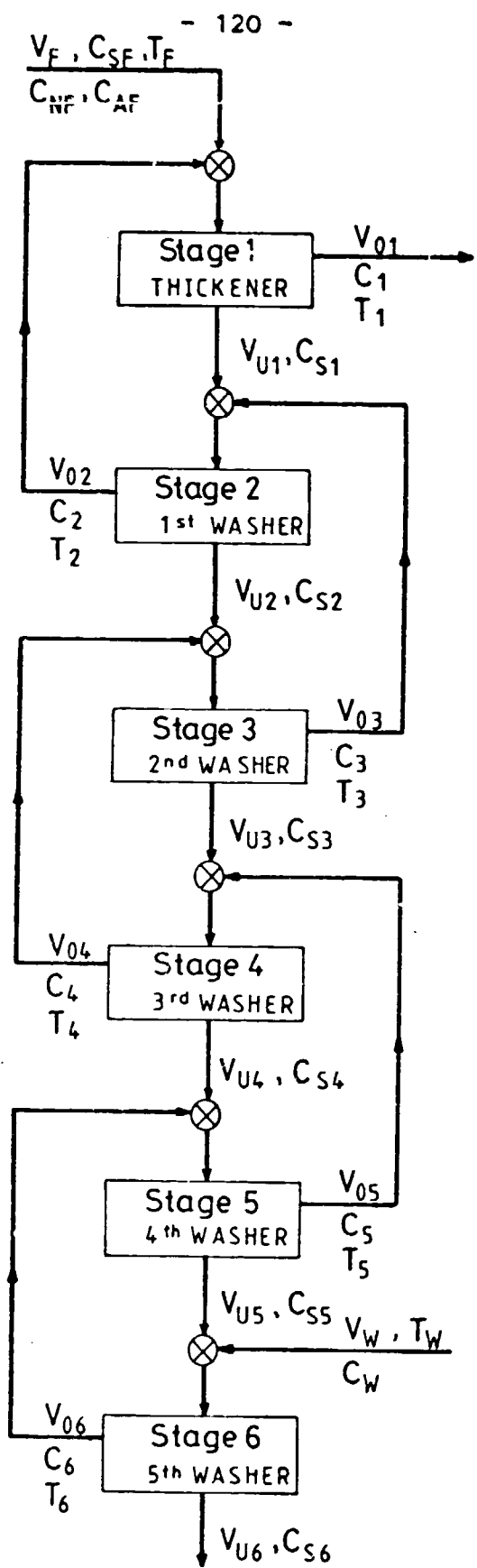


Fig. 48. Flow sheet of settling-washing

$$M_s = M_{rm} = M_B \frac{Fe_{bx}}{Fe_{rm}} \text{ taking the data used earlier}$$

in the case example this would result in:

$$M_s = M_{rm} = 2,306 \cdot 0,4545 = 1,048 \text{ t/t}$$

In this way the readings of solids concentration  $/C_s/$  could directly be used to calculate corresponding liquid volumes of the underflow, as shown in Table below.

The specific weight of solids was taken as  $\rho_s = 3 \text{ t/m}^3$ .

Table 22. Solids concentrations and liquid volumes in underflow

$C_s$ t/m <sup>3</sup>	0.200	0.300	0.400	0.500	0.600	0.700
$V_u$ m <sup>3</sup> /t	4.891	3.144	2.271	1.747	1.397	1.148

Referring to Fig. 48 the underflow volumes can be computed from solids concentrations:

$$V_{u1} = M_{rm} \frac{1 - C_{s1}/\rho_s}{C_{s1}}$$

$$V_{u6} = M_{rm} \frac{1 - C_{s6}/\rho_s}{C_{s6}}$$

The balance of caustic soda can be written for any stage. Denoting the caustic soda concentration by the subscript number indicating the stage to which it belongs, the overflow volume can be evaluated:

$$V_{O1} = V_F + V_W - V_{U6} \quad /1/$$

$$V_{O2} = V_F \frac{C_F - C_1}{C_1 - C_2} \quad /2/$$

$$V_{O3} = V_{U1} \frac{C_1 - C_2}{C_2 - C_3} \quad /3/$$

$$V_{O4} = V_{U2} \frac{C_2 - C_3}{C_3 - C_4} \quad /4/$$

$$V_{O5} = V_{U3} \frac{C_3 - C_4}{C_4 - C_5} \quad /5/$$

$$V_{O6} = V_{U4} \frac{C_4 - C_5}{C_5 - C_6} \quad /6/$$

$$V_W = V_{U5} \frac{C_5 - C_6}{C_6 - C_W} \quad /7/$$

Equation /1/ comes from the overall volume balance of the whole settling-washing operation.

Equation /7/ is important because it determines the red mud wash water which is the largest item in the water balance of the plant.

Mass flow rates /M/ and heat capacities /W = water equivalents/ can be calculated as shown previously. The overall heat balance will be:

1. Unit heat rates in:

$$1.1 \quad Q_F = W_{DIG} - \sum M_{Ei} // T_F$$

$$1.2 \quad Q_W = W_W \times T_W$$

2. Unit heat rates out:

$$2.1 Q_{O1} = W_{O1} \times T_1$$

$$2.2 Q_{U6} = W_{U6} \times T_6$$

$$2.3 Q_{RAD \text{ loss}} = Q_F + Q_W - Q_{O1} - Q_{U6}$$

Remark:  $Q_{U6}$  is regarded as waste heat discharged.

### 7.3 Precipitation

Precipitation of alumina hydrate crystals from super-saturated liquor gradually changes its composition. First of all the alumina concentration will fall. With concentration readings before and after precipitation for example of

$$C_{A1} = 135.5 \text{ kp/m}^3 \quad C_{A2} = 65.7 \text{ kp/m}^3$$

the difference between the two is  $C_{A1} - C_{A2} = 69.8 \text{ kp/m}^3$ . Since the molecular weights of  $\text{Al}_2\text{O}_3$  and  $\text{Al}_2\text{O}_3 \cdot 3\text{H}_2\text{O}$  are 102 and 156, 69.8 kp  $\text{Al}_2\text{O}_3$  means 106.8 kp  $\text{Al}_2\text{O}_3 \cdot 3\text{H}_2\text{O}$ , so that  $106.8 - 69.8 = 37 \text{ kp H}_2\text{O}$  are also taken out of each  $\text{m}^3$  of initial liquor volume. Consequently, the initial caustic soda concentration  $/C_{N1}/$  of  $140 \text{ kp/m}^3$  in the case investigated will increase to:

$$C_{N2} = \frac{C_{N1} \times 1.000}{1.000 - 0.037} = \frac{140}{0.963} = 145.5 \text{ kp/m}^3$$

So the alumina precipitated from one cubicmeter of liquor



$$C_{N2} \left[ \left( \frac{C_A}{C_N} \right)_1 - \left( \frac{C_A}{C_N} \right)_2 \right] = 145.5 / \frac{135.5}{140} - \frac{65.7}{145.5} / = 75.1$$

kp Al<sub>2</sub>O<sub>3</sub>/m<sup>3</sup>

With, for instance,  $V_{AL} = 13.7 \text{ m}^3/\text{t}$ , the alumina output would be  $13.7 \times 75.1 = 1029 \text{ kp Al}_2\text{O}_3/\text{t}$ , that is, 2.9 per cent more than theoretically required.

The precipitation section consists of diverse functional parts, and a flow sheet as shown in Fig. 49 will be helpful for further considerations.

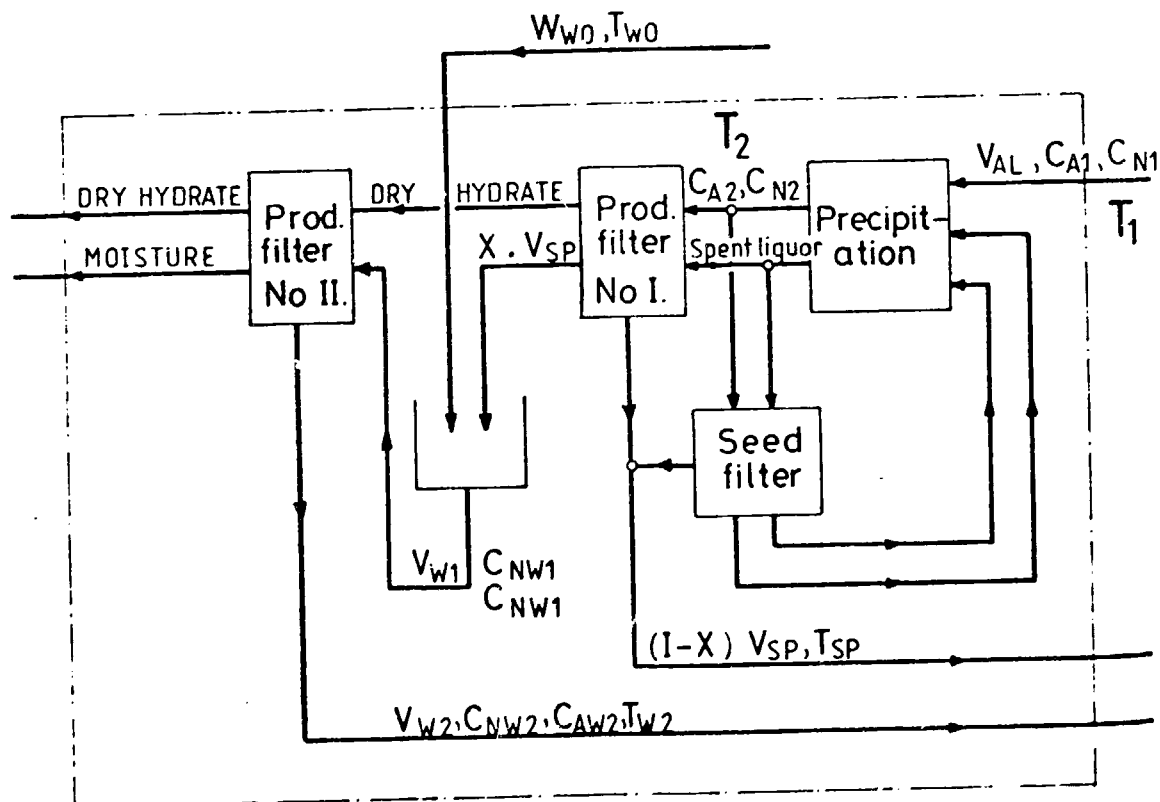


Fig. 49. Functional flow sheet of precipitation

The energy balance of precipitation consists of incoming heat flow rates, the energy generated by the crystallization reaction on the one side, and outgoing heat flow rates and radiation losses on the other side of the balance.

The recycling seed flow must not be considered because it is fully confined within the balance boundary.

The unit heat of aluminate liquor feed is

$$Q_{AL} = 4.1868 \times W_{AL} \times T_{AL1} \quad \text{MJ/t, where}$$

$$W_{AL} = V_{AL} + 4.905 \times 10^{-4} N_{AL} + 2.725 \times 10^{-4} A_{AL}$$

and

$$N_{AL} = V_{AL} \times C_{N1} \text{ /kp Na}_2\text{O/t/}$$

$$A_{AL} = V_{AL} \times C_{A1} \text{ /kp Al}_2\text{O}_3\text{/t/},$$

$V_{AL}$  being the unit volume rate of aluminate liquor;

$C_{N1}$  its caustic soda-,  $C_{A1}$  its alumina concentration.

The product hydrate discharged to calcination consists of the dry material  $\text{Al}_2\text{O}_3 \cdot 3\text{H}_2\text{O}$  which was found to have the unit mass rate

$M_{HD} = 1.029 \text{ t/t}$ , and the moisture represented in

weight per cent would typically be about  $W = 12$  per cent, so the total wet hydrate weight is

$$M_{HW} = /1 + W/M_{HD} = 1.12 \times 1.029 = 1.15 \text{ t/t}$$

The unit heat flow rate of hydrate discharge

$$Q_{HW} = 4.1868/0.2 \times M_{HD} + 1.0/M_{HW} - M_{HD} // T_H \quad /MJ/t/$$

where  $T_H$  is the temperature of product hydrate.

The unit mass of spent liquor can be calculated from the precipitation balance

$$M_{AL} - M_{HD} = M_{SP} \quad t/t \quad \text{and}$$

$$V_{SP} = M_{SP} - 0.0011355 \times C_{N2} - 0.0009396 C_{A2}$$

The wash water intake and outlet may be computed by using concentration readings in the washing process. The required information is gained by stepwise calculations. The portion of spent liquor washed out in the production filter No.I:

$$X \times V_{SP} = V_{WO} \frac{C_{NW1}}{C_2 - C_{NW1}} \quad m^3/t$$

which in unit mass rate is:

$$X M_{SP} = X V_{SP} / 1 + 0.0011355 \times C_{N2} + 0.0009395 C_{A2} / \quad t/t$$

Mass balances around the production filters No.I and No.II:

$$M_{WO} + X M_{SP} = M_{W1} \quad t/t$$

$$M_{W1} - /M_{HW} - M_{HD}/ = M_{W2} \quad t/t \quad \text{which converts into}$$

$$V_{W2} = M_{W2} - 0.0011355 \times C_{NW2} - 0.0009395 \times C_{AW2} \quad m^3/t$$

The remaining portion of spent liquor computes to

$$/1 - x/ V_{SP} = V_{SP} - x V_{SP} \quad m^3/t$$

The concentrations, mass and volume rates of all streams have been found. There is no difficulty in setting up the associated unit heat flow rates.

Heat balance of precipitation:

1. Unit heat rates in:

1.1 Aluminate liquor  $Q_{AL} = 4.1868 \times W_{AL} \times T_1$

1.2 Wash water in  $Q_{WO} = 4.1868 \times W_{AL} \times T_{WO}$

2. Unit heat rates out:

2.1 Product hydrate  $Q_{HW} = 4.1868/0.2M_{HD} + 1.0/M_{HW} - M_{HD} // T_H$

2.2 Spent liquor  $Q_{SP} = 4.1868/1-x/W_{SP} \times T_{SP}$

2.3 Wash water out  $Q_{W2} = 4.1868 \times W_{W2} \times T_{W2}$

2.4 Radiation loss  $Q_{RL} = Q_{AL} + Q_{WO} - /Q_{HW} + Q_{SP} + Q_{W2}/$

Discussion of results:

The radiation loss caused by free cooling of the aluminate liquor during the time of precipitation constitutes the most significant part of the total radiation loss of the cycle. Every modification in precipitation technology resulting in improved liquor utility, expressed by

$$a = C_{N2} \left[ \left( \frac{C_A}{C_N} \right)_1 - \left( \frac{C_A}{C_N} \right)_2 \right] \frac{\text{kp Al}_2\text{O}_3 \text{ precipitated}}{\text{m}^3 \text{ aluminate liquor}}$$

will reduce the unit volume of aluminate liquor by

$$V_{AL} = \frac{1000}{a} \text{ /m}^3\text{/t/}, \text{ and its heat capacity to}$$

$$W_{AL} = \frac{1000}{a} + 4.905 \times 10^{-4} x C_{N1} + 2.725 \times 10^{-4} x C_{A1} \text{ t/t.}$$

The unit rate of hydrate wash water  $V_{WO}$  should be kept as low as possible because it helps to reduce evaporation load. Live steam consumption in the evaporators is proportional to the amount of water to be removed from the liquor cycle.

## 8. Evaporation

### 8.1 Multieffect evaporators

In an ideal evaporator without any heat loss and with negligible temperature difference between the heating steam and the heated water, any ton of steam would evaporate one ton of vapour from the water which would be at the same pressure and temperature as that of the steam.

The condensate of the heating steam would also have the same temperature as the boiling water.

With any temperature difference between the heating steam and the evaporating water, the vapour pressure and temperature would be lower than that of the heating steam, although there would be no significant difference between their respective enthalpies.

The vapour of the first evaporator could be utilized in the second evaporator, with a boiling point below that of the saturation temperature of the first vapour. This way of thinking led to the concept of double- and multi-effect evaporation, where a series of evaporators are linked by heating vapours of gradually decreasing pressure.

The steam consumption rate per unit of evaporated water decreases with the number of effects /n/ applied; steam economy will be better for liquids of lower boiling point elevation, and deteriorate with higher rise of boiling points. Table 23. below gives approximate data.

Table 23. Steam consumption rate per unit of evaporated water

number of steps		1	2	3	4	5	6
$\frac{\text{steam consumed}}{\text{water evaporated}}$	$\left[ \frac{t}{t} \right]$ low	1.1	0.57	0.40	0.30	0.24	0.21
	$\left[ \frac{t}{t} \right]$ high	1.3	0.65	0.48	0.36	0.28	0.24

### 8.2 Co-current evaporator stations

In the flow sheets of Figures 50 and 51 roman numbers denote the sequence of evaporator stages along diminishing vapour pressures. The arabic numbers attached to each roman number indicate the sequence of liquor flow through the individual evaporators.

The cocurrent flow evaporator in Fig. 50 features evaporation stages with both roman and arabic numbers increasing

in the same direction. Liquor enters stage I/1 at high temperature and is heated by live steam. Liquor boils down in succession over II/2, III/3 to IV/t at ever decreasing temperatures, heated by constantly falling temperature vapour. One of the most useful features of cocurrent flow evaporators is the spent liquor preheater series heated by vapours extracted from appropriate evaporator stages, also shown in Fig. 50.

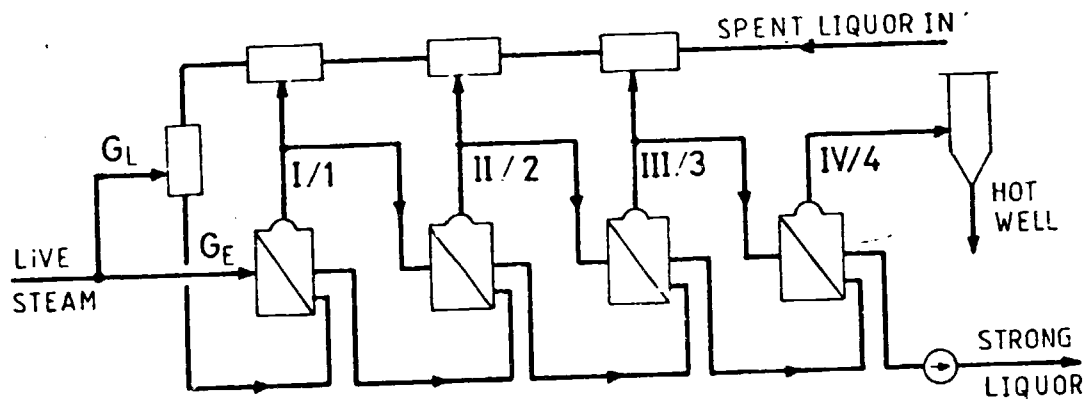


Fig. 50. Cocurrent-flow evaporator

Preheating could at best bring liquor temperature close to the first vapour temperature which would still be lower than the liquor temperature in the first evaporator vessel /at least by the difference of boiling point elevation/. Anyway, the steam economy of the evaporator plant will be the better the more the final preheat temperature will approximate the boiling temperature in the final vessel.

With a  $G_L$  fraction of the total live steam consumption required to bring the liquor to boiling, only the remaining part  $G_E$  would vapourize the liquor.

The multiple use of steam will apply only for that portion of heating steam which is actually engaged in vaporization. Similarly, each portion of vapour extracted from any stage will not precipitate in evaporating in the remaining effects.

### 8.3 Counter current evaporator stations

Spent liquor enters evaporator IV/1 of the counter current flow evaporation scheme in Fig. 51, number IV indicating the vessel with the lowest vapour pressure. So spent liquor feed temperature will be close to the boiling point in the vessel and there is no sense in liquor preheating as practiced in co-current flow evaporation.

Instead, the high temperature liquor discharge from stage I/4 heated by live steam is flashed through a sequence of expanders EI, EII, EIII, EIV, the roman numbers indicating the vapour pressures of the comparative evaporator stages.

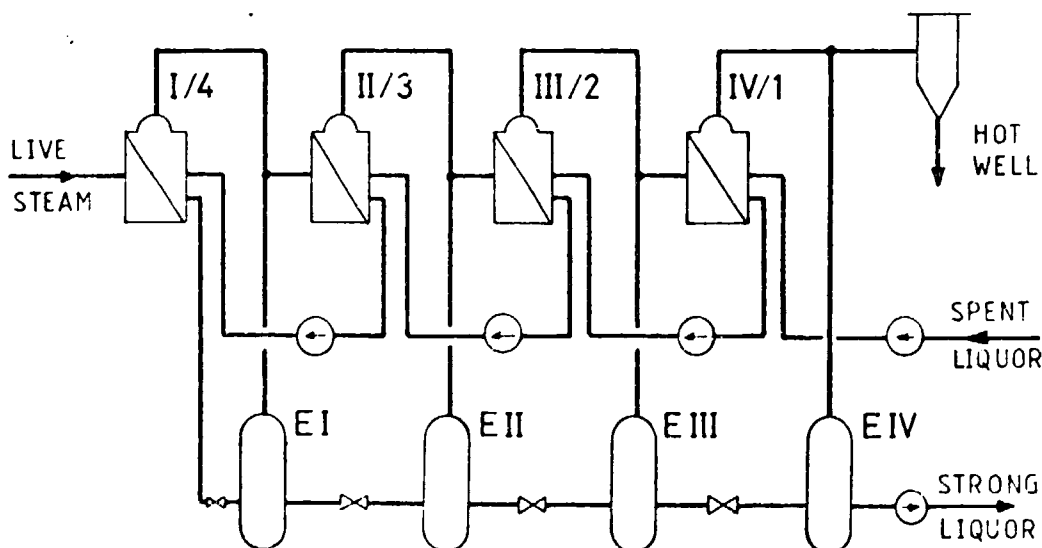


Fig. 51. Counter current evaporator



Additional evaporation takes place in the flashing stages and flashed vapours are fed back to appropriate evaporator stages, contributing effectively to reduction of live steam requirement. Temperatures of both spent liquor feed and slurry liquor discharge will be close to each other.

#### 8.4 Economy of vapour extraction for heating purposes

The advantage of using vapours extracted from the evaporator stages for heating purposes may be elucidated by quantifying live steam requirements of two different solutions serving the same purpose, namely to evaporate  $W_E$  tons of water and additionally raise the temperature of a process liquid  $W_L$  by a temperature difference of  $(T_2 - T_1)$ .

In one case the problem is solved - as shown in Fig. 52 - by using a five-stage multiple effect evaporator with the

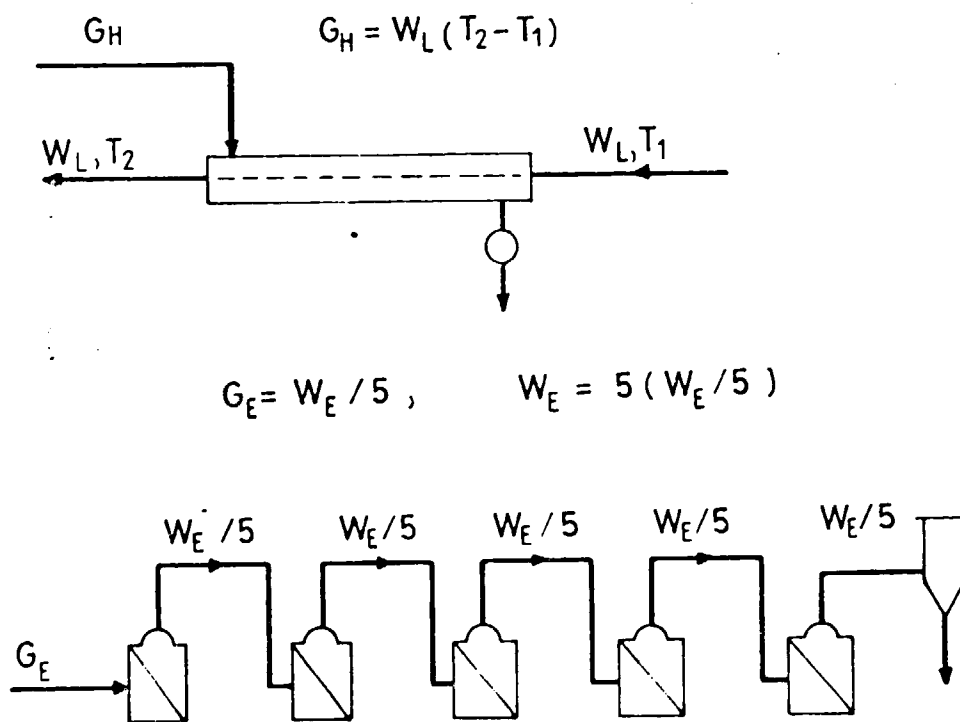


Fig. 52. Case solution No.1

capacity to evaporate a total of  $W_E$  tons of water in five equal parts, and a separate heat exchanger, to raise the temperature of the process liquid  $W_L$ , by  $/T_2 - T_1/$  centigrades.

Total live steam required in case 1:

$$G_1 = G_E + G_H = WE/5 + G_H$$

Another answer to the question is shown on the flow sheet in Fig. 53.

$$G_H = 4 \cdot \frac{G_H}{4} = W_L (T_2 - T_1) \quad G_E' = \frac{W_e'}{5} + 4 \frac{G_H}{4}$$

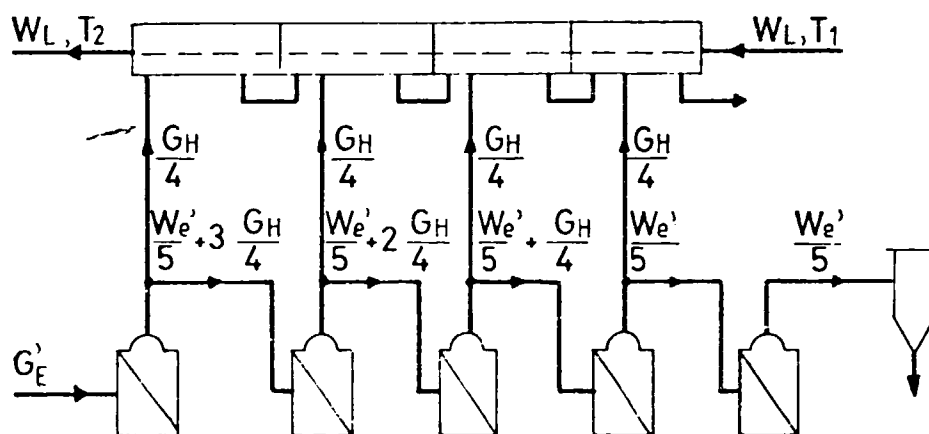


Fig. 53. Case solution No.2

Because total evaporation in both cases is equal

$$\begin{aligned} 5 \frac{W_E}{5} &= 5 \frac{W_E'}{5} + \frac{4G_H}{4} + \frac{3G_H}{4} + \frac{2G_H}{4} + \frac{G_H}{4} = \\ &= 5 \frac{W_E'}{5} + \frac{10 G_H}{4}, \text{ therefore} \end{aligned}$$

$$5 \frac{W_E'}{5} = 5 \frac{W_E}{5} - \frac{10}{4} G_H \quad \text{so}$$

$$\frac{W_E'}{5} = \frac{W_E}{5} - \frac{2}{4} G_H \quad \text{substituting into equation above}$$

$$G_E' = \frac{W_E}{5} - \frac{2}{4} G_H + \frac{4}{4} G_H = \frac{W_E}{5} + \frac{1}{4} G_H$$

Total live steam required in case 2 is:

$$G_2 = G_E' = \frac{W_E}{5} + \frac{1}{2} G_H$$

So the difference in total live steam requirements between the cases is  $G_1 - G_2 = \frac{1}{2} G_H$  i.e. half of the steam required for preheating the liquid  $W_L$  from  $T_1$  to  $T_2$  is saved by using extracted steam.

#### 8.5 Flash evaporators

Heating with live steam can fully be realized in liquor heaters, so the heat transfer takes place always between condensing vapours on the shell side and the process liquor flowing through the tubes of the heat exchanger. /In multiple effect evaporators the condensing vapours heat a boiling liquid./

The flash evaporation is similar to digestion with flash type heat recovery. To get the required quantity of water out of the liquor, either a wide temperature range of flashing, or large volume rates forced through the flashing process is needed.

To increase flashing volume rates, one portion of liquor discharge is recirculated for repeated flashing. Its

use is limited to low caustic concentration types of Bayer cycles where large volumes and small concentration difference between spent and strong liquors are available.

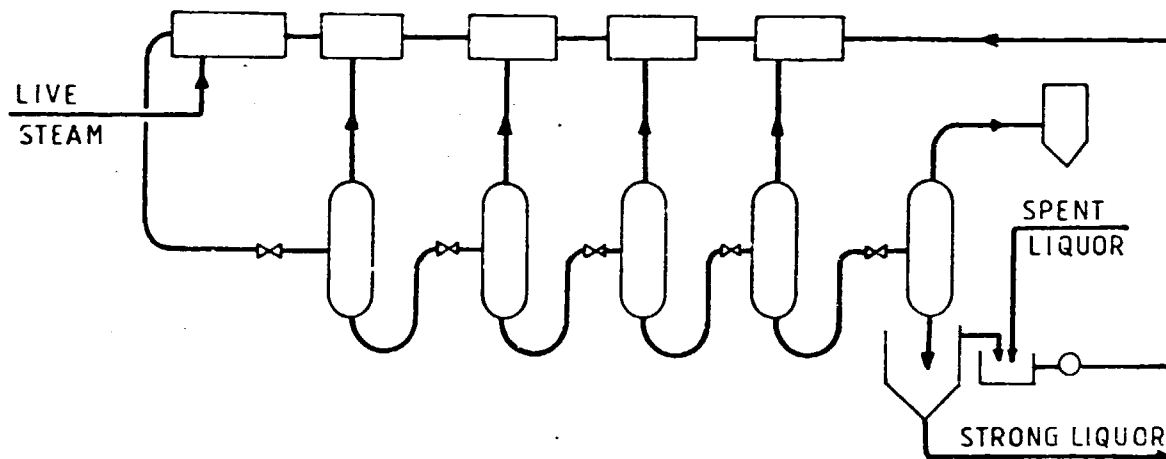


Fig. 54. Flash type evaporator

The steam economy depends mainly on the number of flashing stages applied, and is of similar magnitude to that of the comparable multicolumn evaporators.

#### 8.6 Thermo-compression

Another way of improving steam economy is to rise the vapour pressure by compression to the level of the heating steam. Again, the live steam consumption can be cut sharply. This concept is called thermo-compression. It requires only a single evaporator stage. No hot well loss occurs but additional shaft power is needed to drive the compressor. A small amount of live steam is required to compensate for heat losses.

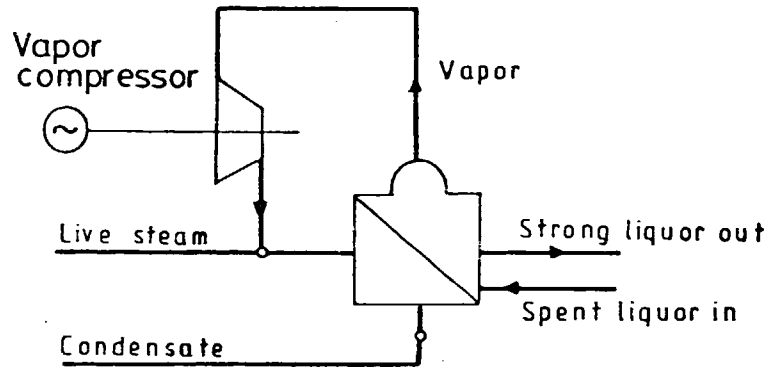


Fig. 55. Thermocompression type evaporator

The overall economy of the thermocompression and the multistage evaporation depends on the local cost ratio of steam and electricity.

Case example as given in Table 24 may serve as guideline for making the choice under the prevailing local price conditions:

Evaporation  $W = 50$  t/h

Boiling point elevation  $T_b = 10$  °C

Total temperature difference of heat transfer  $T = 20$  °C

Table 24. Economy of thermocompression  
/after Kondorossy, Ref. 69/

	Consumption		Energy prices	
	Thermo- compression	5-stage Multieffect	Case I.	Case II.
Live steam	0.3 t/h	12.5 t/h	10 \$/t	30 \$/t
Electricity	-	900 m <sup>3</sup> /h	0.025 \$/m <sup>3</sup>	0.05 \$/m <sup>3</sup>
Energy costs per annum in Case I.	959,100 \$	1,287,000 \$		
	Difference = + 1,269,450 \$			
Energy costs per annum in Case II.	585,000 \$	1,854,450 \$		
	Difference = + 1,269,450 \$			

Remarks: 1/ The installation cost of the thermocompressor unit will be \$ 500,000 more than that of the 5-stage multieffect evaporator unit.

2/ The annual energy costs have been calculated on a basis of 7800 hours per year operation.

The probable choice will be thermocompression in regions with abundant and cheap hydropower, or with costly fuel resources /natural gas, fuel oil/ for steam generation.

When the generation of electricity in a region is based on thermal power stations, the most economical solution will very likely be the application of multieffect or flash type evaporation.

8.7 Energy audit of the evaporation section

The energy audit concentrates upon the heat balance which in turn is footed on the mass balance. They again strongly depend on the process flow sheet of the evaporation section. The procedure can therefore best be shown by taking the existing plant flow sheet /in the case to be discussed, this is a co-current type 4-stage evaporator with feed liquor preheat by extracted vapours from three stages - as given in Fig. 56. - to avoid lengthy generalizations.

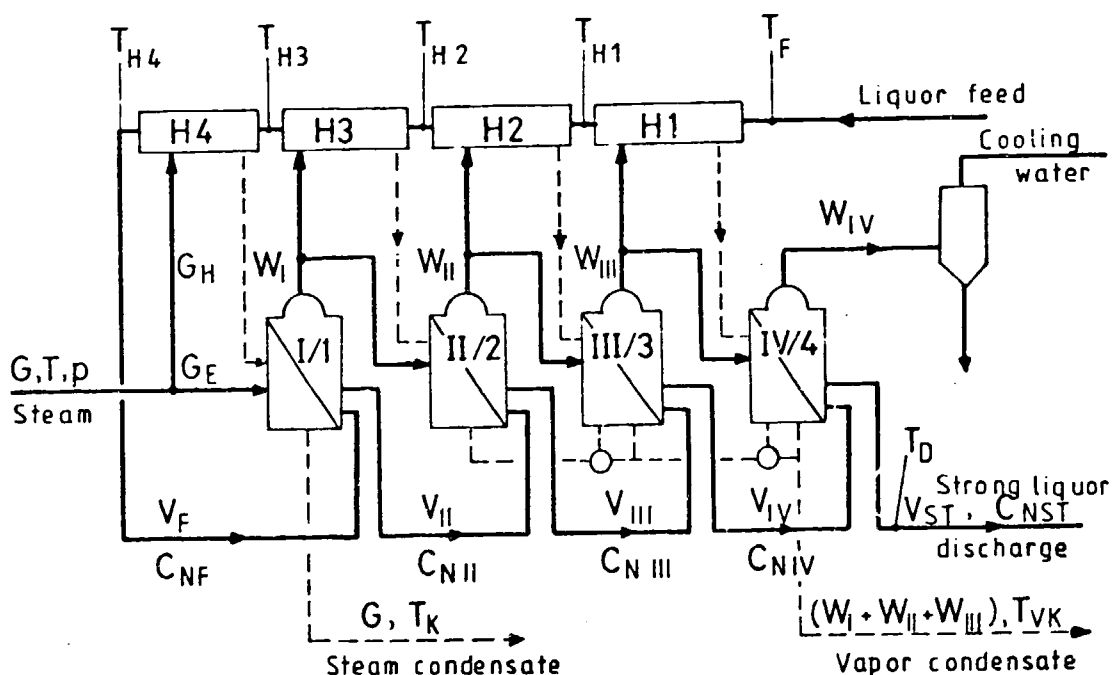


Fig. 56. Evaporation flow sheet

The unit mass flow rate of the liquor feed and its composition can be calculated by known unit volume rates of spent liquor and hydrate wash to be calculated and their respective alumina and soda concentrations:

$$N_F = V_{SP.L} \times C_{N\ SP.L} + V_{HW} \times C_{NHW} \quad /kp\ Na_2O/t/$$

$$A_F = V_{SPL} \times C_{ASP.L} + V_{HW} \times C_{AHW} \quad /kp\ Al_2O_3/t/$$

$$M_F = /V_{SPL} + V_{HW}/ + 1.1355 \times 10^{-3} \times N_F + 0.9395 \times 10^{-3} \times A_F \quad /t/t/$$

The water equivalent /expressing specific heat capacity in Mcal/t, °C/ of liquor feed

$$W_F = M_F - 0.000645 \times N_F - 0.000667 \times A_F \quad /Mcal/t, °C/,$$

and the heat flow of evaporation liquor feed:

$$Q_F = W_F \times T_F \text{ which boils down to}$$

$$Q_F = /V_V + 4.905 \times 10^{-4} \times N_F + 2.725 \times 10^{-4} \times A_F / T_F \quad /Mcal/t/$$

The unit volume rate of strong liquor discharge can be derived from its measured  $C_{NST}$  caustic soda concentration:

$$V_{ST} = V_F \frac{C_{NST}}{C_{NF}} \quad /m^3/t/, \text{ its unit mass rate:}$$

$$M_{ST} = V_{ST} + 1.1355 \times 10^{-3} \times N_{ST} + 0.9395 \times 10^{-3} \times A_{ST} \quad /t/t/,$$

wherein:

$$N_{ST} = V_{ST} \times C_{NST} \quad /kp/m^3/ \quad \text{and}$$

$$A_{ST} = V_{ST} \times C_{NST} \times \frac{A_F}{N_F} \quad /kp/m^3/, \text{ assuming that}$$

the  $C_A/C_N$  ratio remains unchanged during evaporation.



The heat flow by strong liquor discharge

$$Q_{ST} = /V_{ST} + 4.905 \times 10^{-4} \times N_{ST} + 2.725 \times 10^{-4} \times A_{ST} / T_D \quad /Mcal/t/$$

Unit mass of total water evaporated

$$W = W_I + W_{II} + W_{III} + W_{IV} = M_F - M_{ST} \quad /t/t/$$

The unit water masses evaporated in any stage  $/W_I, W_{II}, W_{III}$  and  $W_{IV}/$  can be derived by similar procedure.

The heat content of live steam and vapours can be taken from steam tables by their pressure and temperature readings. With  $h_{ST}''$ ,  $h_I''$ ,  $h_{II}''$ ,  $h_{III}''$  and  $h_{IV}''$  denoting heat contents of live steam and vapours from stage I to IV and condensate heat contents  $h_{ST}'$ ,  $h_I'$ ,  $h_{II}'$ ,  $h_{III}'$ , and  $h_{IV}'$  the overall energy balance will be:

1. Unit heat rates in:

1.1 Liquor feed  $Q_F = 4,1868 / V_F + 4.905 \times 10^{-4} \times N_F + 2.725 \times 10^{-4} \times A_F / T_F$

1.2 Live steam  $Q_{ST} = G \times h_{ST}''$

2. Unit heat rates out:

2.1 Liquor discharge  $Q_D = 4,1868 / V_{ST} + 4.905 \times 10^{-4} \times N_{ST} + 2.725 \times 10^{-4} \times A_{ST} / T_D$

2.2 Vapour to hotwell  $Q_H = W_{IV} \times h_{IV}''$

2.3 Vapour condensate  $Q_{VC} = /W_I + W_{II} + W_{III} / h_{III}'$

2.4 Steam condensate  $Q_{SC} = G \times h_{ST}'$

2.5 Radiation loss  $Q_{RL} = /Q_F + Q_{ST} / - /Q_D + Q_H + Q_{VC} + Q_{SC} /$

An overall survey would furnish the information as given in the energy balance above.

The heat balances of individual evaporator vessels and attached heat exchangers can be calculated /I/1 + H4/, /H/2 + H3/, /III/3 + H2/ and /IV/4 + H1/, for an elaborate analysis.

Upon evaluating the information gained by detailed heat balance calculations, the magnitude of losses should be dealt with. The reject heat loss to the hot well /which can be one of the highest in the cycle process/ will be proportional to the total water evaporated.

The heat loss to the hot well cannot be eliminated as long as there is a need for special evaporation to restore the water balance in the cycle.

Heat consumptions of digestion and evaporation may to some extent substitute each other because evaporation reduces liquor quantity required in the digestion section and thereby cuts heat consumption of the digester.

A case example makes the point clear:

With  $15 \text{ m}^3/\text{t}$  unit liquor rate in digestion, 11.5 GJ/t high temperature heat is needed there. Making higher liquor concentration of digestion by a unit evaporation rate of  $4 \text{ m}^3/\text{t}$ , the heat consumption of the digester drops to 8.7 GJ/t. On the other hand,  $4 \text{ m}^3$  water evaporation requires about 4.5 GJ/t low pressure steam. The total heat consumed in the latter case  $8.7 + 4.5 = 13.2$  GJ/t is higher than 11.5 GJ/t of the low concentration extraction case.

When a back pressure turbine operates in the plant, the merits of low cost cogenerated electricity may again tilt the balance in favour of increased evaporation.

Performance of the evaporation plant can be quantified by relating steam consumption to the evaporated water:

$$\frac{\text{live steam}}{\text{evaporated water}} = \frac{G}{W_I + W_{II} + W_{III} + W_{IV}} = \frac{G}{M_F - M_{ST}}$$

Unit heat rates as computed can easily be converted into heat rates per hour when multiplying by the average alumina output of the plant during the period of auditing.

These data combined with more temperature readings and the heat transfer areas involved, allow the calculation of heat transfer coefficients and heat transfer efficiency in the heat exchangers and evaporators.

#### 9. Calcination

In a calciner plant, high temperature flue gas is generated by the chemical reaction of fuel combustion. The heat content of the fuel gas is gradually dissipated by radiation and convection, with a simultaneous steady decrease of flue gas temperature. Finally, it leaves the calciner at stack temperature.

At the other end, a wet filter cake is fed into the kiln and is heated in counter current heat exchange by cooling flue gases. First the adhesive moisture is vapourized and

superheated. This drying process takes place in contact with flue gas in the 200-600 °C temperature range. At about 900 °C a reaction takes place which absorbs energy: the aluminahydrate crystal structure is split and released water molecules are evaporated. On further heating to about 1200 °C a crystal modification of alumina is taking place, which is important for its use in the smelter.

The process is essentially a counter current heat exchange procedure as illustrated in the functional flow sheet of Fig. 57.

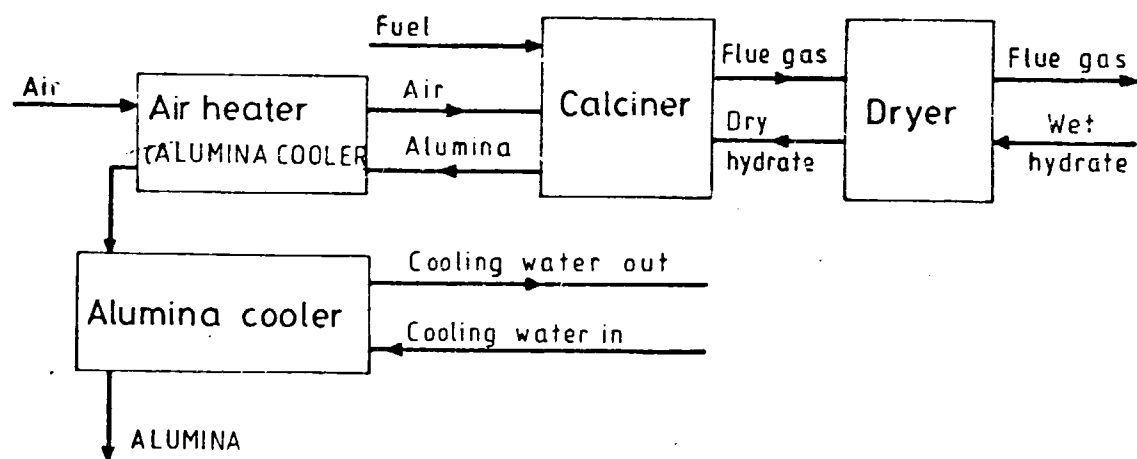


Fig. 57. Functional flow sheet of calcination

There are three basic types of calciner kilns in use:

- the conventional rotary kiln
- the fluid flash calciner
- intermediate types and retrofits.

Characteristic features are shown in the Figures 58 and 59 below.

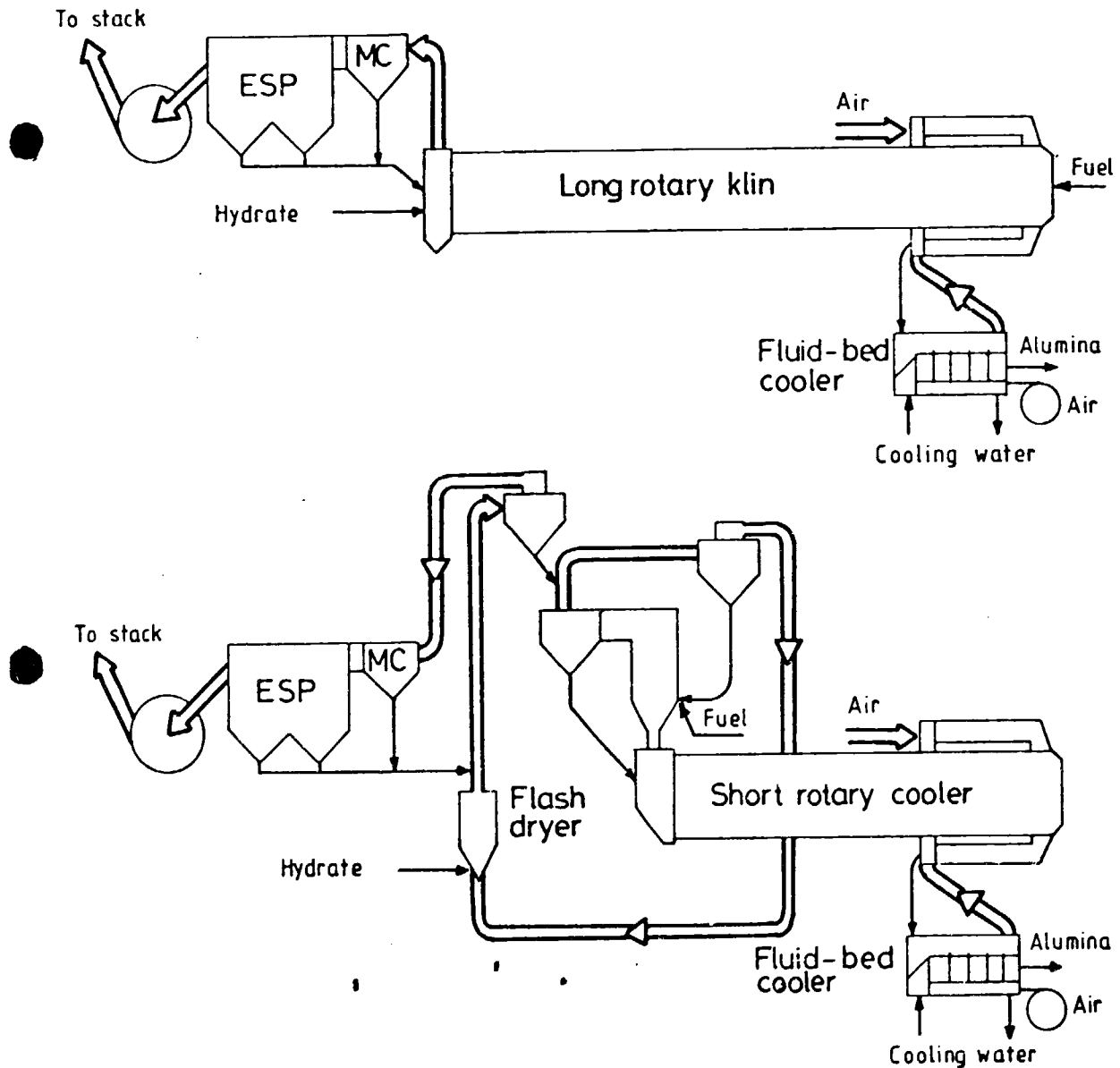


Fig. 58. Retrofitting of rotary kiln with GSC /gas sus-  
pension calciner/  
/after Raahaoye, Ref. 67/

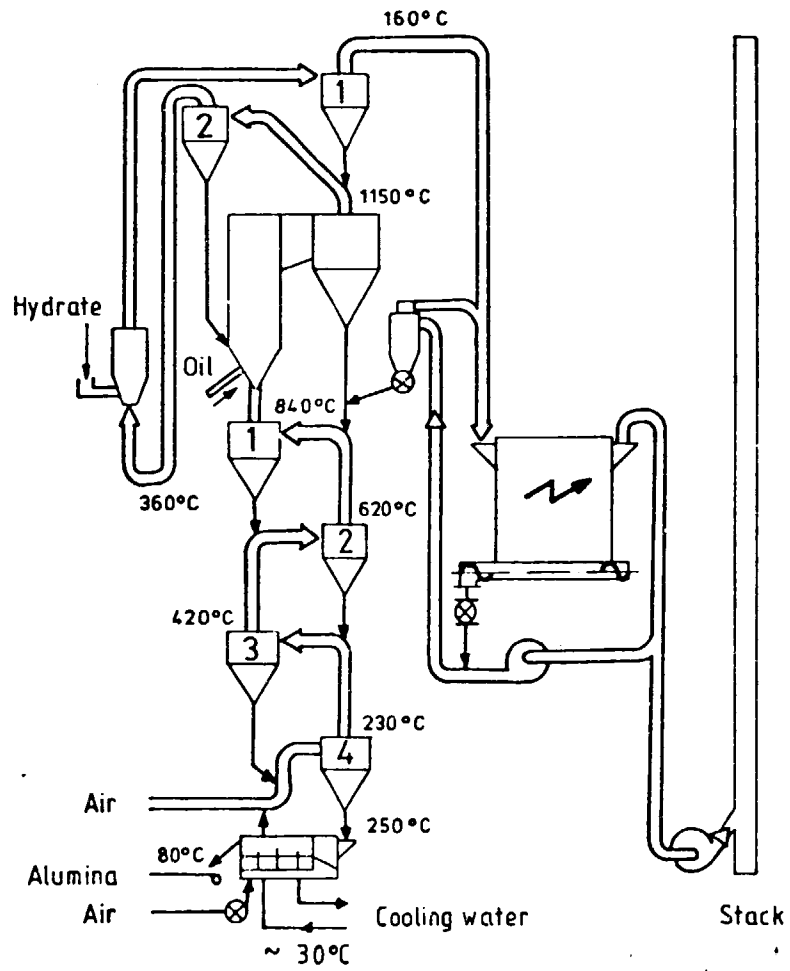


Fig. 59. Fluid flash calciner

Typical unit heat consumptions and main items of energy balances are given in Table 25.

Table 25. Energy balances of calciners

Main items of heat balance	Type of calciner kiln		
	Fluid flash	Rotary kiln	Retrofit
Water evaporation	560	600	600
Reaction heat	2020	2025	2025
Stack loss	270	500	290
Water cooling	250	300	250
Radiation loss	100	1075	635
Heat consumption	3200	4500	3800

It appears that the bad energy efficiency of conventional rotary kilns is mainly due to the large radiation loss. Stack losses may be heavier in older kilns. The remedy may be the addition of a multicyclone type heat exchanger for hydrate drying.

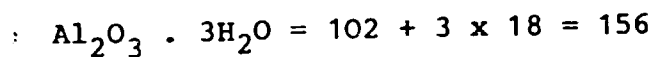
In addition, the heat wasted to cooling water is often large enough to justify the installation of a retrofit of another multicyclone type air preheater.

#### 9.1 Alumina and water balance

Aluminatrichydrate  $/\text{Al}_2\text{O}_3 \cdot 3\text{H}_2\text{O}/$  is converted into alumina during the calcination process. This reaction absorbs energy. The released water of the crystal structure and the moisture of the filler cake vapourizes and leaves the process at stack temperature. Alumina is fed to the proc-

ess at filter cake temperature and discharged at increased temperature.

The weight ratios can be quantified using molar weights of alumina and aluminatrihydrate:



so  $\frac{156}{102} = 1.53$  tons of dry trihydrate make up for 1 ton of calcined alumina.

Moisture of the filter cake is mostly given in weight per cent /W/, so the unit feed rate of filter cake amounts to  $1.53 + W$  tons. The total water feed will be:  
 $1.53 + W - 1 = 0.53 + W$ .

Calculated from the balance of the Bayer cycle and derived from hydrate feed measurements an excess will result over the actual calcined alumina product measurement discharged from the calciner and shipped to buyers. The difference is the alumina loss discharged in form of dust into the environment. The per cent of lost alumina /a/ can be quantified:

$$M_{FC} / 1 - W / \frac{102}{156} / 1 - a / = 1$$

In heat balance calculation aluminahydrate feed may be regarded to consist of alumina and water. The specific heat of alumina is about  $1.64 \text{ MJ/t, } ^\circ\text{C}$ , for water  $4.2 \text{ MJ/t, } ^\circ\text{C}$  can be used.

So the heat content of filter cake feed will be:

$$Q_{FC} = 1.64 + 0.53 + W / 4.2 \quad T_{FC}$$



The heat content of alumina at any stage /before air cooler, after air or water cooler/ may be calculated by multiplying the specific heat of 1.64 MJ/t, °C by the appropriate temperature readings.

The unit reaction energy needed to split the hydrate structure and evaporate the crystal water is about 2020 MJ/t, and the unit energy required to evaporate 1 per cent of filter cake moisture is about 45 MJ/t. So the heat absorbed for reaction and moisture evaporation is

$$Q_{\text{Reaction}} = 2020 \text{ MJ/t}$$

$$Q_{\text{W evap.}} = W \times 45 \text{ MJ/t}$$

So far the product side of the heat exchange process has been discussed. For other items of the heat balance, a detailed investigation of the combustion process with different fuels and varying conditions is essential. The practical outcome will be unit heat rate calculations linked to flue gas and air flows, like stack loss and air preheating.

## 9.2 Heat generation by combustion

In any fuel there are three elements which generate heat by oxidation, namely carbon, hydrogen and sulphur.

By knowing the molecular weights of the elements involved and the reaction heats released, the fundamental combustion equations can be formulated and heat values, oxygen and air quantities required, flue gas quantities and compositions can be derived, as shown in Tables 26 and 27.

Table 26. Combustion equations

Combustion equation Molecular weights	Reaction heat	
	KJ/kmole	KJ/kg
$C + O_2 = CO_2$ 12 + 32 = 44 kp	399,000	33,222
$H_2 + \frac{1}{2} O_2 = H_2O$ 2 + 16 = 18 kp	241,322	120,161
$S + O_2 = SO_2$ 32 + 32 = 64 kp	298,230	9,630

Table 27. Gas volumes and compositions

	Oxygen Quantity	Air Quantity	Flue gas			
			Quantity	Volume per cent		
	m <sup>3</sup> /kp	m <sup>3</sup> /kp	m <sup>3</sup> /kg	CO <sub>2</sub> /SO <sub>2</sub> /	H <sub>2</sub> O N <sub>2</sub>	/SO <sub>2</sub> /
C	1,865	8,924	8,924	20.9	-	79.1
H	5.555	26.58	32.13	-	34.6	65.4
S	0.699	3.342	3.342	20.9	-	79.1

### 9.3 Practical calculations on combustion

Practical combustion calculations should be based on the heat value of the actual fuel, rather than on its composition. A series of tables presented in the followings will make calculations convenient.

Table 28 gives data and formula for volume of air, flue gas and its compositions. Any volume can be computed by multiplying either by the net heat value of the fuel involved to get the corresponding data related to the combustion of one unit quantity of that fuel - or by multiplying by the heat generated for any purpose /for example the fuel heat to calcine one ton of alumina/, to arrive at the related volumes.

Table 29 is a guide to compute excess air ratios from  $\text{CO}_2$  or  $\text{O}_2$  readings in flue gases of different fuels. For the calciner operation where a considerable amount of water is vapourized from the hydrate, it is better to go in for dry flue gas analyses.

Tables 30 and 31 are given for convenience to check up specific air and flue gas volumes.

The specific heat content important to determine actual heat ratios referred to air or flue gas flow rates is given in Table 32.

The information provided in these tables may also be used for combustion calculations of steam boilers: therefore, data on coal firing have been included as well.

Table 28. Oxygen and air requirements and resulting flue gas volumes and compositions

Denomination	Units	Natural gas	Fuel oil	Coal
Oxygen $O_{ideal}$	$m_n^3/MJ$	0.0555	0.0528	0.0554
Air $A=4.76 \times O_{ideal} \times n$	$m_n^3/MJ$	0.2644	0.2515xn	0.2603xn
Dry flue gas $V_{FGV}$	$m_n^3/MJ$	$0.2386+/n-1/0.2644$	$0.2372+/n-1/0.2515$	$0.2527+/n-1/0.2603$
Wet flue gas $V_{FGW}$	$m_n^3/MJ$	$0.2938+/n-1/0.2644$	$0.2680+/n-1/0.2515$	$0.2740+/n-1/0.2603$
CO <sub>2</sub> in flue gas	$m_n^3/MJ$	0.0285	0.0381	0.0461
H <sub>2</sub> O in flue gas	$m_n^3/MJ$	0.0545	0.0308	0.0213
O <sub>2</sub> in flue gas	$m_n^3/MJ$	$0.0555 /n-1/$	$0.0528 /n-1/$	$0.0554 /n-1/$

- Remarks: 1/ The characteristic combustible elements of fuels will determine their heat values according to their share in the composition of the fuels. The data given in the table represent excellent approximations for natural gas and fuel oil, and fairly good ones for coal as compared to detailed calculations based on the actual composition of the fuel.
- 2/ The volume rates of the table are normal cubic meters for each MJ of heat released by burning the fuel in question.

Table 29. Flue gas compositions for different fuels and excess air conditions

Flue gas components		Units	Natural gas	Fuel oil	Coal
Dry flue gas Composition at n=1.0	CO <sub>2</sub>	vol %	11,9	16,1	18,5
	O <sub>2</sub>		-	-	-
	N <sub>2</sub>		88,1	83,9	81,5
Dry flue gas Composition at n>1.0	CO <sub>2</sub>	vol %	$\frac{0,0283 \cdot 100}{0,2386+n-1/0,2644}$	$\frac{0,0381 \cdot 100}{0,2372+n-1/0,2515}$	$\frac{0,0461 \cdot 100}{0,2527+n-1/0,2603}$
	O <sub>2</sub>		$\frac{0,0555/n-1/100}{0,2386+n-1/0,2644}$	$\frac{0,0528/n-1/100}{0,2372+n-1/0,2515}$	$\frac{0,0554/n-1/100}{0,2527+n-1/0,2603}$
	N <sub>2</sub>		100-/(CO <sub>2</sub> +O <sub>2</sub> /	100-/(CO <sub>2</sub> +O <sub>2</sub> /	100-/(CO <sub>2</sub> +O <sub>2</sub> /
Wet flue gas Composition at n=1.0	CO <sub>2</sub>	vol %	9,7	14,2	17,0
	H <sub>2</sub> O		18,5	11,5	1,7
	N <sub>2</sub>		71,8	74,3	75,3
Wet flue gas Composition at n>1.0	CO <sub>2</sub>	vol %	$\frac{0,0285 \cdot 100}{0,2938+n-1/0,2644}$	$\frac{0,0381 \cdot 100}{0,2680+n-1/0,2515}$	$\frac{0,0461 \cdot 100}{0,2740+n-1/0,2603}$
	H <sub>2</sub> O		$\frac{0,0545 \cdot 100}{0,2938+n-1/0,2644}$	$\frac{0,0308 \cdot 100}{0,2680+n-1/0,2515}$	$\frac{0,0213 \cdot 100}{0,2740+n-1/0,2603}$
	O <sub>2</sub>		$\frac{0,0555/n-1/100}{0,2938+n-1/0,2644}$	$\frac{0,0528/n-1/100}{0,2680+n-1/0,2515}$	$\frac{0,0554/n-1/100}{0,2740+n-1/0,2603}$
	N <sub>2</sub>		100-/(CO <sub>2</sub> +H <sub>2</sub> O+O <sub>2</sub> /	100-/(CO <sub>2</sub> +H <sub>2</sub> O+O <sub>2</sub> /	100-/(CO <sub>2</sub> +H <sub>2</sub> O+O <sub>2</sub> /

Remark: Excess air coefficient /n = 1.0/ means ideal amount of air required for complete combustion of fuel.

Table 30. Specific combustion air volumes  $/V_{Air}/$  for different excess air ratios  $/n/$  and fuels

n	Units	Natural gas	Fuel oil	Coal
1.0	m <sup>3</sup> /MJ	0.264	0.252	0.260
1.1	m <sup>3</sup> /MJ	0.291	0.277	0.286
1.2	m <sup>3</sup> /MJ	0.317	0.302	0.312
1.3	m <sup>3</sup> /MJ	0.344	0.327	0.338
1.4	m <sup>3</sup> /MJ	0.370	0.352	0.364
1.5	m <sup>3</sup> /MJ	0.397	0.377	0.391
1.6	m <sup>3</sup> /MJ	0.423	0.402	0.417
1.7	m <sup>3</sup> /MJ	0.450	0.428	0.443
1.8	m <sup>3</sup> /MJ	0.476	0.453	0.469
1.9	m <sup>3</sup> /MJ	0.502	0.478	0.495
2.0	m <sup>3</sup> /MJ	0.529	0.503	0.521

Table 31. Specific wet flue gas volumes  $/V_{FGW}/$  for different excess air ratios  $/n/$  and fuels

	Units	Natural gas	Fuel oil	Coal
1.0	m <sup>3</sup> /MJ	0.294	0.268	0.274
1.1	m <sup>3</sup> /MJ	0.320	0.293	0.300
1.2	m <sup>3</sup> /MJ	0.347	0.318	0.326
1.3	m <sup>3</sup> /MJ	0.373	0.343	0.352
1.4	m <sup>3</sup> /MJ	0.400	0.369	0.378
1.5	m <sup>3</sup> /MJ	0.426	0.394	0.404
1.6	m <sup>3</sup> /MJ	0.452	0.419	0.430
1.7	m <sup>3</sup> /MJ	0.479	0.444	0.456
1.8	m <sup>3</sup> /MJ	0.505	0.469	0.482
1.9	m <sup>3</sup> /MJ	0.532	0.494	0.508
2.0	m <sup>3</sup> /MJ	0.558	0.519	0.534

Table 32. Specific heat content of flue gases  $/q_{FG}/$  and air  $/q_{Air}/$  at different temperatures

Temperature °C	Flue gases at n = 1.0			Air
	Natural gas	Fuel oil	Coal	
100	138.2	138.6	139.0	130.6
200	279.3	280.5	281.8	262.5
300	422.9	425.4	427.9	396.0
400	570.2	574.8	578.2	532.6
500	723.1	729.8	733.9	672.8
600	878.4	886.3	892.6	816.0
700	1040.0	1050.0	1057.6	963.8
800	1202.9	1214.6	1223.4	1112.0
900	1369.1	1382.1	1392.5	1263.2
1000	1538.6	1553.3	1564.6	1416.0
1100	1711.1	1727.1	1739.6	1570.9
1200	1886.2	1903.3	1916.7	1728.3
1300	2060.7	2078.7	2093.0	1884.5
1400	2236.6	2255.4	2270.1	2041.1
1500	2417.9	2436.7	2452.6	2202.7
1600	2600.4	2620.1	2636.8	2364.7
1700	2783.0	2803.5	2818.6	2527.6
1800	2967.2	2987.3	3005.3	2690.4
1900	3151.0	3171.5	3189.9	2853.3
2000	3336.0	3356.1	3374.6	3016.2
2100	3523.2	3542.5	3561.7	3181.1
2200	3710.3	3729.6	3748.0	3345.3
2300	3900.0	3919.3	3940.6	3512.7
2400	4090.5	4108.9	4132.8	3679.8

#### 9.4 Energy audit of calcination

The procedure of making an energy balance of the calcination section is shown by a practical case:

The operating rotary kiln is fired by natural gas and comprises a planetary alumina cooler /or air preheater/ and a multicyclone type hydrate dryer section as shown in Fig. 60.

Flow rates of both fuel gas and hydrate feed can be measured, although the latter is used only to check the alumina losses. An alumina feed and discharge of unit amount is taken because the balance is set up for unit rate of alumina output.

The heat balance around the planetary cooler is only approximative since the temperature of air discharge cannot be measured accurately. The same difficulty arises from the product aspect: temperatures of alumina entering and leaving the cooler cannot be taken precisely. Fortunately, this will not influence the accuracy of the overall heat balance because this portion of heat is recycling.

The real heat losses are actually the waste heat to the water cooler and that rejected to the atmosphere by radiation.



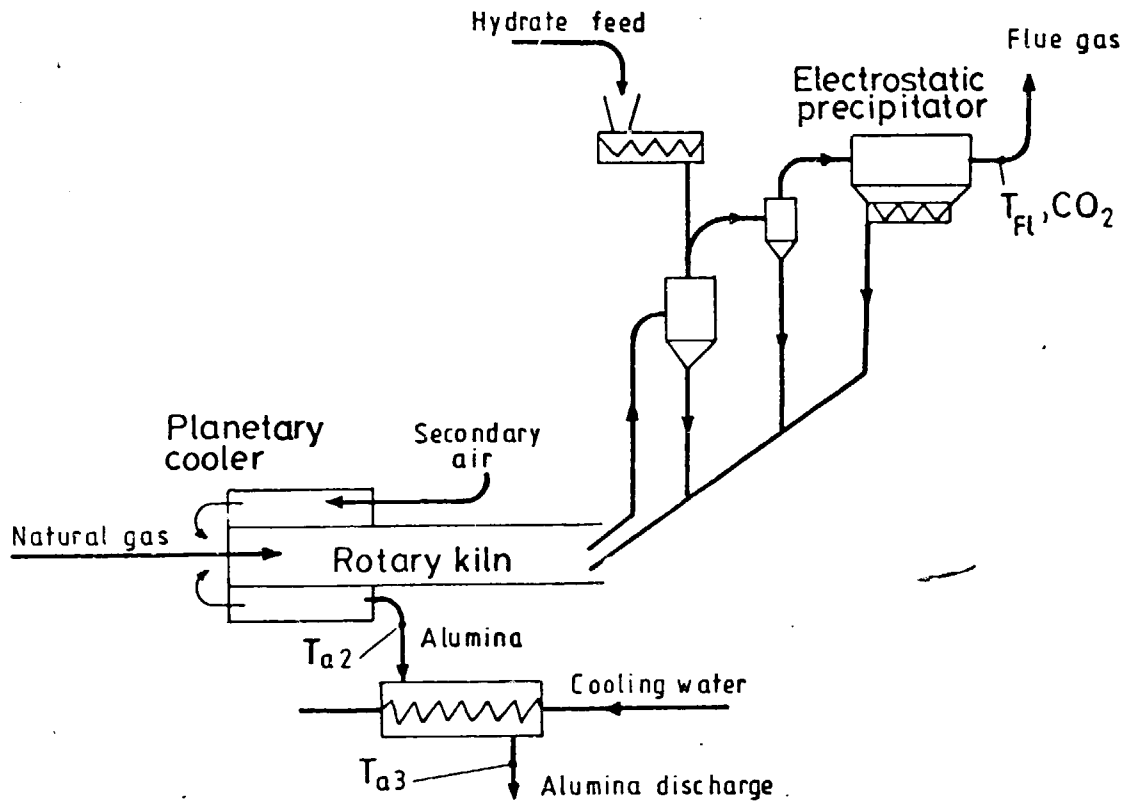


Fig. 60. Calcination flow sheet

Unit heat rate from natural gas combustion:

$$Q_{NG} = V_{NG} \times H_{NG} \quad /MJ/t/$$

where  $V_{NG}$  is the measured unit volume  $/m^3/t/$  of natural gas fired, and

$H_{NG}$  is its heat value  $/MJ/m^3/$ .

From  $CO_2$  or  $O_2$  readings the excess air ratio can be computed using the equations as given in Table 30.

The unit heat input by preheated air becomes:

$$Q_{Air} = Q_{NG} \times V_{Air} / n \times q_{Air} / T / \quad /MJ/t/, \text{ wherein}$$

the specific heat content  $q_{Air} / T /$  are taken from Tables 28 and 32, corresponding to increased stack gas temperature:

$$Q_{STL} = Q_{NG} \left\{ \left[ V_{FGW}^{-/n-1/} V_{Air} \times q_{FG} \right] + /n-1/V_{Air} \times q_{Air} \right\}$$

The energy balance of the calciner:

1. Unit heat rates in:

1.1 Fuel  $Q_{NG} = V_{NG} \times H_{NG}$

1.2 Air  $Q_{Air} = Q_{NG} \times V_{Air} \times q / W^T /$

1.3 Hydrate  $Q_{FC} = \left[ 1.64 \times /0.53+W/ \times 4.2 \right] T_{FC}$

Total  $\sum /Q_{NG} + Q_{Air} + Q_{FC} /$

2. Unit heat rates out /or absorbed/:

2.1 Water evaporation  $Q_{WE} = 45 \times W$

2.2 Reaction heat  $Q_{RE} = 2020$

2.3 Stack loss  $Q_{ST} = Q_{WG} \left\{ \left[ V_{FGW}^{-/n-1/V_{Air}} \right] \times q_{FG} + \right. \\ \left. + /n-1/V_{Air} \cdot q_{Air} \right\}$

2.4 Air cooler  $Q_{A11} = 1.64 /T_{a1} - T_{a2} / = Q_{Air}$

2.5 Water cooler  $Q_{A12} = 1.64 /T_{a2} - T_{a3} /$

Subtotal  $\sum /Q_{WE} + Q_{RE} + Q_{ST} + Q_{Air} + Q_{A12} /$

2.6 Radiation loss  $Q_{RL} = \text{Total} - \text{Subtotal}$

### 10. Electrical energy

In an energy audit of an alumina plant the distribution of the total unit energy consumption of 340 kWh/tonne was found to break up into the portions as given in Table 33.

Table 33. Break up of electrical energy consumption

Plant units	%	Equipment	%
Preparation	8.0	Piston pumps	7
Digestion	11.5	Compressors	10
Settling-washing	21.0	Vacuum pumps	9
Precipitation	30.5	Centrifugal pumps	52
Evaporation	11.8	Tank agitators	12
Calcination	17.2	Fans, others	10
Total	100.0	Total	100

The break up is fairly representative for medium size alumina plants. Centrifugal pumps are the largest consumers among any other group of equipment, and deserve examination.

In an alumina plant there are about 200-250 pumps, and it is best to check the efficiency of the larger types at first.

When grouping all the pumps according to their power requirement it turns out, that it is enough to check the 30-40 largest pumps, which may cover about 67 per cent of the total power required by all the pumps in the plant.

The efficiency is determined by measuring the head  $/H/$  by a manometer and the volume rate  $/V/$  by a flow meter /for liquors and slurries with a magnetic flow meter/ or by tank level gaging. The measurement of the electrical current to calculate power consumption will not present any problem.

The calculated efficiency might be as low as 10-30 % in many cases, and this fact would be a good occasion to start action for energy conservation.

The causes mostly responsible for poor pump efficiencies might be:

- a/ pump is oversized for the actual job
- b/ wide internal running clearances allow high back flow
- c/ period between overhauls is too long
- d/ pumps designed for water are engaged in liquor and slurry service

Fig. 61. Shows typical performance of the same pump when used to transport water or alumina plant slurry.

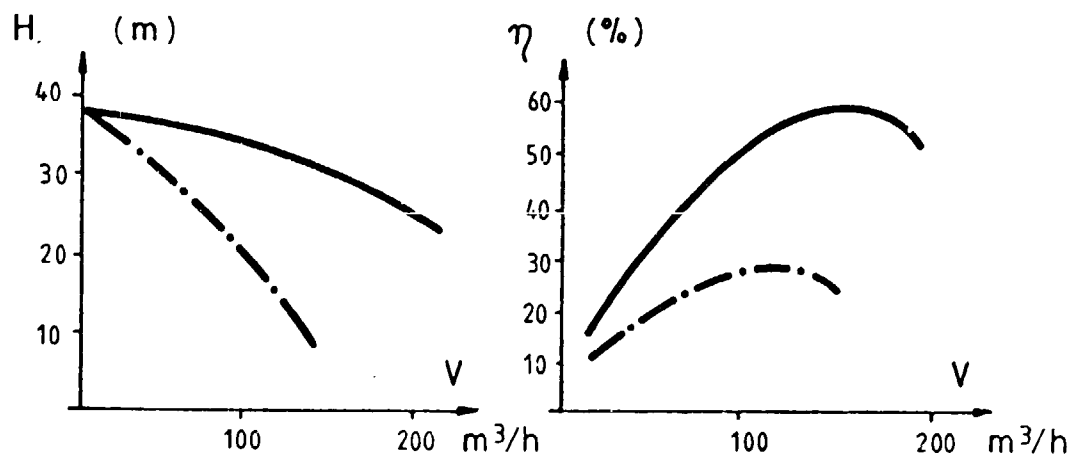


Fig. 61. Head and efficiency curves

One of the promising actions to conserve energy is to substitute pumps designed for water service by special designs capable of pumping slurries with similar efficiencies as water. The proper manufacturer has to be found.

Another general cause for poor performance was found to be the pressure loss at the throttle valve used mostly to set the flow rate delivered by the pump.

A control valve can only become effective if an adequate pressure difference exists across the valve. The throttling curves  $/h_1, h_2, h_3/$  must therefore run higher than the resistance curve of the pipe  $/h_0/$  as shown in Fig. 62. The throttling curves cut the head curve  $/h_0/$  in points  $M_1, M_2, M_3$ , which set the various volume rates  $V_1, V_2, V_3$  as required.

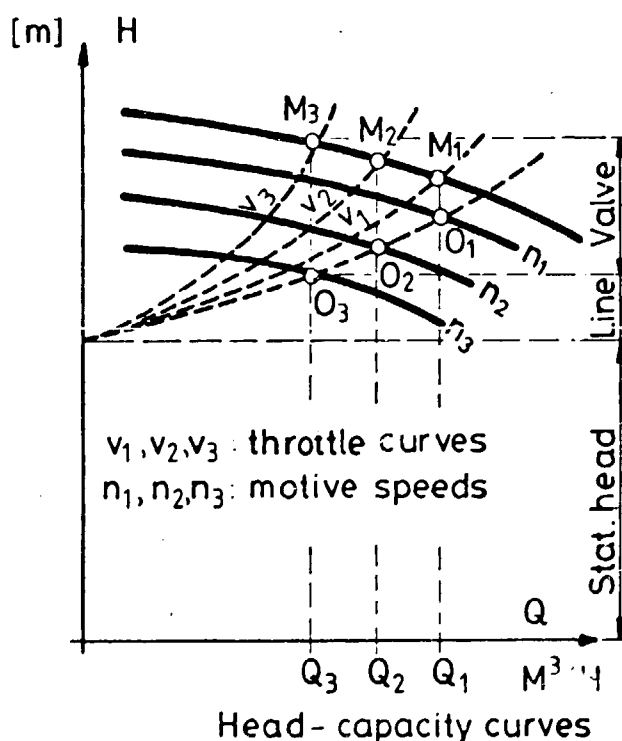


Fig. 62. Head-capacity curves

In order to eliminate this throttle loss variable speed drives can be used instead of control valves. Head curves for speeds  $n_1, n_2, n_3$  are also shown in Fig. 25. which cut the resistance curve of the pipe line in points  $O_1, O_2, O_3$ .

The same volume rates  $V_1-V_2-V_3$  can be adjusted by speed variations  $n_1-n_2-n_3$  as well as by valve throttling  $h_1-h_2-h_3$ , but with an average of about 20 per cent less energy consumed.

In alumina plants both the hydraulic couplings and the variable frequency drives were applied to advantage. Hydraulic couplings are rugged, cheap but their efficiency deteriorates with increasing slip at low volume rates. Another disadvantage is that separate couplings are to be used between every pump and motor.

Fig. 63. shows the efficiencies of the both the variable frequency drive and the hydrodynamic coupling.

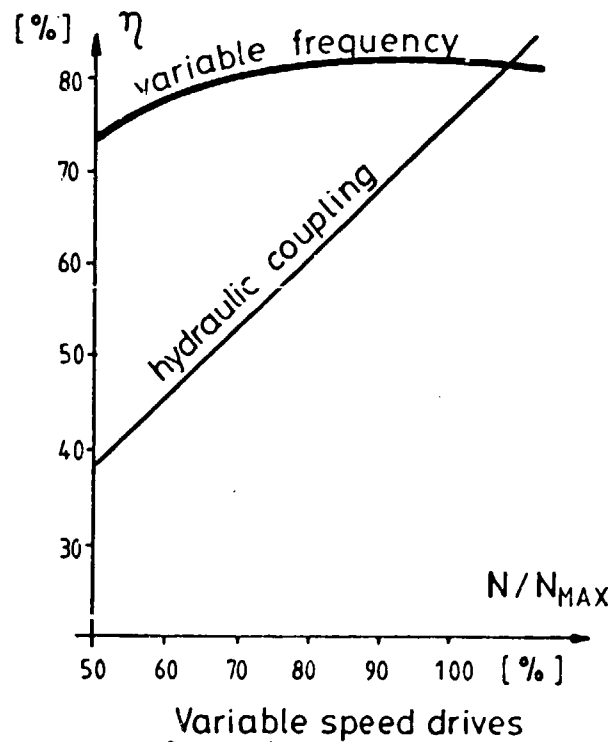


Fig. 63. Variable speed drive efficiencies

In case of variable frequency drives one control device can be applied for a pair of pump motors, where one is operated at a time with the other one as stand-by unit. Even so it is costlier than the simple coupling, but variable frequency speed controls have higher efficiencies in the lower flow rate range.

Pay-out for both speed controls lies within 3 years. Costs for maintenance of pumps are markedly lower, life of the impellers doubles in the average. Generally 20 per cent of electrical energy can be saved by elimination of control valve throttle losses.

#### 11. Cogeneration of electricity and heat

Electricity belongs to the group of secondary energy sources, because it is generated by energy conversion from primary resources /fossil fuels, nuclear fuels, hydropower, solar energy/, which can directly be taken from nature.

Whenever the electricity used in alumina processing is derived from fossil fuel fired thermal power stations it is always worth to consider cogeneration of electricity and heat, because this concept holds a significant potential to conserve primary energy.

The process of energy conversion in a thermal power station is shown in the two parts of Fig. 64. In the lower portion the main equipment components participating in electricity generation can be seen. Fossil fuel fired with combustion air releases a high temperature flue gas, which is cooled down to stack temperature in the process of heat transfer to the water-vapor system.

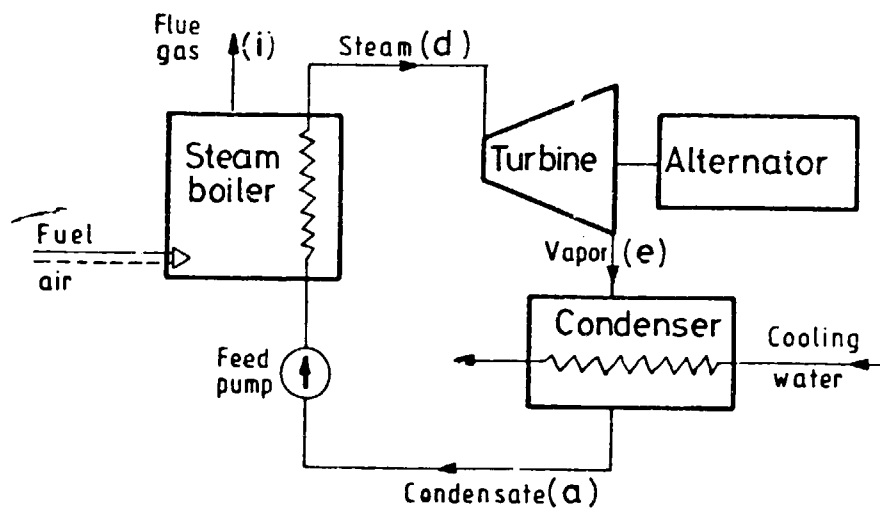
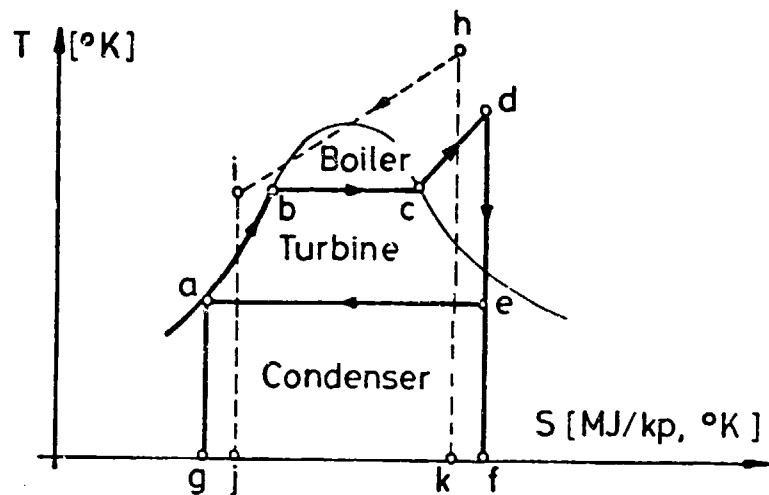


Fig. 64. Thermal power station

The area  $h-i-j-k$  represents the heat transferred from flue gases in the boiler to preheat condensate /a-b/, vaporize /b-c/ and superheat it /e-d/. The total heat absorbed by the area  $a-b-c-d-f-g-a$ , which is equal to the area  $h-k-j-i-h$  delivered by the flue gas side.



The energy converted to shaft power in the turbine is indicated by the area d-e-a-b-c-d, and the heat carried off by the cooling water from the condenser is shown as the area e-f-g-a-e.

Only one portion of the total heat is converted in the turbine to mechanical energy, a substantial portion is lost in the condenser to heat the cooling water stream.

The primary heat equivalent of electricity generated by condensing turbines is around 12 MJ/kWh, which involves the losses of both the boiler and the condenser.

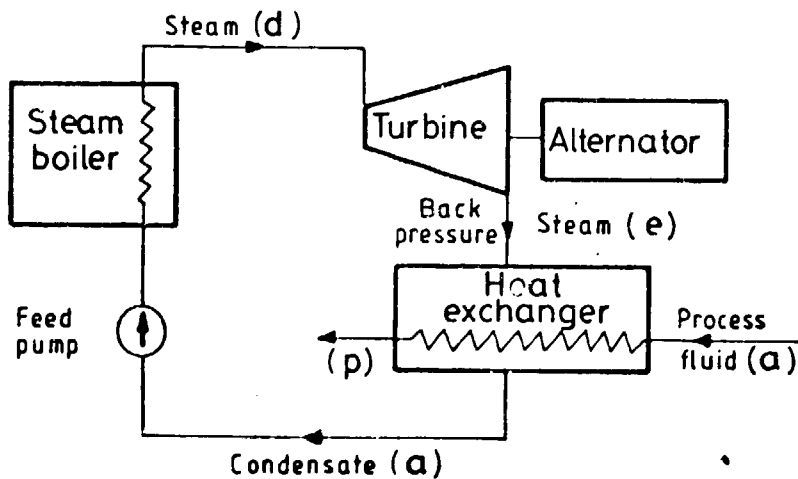
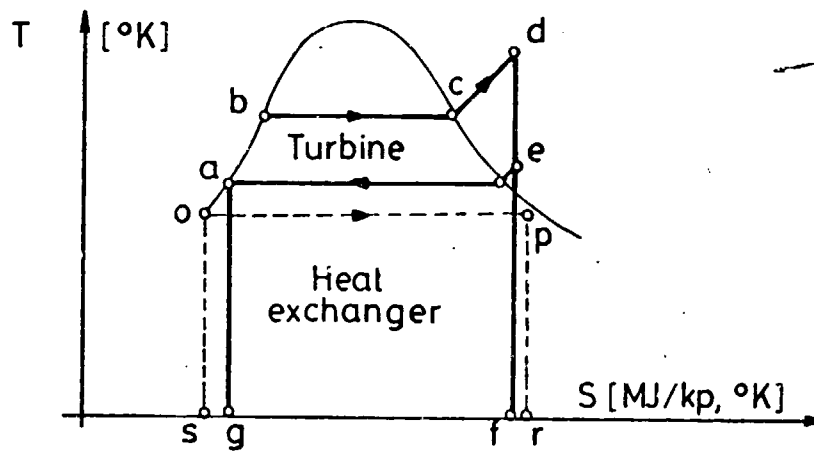


Fig. 65. Cogeneration plant

In an industrial power station as shown in Fig. 65 the part converted to mechanical power is less than in the condensing turbine /the area a-b-c-d-e-a in Fig. 65 is narrower than the corresponding area in Fig. 64/, but the heat content of the back pressure steam is utilized in the heat exchanger. The heat transferred to the process fluid is represented by the area o-p-r-s-o, being equal to area e-a-g-f-e, the heat delivered by the back pressure steam.

So the whole heat content of the steam raised in the boiler /area a-b-c-d-f-g-a/ is fully used, partly for conversion to shaft power in a back-pressure turbine, and partly for process heat supply in heat exchangers.

Back pressure generated electricity needs a primary heat expense of about 6 MJ/kWh.

The ratio of shaft to heat output of a back-pressure turbine depends on the steam pressure and temperature before and after expansion. With steam enthalpies  $h_{p1}$  and  $h_{p2}$  at turbine inlet and outlet, the latent heat of steam at back-pressure  $r_{p2}$  and a turbine nozzle efficiency  $\eta_t$  the shaft to heat ratio can be calculated as

$$\frac{S}{H} = \frac{h_{p1} - h_{p2}}{r_{p2}} \cdot \eta_t$$

Back-pressure power generation entirely depends on low temperature heat requirement of the plant. In one alumina plant audited the back-pressure heat required was  $Q_B = 4500$  MJ/tonne alumina and the shaft to heat ratio  $S/H = 0.13$ ,

so the unit rate of self generated electricity was

$$N_B = \frac{S}{H} \cdot \frac{Q_B}{3,6} = 0,13 \frac{4500}{3,6} = 162 \text{ kWh/t,}$$

because 3,6 MJ = 1 kWh.

The amount of back-pressure power  $N_B$  will depend upon the back-pressure heat demand  $Q_B$  of the plant. Because total electricity consumption  $N_T$  remains the same, the difference must be taken from the utility grid, which might well be a thermal power station having condensing turbines:

$$N_C = N_T - N_B$$

Table 34 shows the effect of back pressure heat demand changes upon the primary heat equivalent  $Q_N$  of the total electrical energy consumption  $N_T$ , calculated with primary heat equivalents of 5,7 MJ/kWh and 12,9 MJ/kWh for the back pressure and the condensing turbines respectively.

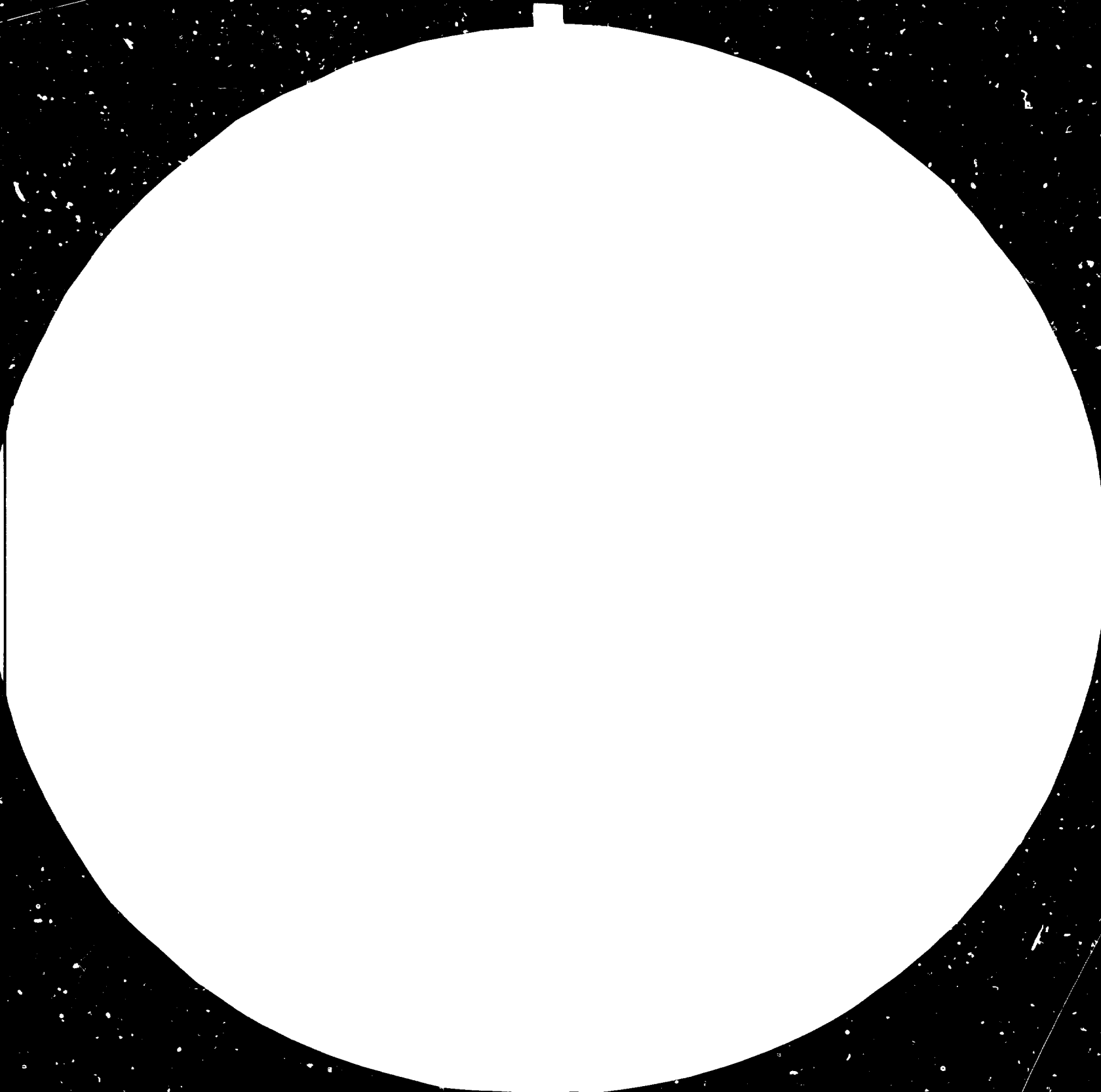
Table 34. Primary heat equivalents

$Q_B$ MJ/t	$N_B$ kWh/t	$N_C$ kWh/t	$Q_N$ MJ/t
-	-	340	4386
1000	36	304	4130
2000	72	268	3879
3000	108	232	3628
4000	144	196	3376
5000	181	159	3118

The advantage of back-pressure power generation can be seen in the decrease of overall primary energy needed  $/Q_N/$  for the same 340 kWh/t unit rate of electricity consumption, by the gradual increase of the back-pressure portion  $N_B$ .

This advantage vanishes when the process cycle is modified to reduce or to eliminate the operation of the evaporation plant. This must be borne in mind whenever such a modification is considered.

84.03.27  
AD. 85.03





28

32

36

40



## MICROSCOPY RESOLUTION TEST CHART

NATIONAL BUREAU OF STANDARDS  
STANDARDS REFERENCE MATERIAL CENTER  
ANDERSON TECHNOLOGY CENTER

Nomenclature and units

A	area of heat transfer surface in $m^2$
a	weight fraction of alumina in ton/ton
$C_A$	concentration of alumina in $kp Al_2O_3/m^3$
$C_N$	caustic concentration in $kp Na_2O/m^3$
G	unit mass rate of steam in ton/ton alumina
H	heat value per unit volume in $MJ/m^3$
$h'$	enthalpy of saturated water in MJ/ton
$h''$	enthalpy of saturated vapor in MJ/ton
K	heat transfer coefficient in $MJ/h, m^2, ^\circ C$
M	unit mass of process fluid in ton/ton alumina
Q	unit quantity of heat in MJ/ton alumina
q	specific heat capacity in $MJ/ton, ^\circ C$
r	latent heat of vapor in MJ/ton
S	entropy of process fluid MJ/ton, $^\circ K$
T	temperature in $^\circ C$ or $^\circ K$
$T_i'$	feed temperature of stream i in $^\circ C$
$T_i''$	discharge temperature of stream i in $^\circ C$
V	unit volume in $m^3/ton$ alumina
W	unit water equivalent Mcal/ $^\circ C$ , ton alumina
w	unit water content in ton water/ton
X	mass or volume fraction in ton/ton or $m^3/m^3$
$\eta$	efficiency in %
$\phi$	efficiency of heat transfer in %

Conversion of units

BTU	=	1,055 KJ
Mcal	=	4,1868 MJ
$^\circ C$	=	$(^\circ F - 32) / \frac{5}{9}$



## REFERENCES

- /1/ Kapolyi, L.: Expected Development of the Aluminium Industry, and the Human Environment. "Alumina Production until 2000" Proceedings of Int. Symp. of ICSOBA, held in Tihany, Hungary, Oct. 6-9. 1981. pp 15-26.
- /2/ Fitzgerald, M.D. and Pollio, G.: Aluminium: The Next Twenty Years. J. of Metals, Dec. 1982. pp 37-42.
- /3/ Brondyke, K.J.: The Aluminium Industry in 1982 and Outlook for the 80's. J. of Metals, April 1983, pp 63-67.
- /4/ Testin, R.F.: Aluminium Recycling - Potential and Problems. J. of Metals, Sept. 1981, pp 21-25.
- /5/ Russell, A.S.: Pitfalls and Pleasures in New Aluminium Process Development. J. of Metals, June 1981. pp 132-139.
- /6/ Grjotheim, K. and Welch, B.: Impact of Alternative Processes for Aluminium Production on Energy Requirements. J. of Metals, Sept. 1981. pp 26-32.
- /7/ Balabanov, T.: Industrial Energy Requirements and Some Policy Implications for Developing Countries. High-level Expert Group Meetings Preparatory to the Fourth General Conference of UNIDO. "Energy and Industrialization" Oslo, Norway, 29 August - 2 September 1983. ID/WG. 402/6. 9. Aug. 1983.

- /8/ Bielfeldt, K. and Winkhaus, G.: Challenge to Alumina Production Technology in the 80's. "Alumina Production until 2000". Proceedings of Int. Symposium of ICSOBA, held in Tihany Hungary. Oct 6-9. 1981. pp 111-119.
- /9/ Cochran, C.N.: Energy Balance of Aluminium - from Production to Application. J. of Metals, July 1981. pp 45-48.
- /10/ Russell, A.S.: Energy Savings in Aluminium Production, Use, and Recycling. J. of Metals, July 1983. pp 51-55.
- /11/ Laue, H.J.: Nuclear Energy for Developing Countries. High-level Expert Group Meetings Preparatory to the Fourth General Conference of UNIDO. "Energy and Industrialization", Oslo, Norway, 29 Aug - 2 Sept. 1983. ID/WG 402/8 Aug. 1983.
- /12/ Heindl, R.A.: Aluminium and Energy, Paper of Bureau of Mines. /USA/.
- /13/ Lotze, J.: Economic Evaluation of World's Bauxite Resources. Proceedings of 4th Int. Congress of ICSOBA /Athens/ 1978, Vol. 2. p 494.
- /14/ Lotze, J.: The Influence of Bauxite Pricing on the Development of Bauxite Resources with Particular Reference to Fiscal Costs. Paper presented on the 5th Int. Congress of ICSOBA, Sept 26/28, 1983 Zagreb, Yugoslavia

- /15/ Solymár, K., Zámbo, J. and Siklósi, P.: Technological Evaluation of Monohydrate Bauxites. Paper prepared for the Int. Bauxite Symposium to be held in Los Angeles, 1983.
- /16/ Hill, V. G., Ostojic, S., and Robson, R.: On Bauxite Assays and the Relative Valuation of Bauxites Traded. Paper presented on the 5th Int. Congress of ICSOBA, Sept. 26/28. 1983. Zagreb, Yugoslavia.
- /17/ Teas, E.B., and Kotte, J.J.: The Effect of Impurities on Processing Efficiencies and Methods for Impurity Control and Removal. J. of Geol. Soc. of Jamaica, Proceedings of Bauxite Symposium IV., June 1980. pp 100-129.
- /18/ Group Training in Production of Alumina, UNIDO-ALUTERV-FKI, Budapest, 1979. Vol. 1. Principles and Methods of Bauxite Prospecting. Edited by Dr. Komlóssy, Gy., Szantner, F., and Dr. Vörös, I.
- /19/ Solymár, K., Gadó, P., Tomcsányi, L. and Bulkai, D.: Profile of Transferring Technology in Testing, Investigation and Evaluation of Bauxite. UNIDO/I.O. 466. 15. Sept. 1981.
- /20/ Donaldson, D.J.: Energy Savings in the Bayer Process. J. of Metals. Sept. 1981. pp 37-41.
- /21/ Lang, G., Solymár, K., and Steiner, J.: Prospects of Bayer Plant Energy Conservation. Light Metals 1981. pp 201-214.

- /22/ Chin, L.A.D.: Energy Demand and Supply in Bayer Alumina Plants. "Alumina Production until 2000" Proceedings of Int. Symp. of ICSOBA, held in Tihany, Hungary, Oct. 6-9. 1981. pp 215-228.
- /23/ Lang, G., and Veres, G.: Alumina Process and Energy Supply Systems Interfacing. "Alumina Production until 2000". Proc. of Int. Symp. of ICSOBA, 1981. pp 229-235.
- /24/ Cresswell, P.J., and Milne, D.J.: A Hydrothermal Process for Recovery of Soda and Alumina from Red Mud, Light Metals, 1982. pp 227-238.
- /25/ Perry, K.W., and Russel, A.S.: Advances and Prospects in Alumina Technology. Journal of Metals, 1982. October pp 48-53.
- /26/ Tóth, B., Vörös, I., and Zámbo, J.: Situation and Development of the Hungarian Alumina Industry. "Alumina Production until 2000". Proc. of Int. Symp. of ICSOBA, 1981. pp 271-282.
- /27/ German Patent, No 579.114
- /28/ Lányi, B.: Der schnelle, kontinuierliche Bauxitaufschluss. Symposium of ICSOBA, Zagreb, Oct. 1-3, 1963, Tom. III. pp 105-117.
- /29/ Bielfeldt, K. and Arnsward, W.: Probleme des Bauxitaufschlusses, Aluminium 43. /1967./ pp 355-360.
- /30/ Bielfeldt, K.: Practical Experiences with Tube Digester. J. of Metals, Sept. 1963. pp 48-54.

- /31/ Hungarian Patents No's 157.057 /1968/, 177.161 /1977/;  
US Patent No 3.586.487
- /32/ Wargalla, G. and Brandt, W.: Processing of Diasporic  
Bauxites, Light Metals, 1981. pp 83-100.
- /33/ Mrs. Orbán, M., Imre, A. and Stefániai, V.: Complex  
Mineralogical Investigation and Characterization of  
Red Mud and its Components. TRAVAUX de l'ICSOBA, 1976.  
No 13. pp 491-505.
- /34/ Hungarian Patents No's 164.863 /1972/, 166.061 /1973/,  
169.643 /1974/ and 173.698 /1976/; US Patents No's  
4.026.989, 3.944.648, 4.091.071 and 4.225.838
- /35/ Solymár, K., Mátyási, J. and Tóth, B.: Digestion of  
Hungarian Goethitic Bauxites with Additives. TRAVAUX  
de l'ICSOBA 1976. No 13. pp 299-312.
- /36/ Solymár, K., Ferenczi, T. and Zöldi, J.: The Effects  
of Technology on the Properties of Red Mud. TRAVAUX  
de l'ICSOBA 1979. No 15. pp 287-305.
- /37/ Orbán, F., 'Sigmund, G., Siklósi, P., Solymár, K. and  
Steiner, J.: Advances in Bayer Process Design. Journal  
of Geol. Soc. Jamaica, Proceedings of Bauxite Symposium  
IV. June 23-26.1980. pp 68-87.
- /38/ Beneslavsky, S.I., Tikhonov, N.N., Jashunin, P.V.:  
The chemical composition and the main technological  
characteristics of Rumanian bauxites. Trudy VAMI, No.  
62. pp 5-11 /1968/ /in Russian/

- /39/ Malts, N.S., Medvedev, V.V., Levina, T.S.: Effect of lime at the digestion of monohydroxide type bauxites in the Bayer process. Trudy VAMI, No 77. pp 16-23 /1971/ /in Russian/
- /40/ Mercier, H., Magrone, R.: Influence de l'addition de chaux a l'attaque alcaline en voie humide des bauxites a dispoire. ICSOBA 3e congres, Nice 1973. pp 513-521.
- /41/ Delyannis, E.: Alkaline treatment of diasporic bauxites. Proc. of the Second Int. Symp. of ICSOBA, Vol. 3. pp 69-76.
- /42/ French Patent No 1.280.009 /1960/ Soc. Pechiney
- /43/ Tikhonov, N.N., Lapin, A.A.: The main technological parameters and technical-economical indices during treatment of different quality bauxites by Bayer's method. Mineralogical and Technological Evaluation of Bauxites. Proc. VAMI-FKI pp 201-212, Budapest 1975.
- /44/ Mercier, H., Noble, M.: Optimization of the alkaline treatment of the different bauxite varieties. Light Metals 1974, Vol. 2. pp 777-786. 103th AIME Annual Meeting
- /45/ Tikhonov, N.N., Jashunin, P.V., Beneslavsky, S.I., Bikova, A.B., Bessonova, E.J.: Solubility of the aluminium hydroxide content of bauxites of different mineralogical type in caustic aluminate solutions. II. Communication. Trudy VAMI, No 77 pp 5-8 /1971/ /in Russian/

- /46/ Solymár, K.: Evaluation of Soviet and Hungarian bauxite reference standards from the view of the Bayer cycle. Mineralogical and Technological Evaluation of Bauxites. pp 229-265. Proc. VAMI-FKI, Budapest /1975/
- /47/ Hungarian Patent No 159.725 /1969/  
Greek Patent No 41.701  
French Patent No 2.060.436  
Soviet Patent No 474.227
- /48/ Coumoulos, G.D.: Processing Diasporic Bauxites. The Greek Bauxite Case. Paper prepared for the Int. Bauxite Symposium to be held in Los Angeles, Febr. 26 - March 2. 1984.
- /49/ Solymár, K., and Steiner J.: Energy and Technological Advantages of Tube Digestion and Digestion with Additives. J. Geol. Soc. Jamaica Proceedings of Bauxite Symposium V. June 21-24. pp 223-232. 1982.
- /50/ Solymár, K. and Ferenczi, T.: New Possibilities for Processing Diasporic Bauxites. Proceedings of 4th ICSOBA International Congress, Vol. 3. 1978. pp 388-403.
- /51/ Minai, S. et al.: Sandy Alumina Conversion. Light Metals 1978. p 95
- /52/ Tschamper, O.: Improvements by the New Alusuisse Process for Producing Coarse Aluminium Hydrate in the Bayer Process. Light Metals 1981. pp 115.
- /53/ Tschamper, O.: The New Alusuisse Process for Producing Coarse Aluminium Hydrate in the Bayer Process. J. of Metals, April 1982. pp 36-39.

- /54/ Kirke, E.A.: Recent Trends in Bayer Precipitation Practice. Chemical Engineering in Australia, 1982. March Ch.E.J./1/ pp 35-39.
- /55/ Gnyra, B. and Leve, G.: Review of Bayer Organics - Oxalate Control Processes. Light Metals 1979. pp 151-161.
- /56/ Deabriges, J., Noble, M., and Magrone, R.: Purification of Bayer liquors by barium salts. Light Metals 1977. Vol. 2. pp 15-22.
- /57/ Yamada, K., Harato, T. and Kato, H.: Oxidation of Organic Substances in the Bayer Process, Light Metals, 1981. pp 117-128.
- /58/ Pohland, H.H. and Tieleus, A.J.: A New Bayer Liquor Purification Process. Light Metals, 1983. pp 211-221. Publisher: The Metallurgical Society of AIME.
- /59/ Pearse, M.J. and Sartowski, Z.: Application of Special Chemicals/Flocculants and Dewatering Aids/ for Red Mud Separation and Hydrate Filtration. Paper prepared for the Int. Bauxite Symposium, to be held in Los Angeles, Febr. 26 - March 2. 1984.
- /60/ Baksa, Gy., Valló, F., Kalocsai, F. and Vitéz, J.: Cycle Cleaning Possibilities in Bayer Alumina Process. TRAVAUX de l'ICSOBA, 1982. /Vol. 12./ - No. 17. pp 97-116.
- /61/ Fritschy, R.C.: Energy and Efficiencies in Alumina Production. Chemical Engineering in Australia, Vol. Ch.E.J. No 1. March 1982.



- /62/ Young, R.C.: Chemistry of Bayer Liquor Causticization. Light Metals, 1982. pp 97-117.
- /63/ Lectard, D.: Mechanism of Causticization of Overflowing Liquor from Washing Muds. TRAVAUX de l'ICSOBA, 1982. /Vol. 12./ No 17. pp 149-156.
- /64/ Vörös, I.: Causticization of Sodium Aluminium Silicates of the Bayer Alumina Plant. Proc. of the Res. Int. for Non-Ferrous Metals, Budapest, IX. Akadémiai Kiadó /Publishing House of the Hung. Acad. of Sci. Budapest, 1971. pp 105-113.
- /65/ Vörös, I., Bujdosó, E., Mrs. Orbán, M. and Tóth, L.: Causticization of Red Mud. TRAVAUX de l'ICSOBA, 1974. No 12. pp 121-133.
- /66/ Riffaud, J.P. and Deschenes, R.: Process control at ALCAN : Evolution and Future Trends. "Alumina Production until 2000". Proceedings of the Int. Symp. of ICSOBA, held in Tihany, Hungary, Oct. 6-9. 1981. pp 193-206.
- /67/ Raahauge, B.E., Theil, J., Lind-Nielsen, B. and Theisen, K.: Energy Saving Production of Alumina with Gas Suspension Calciner. Paper presented on AIME 111th Annual Meeting, Dallas, USA, February, 1982.
- /68/ Bosnjakovic, Fr.: Technische Thermodynamik. Erster Teil. Verlag von Theodor Steinkopff, Dresden und Leipzig. 1948.
- /69/ Kondorossy, P.: Wirtschaftlichkeit der Thermokompression. VDI-Berichte, Nr. 383, 1980.

